2011

Dynamics and Control of Two Degree-of-Freedom Suspension System with Application to Rehabilitation

Chi-Hung Cheng
Lehigh University

DYNAMICS AND CONTROL OF TWO DEGREE-OF-FREEDOM SUSPENSION SYSTEM WITH APPLICATION TO REHABILITATION

by

Chi-Hung Cheng

A Thesis

Presented to the Graduate and Research Committee

of Lehigh University

in Candidacy for the Degree of

Master of Science

in

Mechanical Engineering and Mechanics

Lehigh University

May, 2011

This thesis is accepted and approved in partial fulfillment of the requirements for the Master of Science.

_____

Date

_____

Thesis Advisor

_____

Chairperson of Department

ACKNOWLEDGMENTS

Here I appreciate the support from my family. Without their encouragement, I would not have this honor to present this thesis. I also appreciate the aids and instruction from my advisor Dr. Meng-Sang Chew. He does teach me a lot in how to do a research and offer me many insightful opinions.

TABLE OF CONTENTS

LIST OF TABLES

LIST OF FIGURES

Chapter 2

Chapter 3

Chapter 4

Tables of Nomenclature

Length

l_1	length of link #1
l_2	length of link #2
l_3	length of link #3
l_4	length of link #4
l_{41}	length of the lower part of link #4
l_{42}	length of the upper part of link #4
l_{k1}	attachment point of spring #1
l_{k2}	attachment point of spring #2
l_{s1}	extension of spring #1
l_{s2}	extension of spring #2
l_{s10}	the length before extension of spring #1
l_{s20}	the length before extension of spring #2

Mass & Weight

m_1 , w_1	mass, weight of link #1, respectively
m_2 , w_2	mass, weight of link #2, respectively
m_3 , w_3	mass, weight of link #3, respectively
m_4 , w_4	mass, weight of link #4, respectively

m_a , w_a	mass, weight of suspended mass, respectively

Angle

θ_1, θ_2	generalized coordinates
φ_1	angle measured from link #1 to spring #1
φ_2	angle measured from link #41 to spring #2

Coefficient

g	gravitational acceleration
K_1, K_2	spring constant
f	frequency of walking pace

Controller Parameter

ε	Error in angular displacements
$\dot{\varepsilon}$	Error in angular velocityies
g_d	gain for ε
g_v	gain for $\dot{\varepsilon}$
γ	gain in adaption tuner

ABSTRACT

DYNAMICS AND CONTROL OF TWO DEGREE-OF-FREEDOM SUSPENSION SYSTEM WITH APPLICATION TO REHABILITATION

Chi-Hung Cheng

Lehigh University, 2011

Director: Dr. M. Chew

A two degree-of-freedom suspension system for gravity compensation is presented. The system utilizes a parallelogram linkage plus one extra link with two springs to support the test article to insure that it can move freely in a planar working space. Lagrange's equation is employed in the analysis of dynamics of the system. The motion deviation of the system due to the inertia of the links is presented. The characteristics of system response to forces applied in different directions are also discussed.

To overcome these issues, feed-forward adaptive control is introduced and exhibits an outstanding performance in trajectory control. The new application of the system in rehabilitation is considered. The variation of suspension force with respect to vertical displacement of center of mass of human body is also analyzed. The assumption based on the analysis is used in a later simulation. The simulation shows excellent performance of the system.

Chapter1

Introduction

The design of suspension system for gravity compensation purpose is not a new topic of research. Decades before, the engineers have used different methods to try to remove the gravitational effect on the suspended mass. The mechanism includes band wheel drives, counter weights, linkage with springs. A major application of these kinds of the gravity compensation devices is to attempt to create a zero gravity environment for lab experiments to simulate the environment in space and this is indeed what the devices are built for at first[1].

Recently many researchers are starting to look for new possibilities in the applications of these devices. The idea is inspired by the wearable robot, so called “exoskeleton”. The most general definition of a wearable robot is the device which can amplify human power, so that people who wear it is capable doing something beyond human capabilities, such as maneuvering hundreds of kilogram weight easily [6]. If it is worn by a senior or someone handicapped, the device can also allow them to do something that is simple for normal people, like taking a walk, grabbing a drink. The idea: apply a suspension system design for rehabilitation and orthotics.

Unfortunately, when people speak of exoskeletons, the impression of countless power lines connected to the back along with giant actuators at the joints pops up in their mind. In fact,

with a sophisticated mechanism design, the burden of huge power source could be eased. In 2003, the team of the Mechanical Systems Lab in University of Delaware creates a gravity balancing mechanism to directly ease the load on the lower limb while walking without the use of a power source [8,9].

In the following chapters, the new application of a two degree-of-freedom suspension system will be presented and the control method will be introduced. Details of the design and the characteristics of system response well be discussed in Chapter 2. In Chapter 3, the feed-forward adaptive control is presented and its effectiveness will be demonstrated [2~5]. The final part, Chapter 4, deals with application in the area of rehabilitation [7,10]. The advantage and the most special place of the device compared with robotic manipulator are springs carry the load as well as gravitational effect of the linkage while the linkage inertia is the only part that needs to be taken care by motors. This means the power consumption will be much lower and the maintenance costs will be much smaller. All in all, the combination of sophisticated mechanism design integrated to a simple control method can bring a more useful invention.

Chapter 2

Two Degree-of- Freedom Suspension System

The objective of the two degree-of-freedom suspension system is to eliminate the gravitational effects on a suspended mass. However, the inertia of the linkage causes a delayed system response to the applied force or impulse and its capacity to remove the gravitational effect on the test article is compromised. In this chapter, the system dynamics is present using Lagrange equation for both impulse and force cases and then compared with the real trajectories of an ideal massless suspension system to see how the inertia of the links compromises the performance of the device.

2.1 Concept of the Suspension System

As shown in the Fig. 2.1, the system consists of a parallelogram linkage. The links l_1, l_2, l_3, and one extra link, l_4, provide a two degree-of-freedom system to insure the suspended mass can be moved freely in a planar work space. Each part is supported by one zero free-length spring. For link #4, the length from the end C to the pivot B and from pivot B to point A are the same ($l_{41} = l_{42}$). The positions of the spring attachment point, F and D, are chosen base on the weight of suspended mass. The point O_1 on the lower left corner of the parallelogram linkage is the origin of the coordinate system. The suspended mass is attached on the upper end C of link #4. In the following derivation, we assume that the link is uniform,

the test article is attached right on the end of link #4, and the joints are frictionless. In our case, we assume the lengths, $\overline{AB}$ and $\overline{BC}$, are the same.($l_{41} = l_{42}$)

Since the mass is suspended at point C of the link #4, the length, l_{k2}, from pivot B to the spring attachment point D can be determined by the static equilibrium of the mass (the total moment acting on the link #4 equals to zero).

$$w_a l_{42} Sin\theta_2 - K_2 \left(l_{s2} - l_{s20}\right) Sin\varphi_2 l_{41} = 0 \tag{2.1}$$

Where w_a is the weight of the article attached at point C.

Assuming the spring has zero free-length, the length of the spring #2 before extension, l_{s20}, is zero. From the geometry, it can be deduced:

$$l_{s2} = \frac{l_{k2} Sin\theta_2}{Sin\varphi_2} \tag{2.2}$$

Therefore, equation (2.1) becomes:

$$w_a l_{42} Sin\theta_2 = K_2 l_{s2} Sin\varphi_2 l_{41} = K_2 \frac{l_{k2} Sin\theta_2}{Sin\varphi_2} Sin\varphi_2 l_{41} = K_2 l_{41} l_{k2} Sin\theta_2 \tag{2.3}$$

In the design, the lengths $l_{41} = l_{42}$ of link #4. Therefore equation (2.3) can then be simplified to:

$$l_{k2} = \frac{w_a}{K_2} \tag{2.4}$$

The length l_{k1} from ground pivot O_1 to the attachment point F of spring #1 can be obtained through a similar procedure. For the parallelogram linkage, the static equilibrium equation can then be written as:

$$K_1\left(l_{s1}-l_{s10}\right)l_1 Sin\varphi_1-\left(w_a+m_4 g\right)l_1 Cos\theta_1-\left(\frac{m_1}{2}l_1+\frac{m_2}{2}l_2+m_3 l_1\right)gCos\theta_1=0 \tag{2.5}$$

From geometry, it can be shown that:

$$l_{s1}=\frac{l_{k1}Cos\theta_1}{Sin\varphi_1} \tag{2.6}$$

If spring #1 is zero free-length, and the length of l_1 and l_2 are equal, then equation (2.5) becomes:

$$K_1\frac{l_{k1}Cos\theta_1}{Sin\varphi_1}l_1 Sin\varphi_1=K_1 l_{k1}l_1 Cos\theta_1=\left(m_a+\frac{m_1}{2}+\frac{m_2}{2}++m_3+m_4\right)gl_1 Cos\theta_1 \tag{2.7}$$

After simplification, the length, l_{k1}, can be expressed as:

$$l_{k1}=\frac{\left(m_a+\frac{m_1}{2}+\frac{m_2}{2}++m_3+m_4\right)g}{K_1} \tag{2.8}$$

For the case where the inertia of the linkage is zero, we can find:

$$l_{k1}=\frac{w_a}{K_1} \tag{2.9}$$

Equations (2.4) and (2.8) show that the force supported by the device can be readily adjusted by changing the lengths l_{k1} and l_{k2} for given spring constants K_1 and K_2.

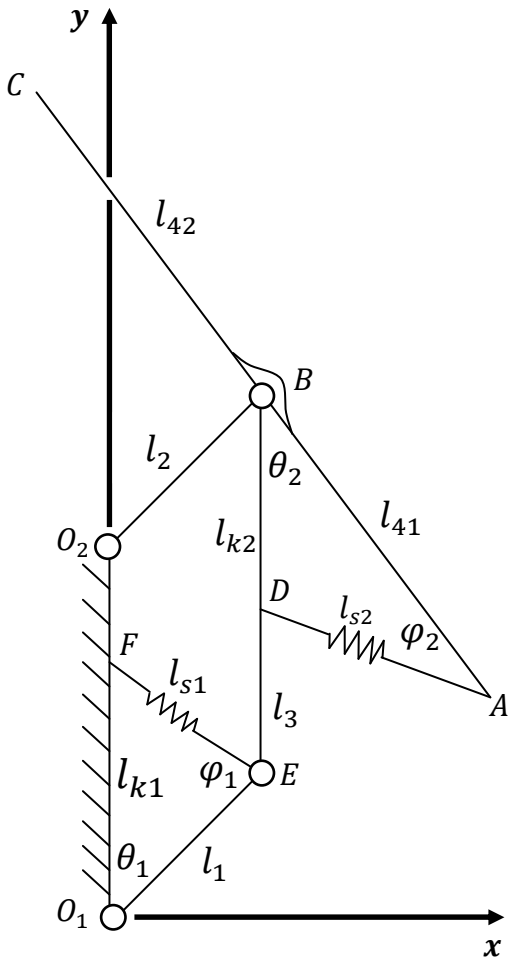

Fig. 2.1: Concept of the Two Degree-of-freedom Suspension System.

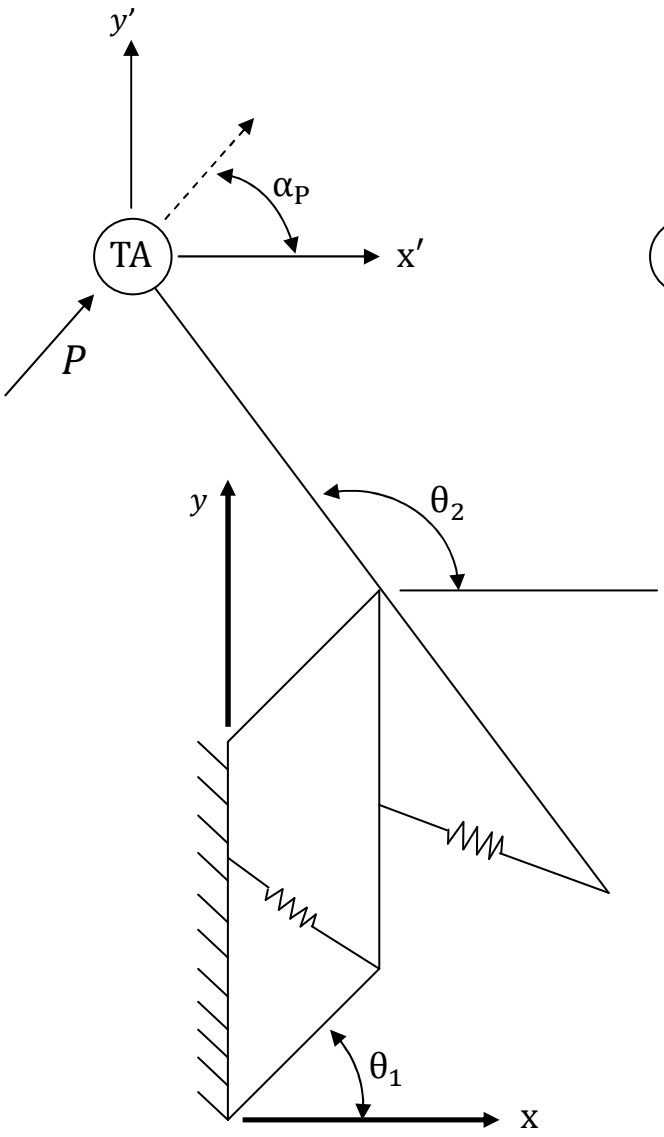

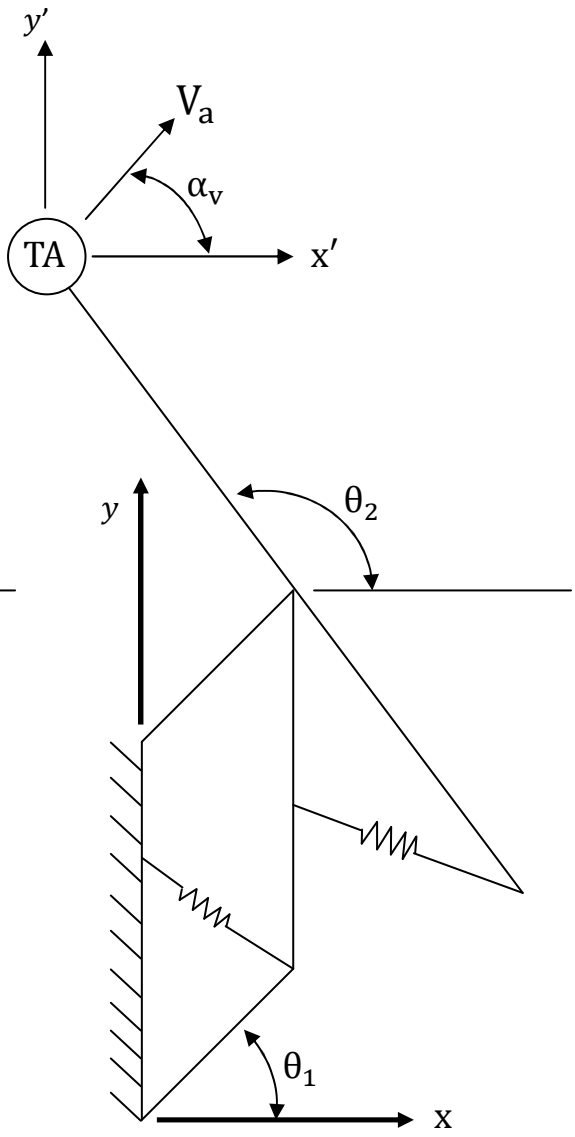

Fig. 2.2(a) Fig. 2.2(b)

Fig. 2.2(a): The Angle of the Force Applied on The Test Article.
Fig. 2.2(b): The Initial Angle of Motion of the Test Article.

2.2 Dynamics of the System under Impulsive Force Applications

In this section, the system dynamic equation for impulsive force case will be fully discussed. Then the initial condition of the system will be determined. Figure 2.2(a) shows the force applied on the test article and Figure 2.2(b) presents the angle of motion of the test article.

2.2.1 Lagrange's Equation for Impulsive force

Friction at the joints is neglected. The whole system is conservative and Lagrange's equation is applied to determine the motion of the system. Figure 2.2 shows the generalized coordinates, θ_1 and θ_2. For an Impulsive system, kinetic and the potential energies are considered in Lagrange's equation.

The motion of the links includes both translation and rotation. The total kinetic energy of the system is:

$$K.E. = \sum_{i=1}^{4} \frac{1}{2} m_i \left(\dot{x}_i^2 + \dot{y}_i^2 \right) + \sum_{i=1}^{4} \frac{1}{2} I_i \left(\dot{\theta}_{1i}^2 + \dot{\theta}_{2i}^2 \right) + \frac{1}{2} m_a \left(\dot{x}_a^2 + \dot{y}_a^2 \right)$$

(2.10)

Now consider the kinetic energy of links #1 and #2 in pure rotation.

$$T_1 = T_2 = \frac{1}{2} I_1 \omega_1^2 = \frac{1}{2} \bullet \frac{1}{3} m_1 l_1^2 \bullet \dot{\theta}_1^2 = \frac{1}{6} m_1 l_1^2 \dot{\theta}_1^2 \qquad (2.11)$$

The kinetic energy of link #3 in pure translation is given by:

$$\begin{aligned}
&\vec{R}_3 = l_1 Cos\theta_1 \hat{i} + \left(l_1 Sin\theta_1 + \frac{1}{2} l_3 \right) \hat{j} \\
&\vec{V}_3 = -l_1 \dot{\theta}_1 Sin\theta_1 \hat{i} + l_1 \dot{\theta}_1 Cos\theta_1 \hat{j} \\
&T_3 = \frac{1}{2} m_3 V_3^{\,2} = \frac{1}{2} m_3 l_1^{\,2} \dot{\theta}_1^{\,2}
\end{aligned} \tag{2.12}$$

The kinetic energy of link # 4 can be shown to be: (Translation and Rotation)

$$\begin{aligned}
&\overrightarrow{R_4} = l_1 Cos\theta_1 \hat{i} + \left(l_1 Sin\theta_1 + l_3 \right) \hat{j} \\
&\overrightarrow{V_4} = -l_1 \dot{\theta}_1 Sin\theta_1 \hat{i} + l_1 \dot{\theta}_1 Cos\theta_1 \hat{j} \\
&T_4 = \frac{1}{2} m_4 V_4^{\,2} + \frac{1}{2} I_4 \omega_4^{\,2} = \frac{1}{2} m_4 l_1^{\,2} \dot{\theta}_1^{\,2} + \frac{1}{2} \times \frac{1}{12} m_4 l_4^{\,2} \dot{\theta}_2^{\,2} = \frac{1}{2} m_4 l_1^{\,2} \dot{\theta}_1^{\,2} + \frac{1}{6} m_4 l_{41}^{\,2} \dot{\theta}_2^{\,2}
\end{aligned} \tag{2.13}$$

Finally, is the kinetic energy of the test article in pure translation is given by:

$$\begin{aligned}
&\overrightarrow{R_a} = \left(l_1 Cos\theta_1 + l_{42} Cos\theta_2 \right) \hat{i} + \left(l_1 Sin\theta_1 + l_3 + l_{42} Sin\theta_2 \right) \hat{j} \\
&\overrightarrow{V_a} = \left(-l_1 \dot{\theta}_1 Sin\theta_1 - l_{42} \dot{\theta}_2 Sin\theta_2 \right) \hat{i} + \left(l_1 \dot{\theta}_1 Cos\theta_1 + l_{42} \dot{\theta}_2 Cos\theta_2 \right) \hat{j} \\
&T_a = \frac{1}{2} m_a V_a^2 = \frac{m_a}{2} \left[l_1^{\,2} \dot{\theta}_1^{\,2} + l_{42}^{\,2} \dot{\theta}_2^{\,2} + 2 l_1 l_{42} \dot{\theta}_1 \dot{\theta}_2 \left(Cos\theta_1 Cos\theta_2 + Sin\theta_1 Sin\theta_2 \right) \right] \\
&\quad = \frac{1}{2} m_a \left[l_1^{\,2} \dot{\theta}_1^{\,2} + l_{42}^{\,2} \dot{\theta}_2^{\,2} + 2 l_1 l_{42} \dot{\theta}_1 \dot{\theta}_2 Cos\left(\theta_1 - \theta_2 \right) \right]
\end{aligned} \tag{2.14}$$

The total kinetic energy with test article can be shown as:

$$\begin{aligned}
T &= \frac{1}{2} m_a \left[l_1^{\,2} \dot{\theta}_1^{\,2} + l_{42}^{\,2} \dot{\theta}_2^{\,2} + 2 l_1 l_{42} \dot{\theta}_1 \dot{\theta}_2 Cos\left(\theta_1 - \theta_2 \right) \right] \\
&\quad + \frac{1}{6} m_1 l_1^{\,2} \dot{\theta}_1^{\,2} + \frac{1}{6} m_2 l_1^{\,2} \dot{\theta}_1^{\,2} + \frac{1}{2} m_3 l_1^{\,2} \dot{\theta}_1^{\,2} + \frac{1}{2} m_4 l_1^{\,2} \dot{\theta}_1^{\,2} + \frac{1}{6} m_4 l_{41}^{\,2} \dot{\theta}_2^{\,2} \\
&= \left(\frac{1}{2} m_a + \frac{1}{6} m_1 + \frac{1}{6} m_2 + \frac{1}{2} m_3 + \frac{1}{2} m_4 \right) l_1^{\,2} \dot{\theta}_1^{\,2} \\
&\quad + \left(\frac{1}{2} m_a + \frac{1}{6} m_4 \right) l_{42}^{\,2} \dot{\theta}_2^{\,2} + m_a l_1 l_{42} \dot{\theta}_1 \dot{\theta}_2 Cos\left(\theta_1 - \theta_2 \right) \\
&= \left(\frac{1}{2} m_a + \frac{1}{3} m_1 + \frac{1}{2} m_3 + \frac{1}{2} m_4 \right) l_1^{\,2} \dot{\theta}_1^{\,2} + \left(\frac{1}{2} m_a + \frac{1}{6} m_4 \right) l_{42}^{\,2} \dot{\theta}_2^{\,2} \\
&\quad + m_a l_1 l_{41} \dot{\theta}_1 \dot{\theta}_2 Cos\left(\theta_1 - \theta_2 \right)
\end{aligned} \tag{2.15}$$

There are two kinds of potential energy considered here, gravitational potential energy and elastic potential energy due to the spring. The total potential energy is as follows:

$$P.E. = P.E._{grav} + P.E._{spring} = \sum_{i=1}^{4} m_i g h_{yi} + \sum_{n=1}^{2} \frac{1}{2} K_n \left(x_n - x_{n0} \right)^2 \quad (2.16)$$

Where h_{yi} is the height of the center of mass of link # i, K_n is the spring constant is spring # n, x_n is the length of the spring # n after elongation and x_{n0} is the original length of the spring # n.

The total gravitational potential energy of the links and test article is given:

$$P.E._{grav} = \left(\frac{1}{2} w_1 + \frac{1}{2} w_2 + w_3 + w_4 + w_a \right) l_1 Sin\theta_1 + \left(w_2 + \frac{1}{2} w_3 + w_4 + w_a \right) l_3 + w_a l_{42} Sin\theta_2 \quad (2.17)$$

The elastic potential energy of the elastic spring is given by:

$$P.E._{spring} = \frac{1}{2} K_1 \left(x_1 - x_{10} \right)^2 + \frac{1}{2} K_2 \left(x_2 - x_{20} \right)^2 \quad (2.18)$$

Since all the springs have zero free-length, x_{n0} equals to zero, so that x_1 and x_2 equal l_{s1}, l_{s2} respectively. From the law of cosines:

$$l_{s1} = \left[{l_{k1}}^2 + {l_1}^2 - 2 l_{k1} l_1 Sin\theta_1 \right]^{1/2}, \; l_{s2} = \left[{l_{k2}}^2 + {l_{41}}^2 - 2 l_{k2} l_{41} Sin\theta_2 \right]^{1/2} \quad (2.19)$$

Equation (2.18) can be shown to be:

$$P.E._{spring} = \frac{1}{2} K_1 \left[{l_{k1}}^2 + {l_1}^2 - 2 l_{k1} l_1 Sin\theta_1 \right] + \frac{1}{2} K_2 \left[{l_{k2}}^2 + {l_{41}}^2 - 2 l_{k2} l_{41} Sin\theta_2 \right] \quad (2.20)$$

Lagrange equation without force and moment takes the form:

$$\frac{d}{dt}\left(\frac{\partial L}{\partial \dot{q}_i}\right)-\frac{\partial L}{\partial q_i}=0 \qquad q_1=\theta_1,\ \ q_2=\theta_2 \qquad L=T-V \tag{2.21}$$

Where T is the total kinetic energy of the system, V is the total potential energy which includes the gravitational and elastic contributions.

$$\begin{aligned} L &= T-V = K.E.-P.E. \\ &= \left(\frac{1}{2}m_a+\frac{1}{6}m_1+\frac{1}{6}m_2+\frac{1}{2}m_3+\frac{1}{2}m_4\right)l_1^{\,2}\dot{\theta}_1^{\,2}+\left(\frac{1}{2}m_A+\frac{1}{6}m_4\right)l_{42}^{\,2}\dot{\theta}_2^{\,2} \\ &\quad + m_A l_1 l_{41}\dot{\theta}_1\dot{\theta}_2 Cos\left(\theta_1-\theta_2\right)-\left(\frac{1}{2}w_1+\frac{1}{2}w_2+w_3+w_4+w_a\right)l_1 Sin\theta_1 \\ &\quad -\left(w_2+\frac{1}{2}w_3+w_4+w_a\right)l_3-w_a l_{42}Sin\theta_2-\frac{1}{2}k_1\left[l_{k1}^{\,2}+l_1^{\,2}-2l_{k1}l_1 Sin\theta_1\right] \\ &\quad -\frac{1}{2}k_2\left[l_{k2}^{\,2}+l_{41}^{\,2}-2l_{k2}l_{41}Sin\theta_2\right] \end{aligned} \tag{2.22}$$

For generalized coordinates θ_1, Lagrange's equation is as follows:

$$\begin{aligned} \frac{d}{dt}\left(\frac{\partial L}{\partial \dot{\theta}_1}\right)-\frac{\partial L}{\partial \theta_1} &= \left(m_a+\frac{1}{3}m_1+\frac{1}{3}m_2+m_3+m_4\right)l_1^{\,2}\ddot{\theta}_1+m_a l_1 l_{42}\ddot{\theta}_2 Cos\left(\theta_1-\theta_2\right) \\ &\quad + m_a l_1 l_{42}\dot{\theta}_2^{\,2}Sin\left(\theta_1-\theta_2\right)+\left(\frac{1}{2}w_1+\frac{1}{2}w_2+w_3+w_4+w_a\right)l_1 Cos\theta_1 \\ &\quad - k_1 l_{k1} l_1 Cos\theta_1 \end{aligned} \tag{2.23}$$

For generalized coordinates θ_2, Lagrange's equation can be shown as:

$$\begin{aligned} \frac{d}{dt}\left(\frac{\partial L}{\partial \dot{\theta}_2}\right)-\frac{\partial L}{\partial \theta_2} &= \left(m_a+\frac{1}{3}m_4\right)l_{42}^{\,2}\ddot{\theta}_2+m_a l_1 l_{42}\ddot{\theta}_1 Cos\left(\theta_1-\theta_2\right) \\ &\quad - m_a l_1 l_{42}\dot{\theta}_1^{\,2}Sin\left(\theta_1-\theta_2\right)+w_A l_{42}Cos\theta_2-k_2 l_{k2} l_{42}Cos\theta_2 \end{aligned} \tag{2.24}$$

Equations (2.23) and (2.24) can be expressed in the state space form:

$$\begin{bmatrix} A_{11} & A_{12} \\ A_{21} & A_{22} \end{bmatrix} \dot{X} = \begin{bmatrix} 0 & \mathrm{B}_{12} \\ \mathrm{B}_{21} & 0 \end{bmatrix} X^2 + \begin{bmatrix} D_1 \\ D_2 \end{bmatrix} \qquad X = \begin{bmatrix} \dot{\theta}_1 \\ \dot{\theta}_2 \end{bmatrix} \qquad \dot{X} = \begin{bmatrix} \ddot{\theta}_1 \\ \ddot{\theta}_2 \end{bmatrix} \tag{2.25}$$

Where:

$$A_{11} = \left(m_a + \frac{1}{3} m_1 + \frac{1}{3} m_2 + m_3 + m_4 \right) l_1^{\,2}$$
$$A_{12} = m_a l_1 l_{41} Cos\left(\theta_1 - \theta_2\right)$$
$$A_{21} = m_a l_1 l_{41} Cos\left(\theta_1 - \theta_2\right)$$
$$A_{22} = \left(m_a + \frac{1}{3} m_4 \right) l_{41}^{\,2}$$
$$\mathrm{B}_{12} = -m_a l_1 l_{41} Sin\left(\theta_1 - \theta_2\right)$$
$$\mathrm{B}_{21} = m_a l_1 l_{41} Sin\left(\theta_1 - \theta_2\right)$$
$$D_1 = -\left(\frac{1}{2} w_1 + \frac{1}{2} w_2 + w_3 + w_4 + w_a \right) l_1 Cos\theta_1 + k_1 l_{k1} l_1 Cos\theta_1$$
$$D_2 = -w_a l_{42} Cos\theta_2 + k_2 l_{k2} l_{42} Cos\theta_2$$

If the linkage is massless, the whole equations can be simplified as:

$$\begin{bmatrix} A_{11} & A_{12} \\ A_{21} & A_{22} \end{bmatrix} \dot{X} = \begin{bmatrix} 0 & \mathrm{B}_{12} \\ \mathrm{B}_{21} & 0 \end{bmatrix} X^2 + \begin{bmatrix} D_1 \\ D_2 \end{bmatrix} \qquad X = \begin{bmatrix} \dot{\theta}_1 \\ \dot{\theta}_2 \end{bmatrix} \qquad \dot{X} = \begin{bmatrix} \ddot{\theta}_1 \\ \ddot{\theta}_2 \end{bmatrix} \tag{2.26}$$

Where:

$$A_{11} = m_a l_1^{\,2}$$
$$A_{12} = m_a l_1 l_{42} Cos\left(\theta_1 - \theta_2\right)$$
$$A_{21} = m_a l_1 l_{42} Cos\left(\theta_1 - \theta_2\right)$$
$$A_{22} = m_a l_{42}^{\,2}$$
$$\mathrm{B}_{12} = -m_a l_1 l_{41} Sin\left(\theta_1 - \theta_2\right)$$
$$\mathrm{B}_{21} = m_a l_1 l_{41} Sin\left(\theta_1 - \theta_2\right)$$
$$D_1 = -w_a l_1 Cos\theta_1 + k_1 l_{k1} l_1 Cos\theta_1$$
$$D_2 = -w_a l_{42} Cos\theta_2 + k_2 l_{k2} l_{42} Cos\theta_2$$

The matrix equation (2.25) is the dynamic equation for a real system, where the mass of the linkage is considered. For the ideal case where in the mass of the links are neglected, the governing equations of system dynamics are given by the matrix equation (2.26). In the following simulation, the system dynamics described by Eq. (2.25) is called in dynamic condition" and the dynamics described by Eq. (2.26) is referred to as in kinematic condition.

2.2.2 Initial Condition for Impulsive Force

Impulsive force just exists for a very short time and the mass of linkage also absorbs part of that impulsive force, so that there should be noticeable difference between the real (with linkage inertia), and the ideal case (without linkage inertia) in the collision angle of the impulse and the initial moving angle of the test article. In the following discussion, the initial condition of the real case (linkage has mass) will be called the kinetic initial condition, and the initial condition of the ideal case (linkage is massless) will be called the kinematic initial condition.

First, the kinetic initial condition is determined by Lagrange's impulsive equation. It is a special form of Lagrange's equation which the derivative of momentum is reduced to momentum itself and force is reduced to impulse. It takes the form:

$$\frac{\partial T}{\partial \dot{q}_i} = \sum_{j=1}^{n} \vec{P}_j \bullet \frac{\partial \vec{R}_j}{\partial q_i} \qquad q_1 = \theta_1, \;\; q_2 = \theta_2 \tag{2.27}$$

Here the $\vec{P}$ denotes the impulsive force applied to the test article with $\vec{P} = \vec{F} \bullet \Delta t$.

Where:

$$\vec{P} = P \bullet Cos\alpha_P \hat{i} + P \bullet Sin\alpha_P \hat{j} \tag{2.28}$$

$\vec{R}_a$ is the position vector of the test article and is given by Eq. (2.14):

$$\vec{R}_a = \left(l_1 Cos\theta_1 + l_{42} Cos\theta_2\right)\hat{i} + \left(l_1 Sin\theta_1 + l_3 + l_{42} Sin\theta_2\right)\hat{j}$$

$\hat{i}$ and $\hat{j}$ are the unit vectors in X and Y directions respectively.

The LHS of Eq. (2.27) is given by:

$$\begin{aligned} \frac{\partial T}{\partial \dot{\theta}_1} &= \left(m_a + \frac{1}{3}m_1 + \frac{1}{3}m_2 + m_3 + m_4\right) l_1{}^2 \dot{\theta}_1 + m_a l_1 l_{41} \dot{\theta}_2 Cos\left(\theta_1 - \theta_2\right) \\ \frac{\partial T}{\partial \dot{\theta}_2} &= \left(m_a + \frac{1}{3}m_4\right) l_{42}{}^2 \dot{\theta}_2 + m_a l_1 l_{42} \dot{\theta}_1 Cos\left(\theta_1 - \theta_2\right) \end{aligned} \tag{2.29}$$

The second terms on the RHS of the Eq. (2.27) is given by:

$$\begin{aligned} \frac{\partial \vec{R}_a}{\partial \theta_1} &= -l_1 Sin\theta_1 \hat{i} + l_1 Cos\theta_1 \hat{j} \\ \frac{\partial \vec{R}_a}{\partial \theta_2} &= -l_{42} Sin\theta_2 \hat{i} + l_{42} Cos\theta_2 \hat{j} \end{aligned} \tag{2.30}$$

The RHS of Eq. (2.27) can be shown to be:

$$\begin{aligned} \vec{P} \bullet \frac{\partial \vec{R}_a}{\partial \theta_1} &= -Pl_1 Cos\alpha_P Sin\theta_1 + Pl_1 Sin\alpha_P Cos\theta_1 \\ \vec{P} \bullet \frac{\partial \vec{R}_a}{\partial \theta_2} &= -Pl_{42} Cos\alpha_P Sin\theta_2 + Pl_{42} Sin\alpha_P Cos\theta_2 \end{aligned} \tag{2.31}$$

Using Eq. (2.29) and Eq. (2.31), Lagrange's Impulsive equation is given by:

$$\left(m_a+\frac{1}{3}m_1+\frac{1}{3}m_2+m_3+m_4\right)l_1^{\,2}\dot{\theta}_1+m_a l_1 l_{41}\dot{\theta}_2 Cos\left(\theta_1-\theta_2\right)=-Pl_1 Cos\alpha_P Sin\theta_1 + Pl_1 Sin\alpha_P Cos\theta_1 \qquad (2.32)$$

$$\left(m_a+\frac{1}{3}m_4\right)l_{42}^{\,2}\dot{\theta}_2+m_a l_1 l_{42}\dot{\theta}_1 Cos\left(\theta_1-\theta_2\right)=-Pl_{42} Cos\alpha_P Sin\theta_2+Pl_{42} Sin\alpha_P Cos\theta_2$$

Let Eq. (2.32) be expressed as:

$$C_1\dot{\theta}_1+C_2\dot{\theta}_2=Q_1$$

$$C_3\dot{\theta}_1+C_4\dot{\theta}_2=Q_2$$

Thus, the initial angular velocity, $\dot{\theta}_1$ and $\dot{\theta}_2$, can be determined and represent in the form:

$$\dot{\theta}_1=\frac{C_4Q_1-C_2Q_2}{C_1C_4-C_2C_3}$$
$$\dot{\theta}_2=\frac{C_3Q_1-C_1Q_2}{C_2C_3-C_1C_4} \qquad (2.33)$$

Then the direction of motion of the test article can be found by the Eq. (2.14):

$$\alpha_{Vimpact}=\tan^{-1}\left(\frac{l_1\dot{\theta}_1 Cos\theta_1+l_{42}\dot{\theta}_2 Cos\theta_2}{-l_1\dot{\theta}_1 Sin\theta_1-l_{42}\dot{\theta}_2 Sin\theta_2}\right) \qquad (2.34)$$

Though the value of arctan is between $\pm\frac{\pi}{2}$, the appropriate value of the angle can be selected by the impact angle.

Next, the kinematic initial condition is considered. If the linkage has no mass, the angle of the impulse applied, α_P, is the same as the angle of the motion of the test article, α_V. The velocity vector of the test article in generalized coordinates, θ_1 and θ_2, is given by Eq. (2.14) :

$$\vec{V}_a=\left(-l_1\dot{\theta}_1 Sin\theta_1-l_{42}\dot{\theta}_2 Sin\theta_2\right)\hat{i}+\left(l_1\dot{\theta}_1 Cos\theta_1+l_{42}\dot{\theta}_2 Cos\theta_2\right)\hat{j}$$

Since $\vec{P} = m_a \vec{V}_a$, the kinematic initial condition, $\dot{\theta}_1$ and $\dot{\theta}_2$, can be determined by solving the following equations:

$$\begin{aligned} \frac{P \bullet Cos\alpha_P}{m_a} &= -l_1 \dot{\theta}_1 Sin\theta_1 - l_{42} \dot{\theta}_2 Sin\theta_2 \\ \frac{P \bullet Sin\alpha_P}{m_a} &= l_1 \dot{\theta}_1 Cos\theta_1 + l_{42} \dot{\theta}_2 Cos\theta_2 \end{aligned} \tag{2.35}$$

Then the kinematic initial condition is obtained by solving Eq. (2.35):

$$\begin{aligned} \dot{\theta}_1 &= -\frac{PCos(\alpha_P - \theta_2)}{m_a l_1 Sin(\theta_1 - \theta_2)} \\ \dot{\theta}_2 &= \frac{PCos(\alpha_P - \theta_1)}{m_a l_{42} Sin(\theta_1 - \theta_2)} \end{aligned} \tag{2.36}$$

2.2.3 Simulation under Impulsive Force Applications

The simulation time, t_s, starts from zero and is stopped when any of the links hits the boundaries of the working space in the kinematic condition. The stopping criteria are:

$$-\frac{\pi}{2} \le \theta_1 \le \frac{\pi}{2} \quad \text{and} \quad \frac{\pi}{2} \le \theta_2 \le \pi + \theta_1 \tag{2.37}$$

Aluminium alloy 6063-T52 rectangular tube is chosen as the material of the linkage and the dimension is 2”x2” (width & height) and 1/4” in thickness. In the simulation, the impulsive force, 10 (kgm/s) in magnitude, is applied in various angles, α_P , from 90 degree to 270 degree in steps of 45 degree. More details of the system parameters setup for simulation are listed in the Table A.1. The working space of the device and the initial position of the test article are shown in Fig. 2.3

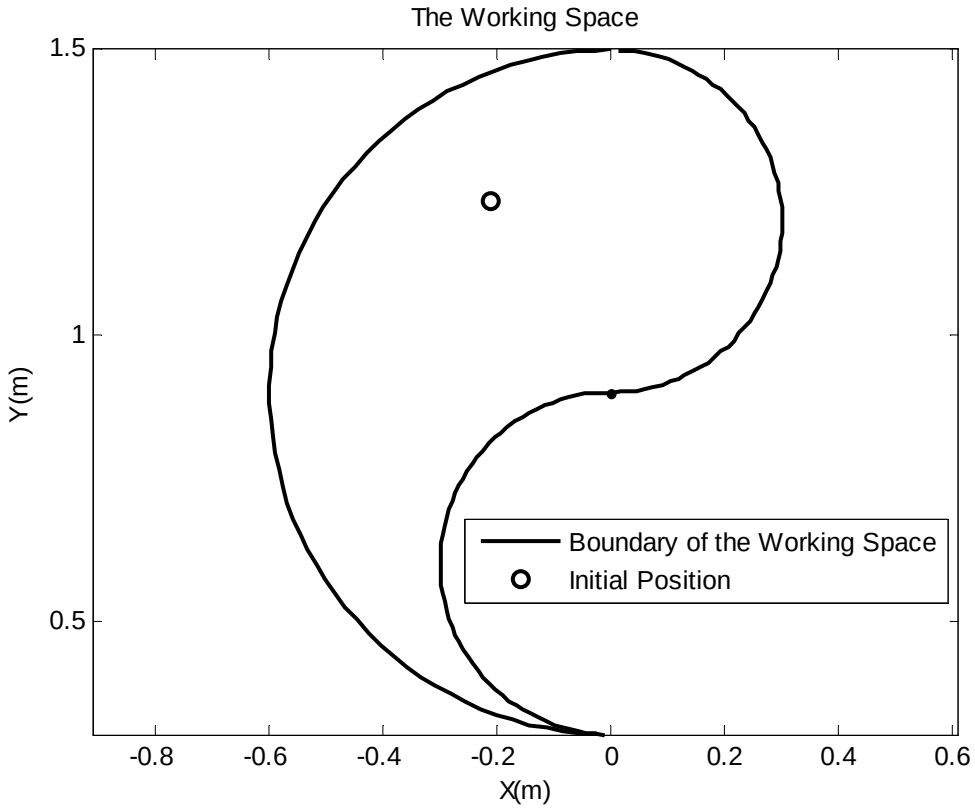

Fig. 2.3: The Boundary of the Working Space and the Initial Position of the Test Article

$(1)\,\alpha_P = \frac{\pi}{2}$

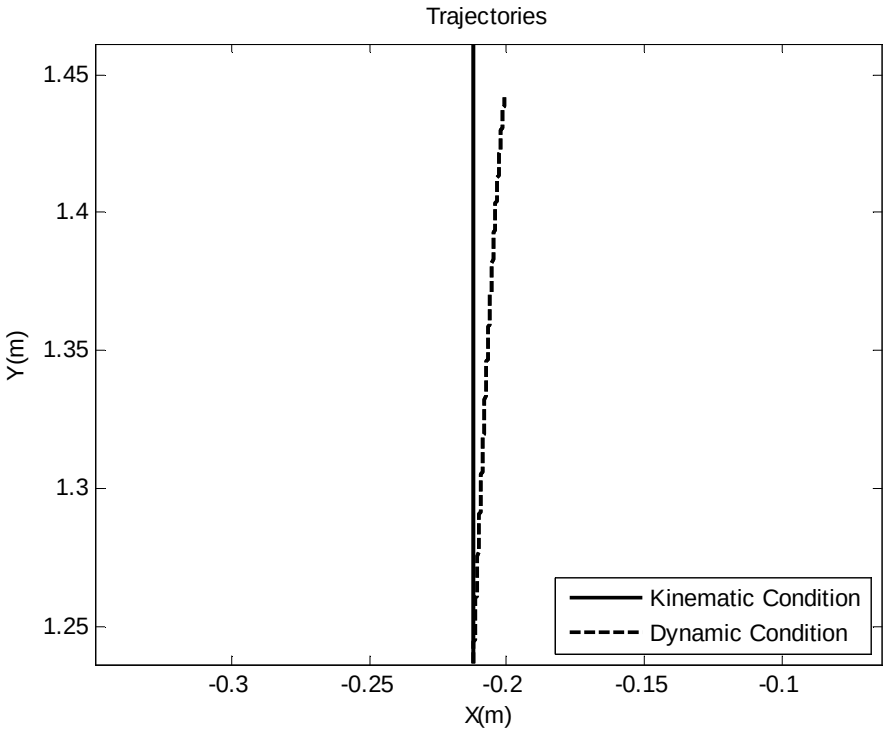

Fig. 2.4(a): Trajectories of the Test Article Due to an Impulsive Force Applied at 90 Degrees in Kinematic and Dynamic Condition

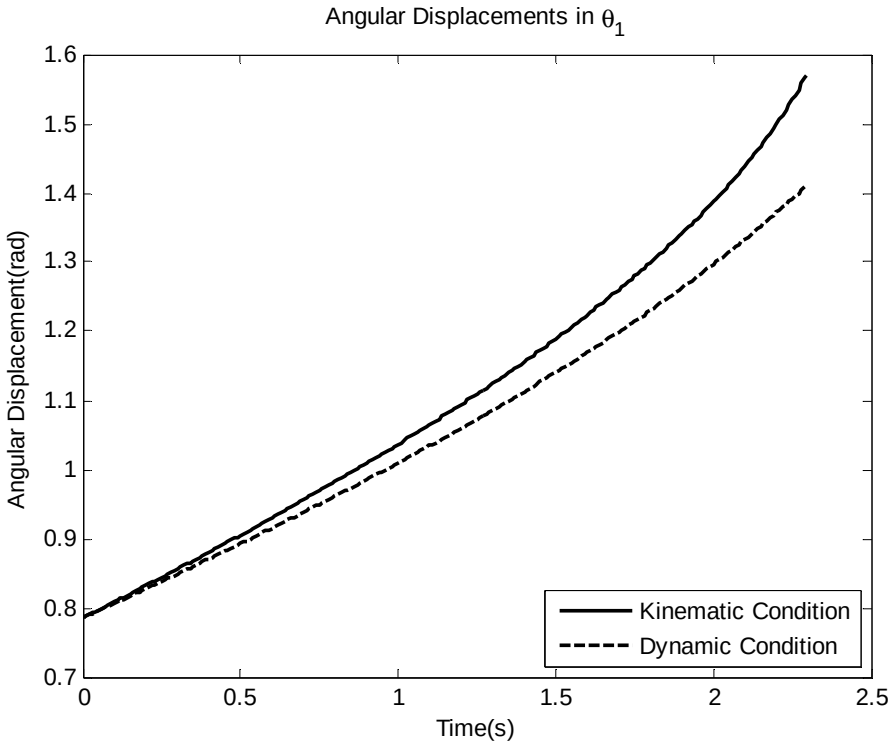

Fig. 2.4(b): Displacements of the Test Article in θ_1 Due to an Impulsive Force Applied at 90 Degrees in Kinematic and Dynamic Condition

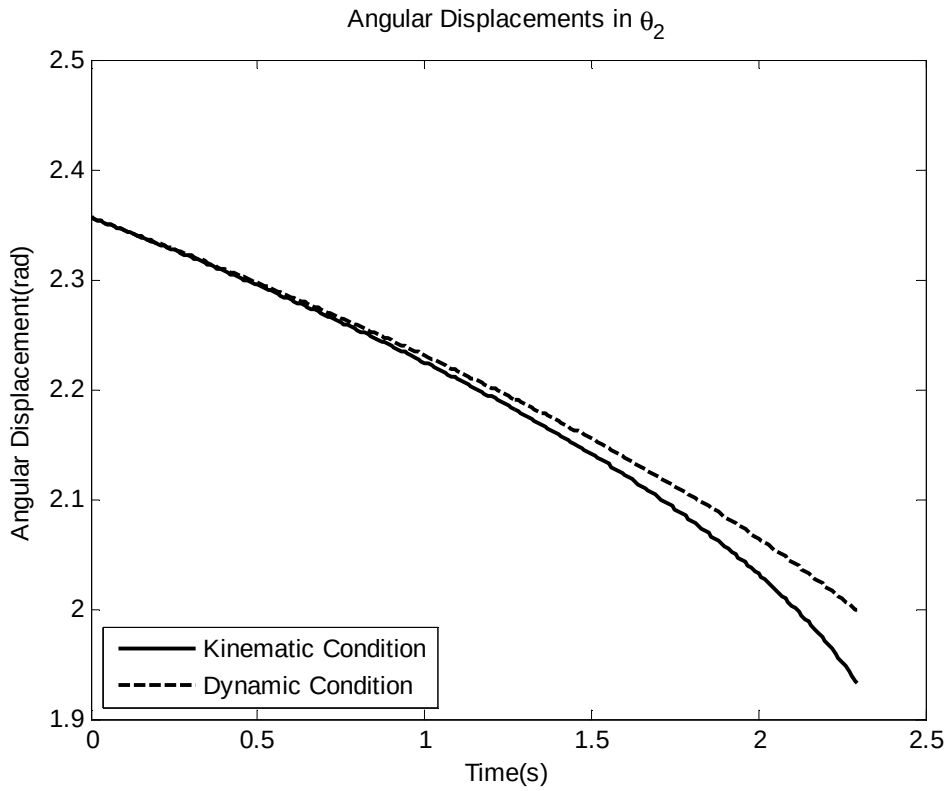

Fig. 2.4(c): Displacements of the Test Article in θ_2 Due to an Impulsive Force Applied at 90 Degrees in Kinematic and Dynamic Condition

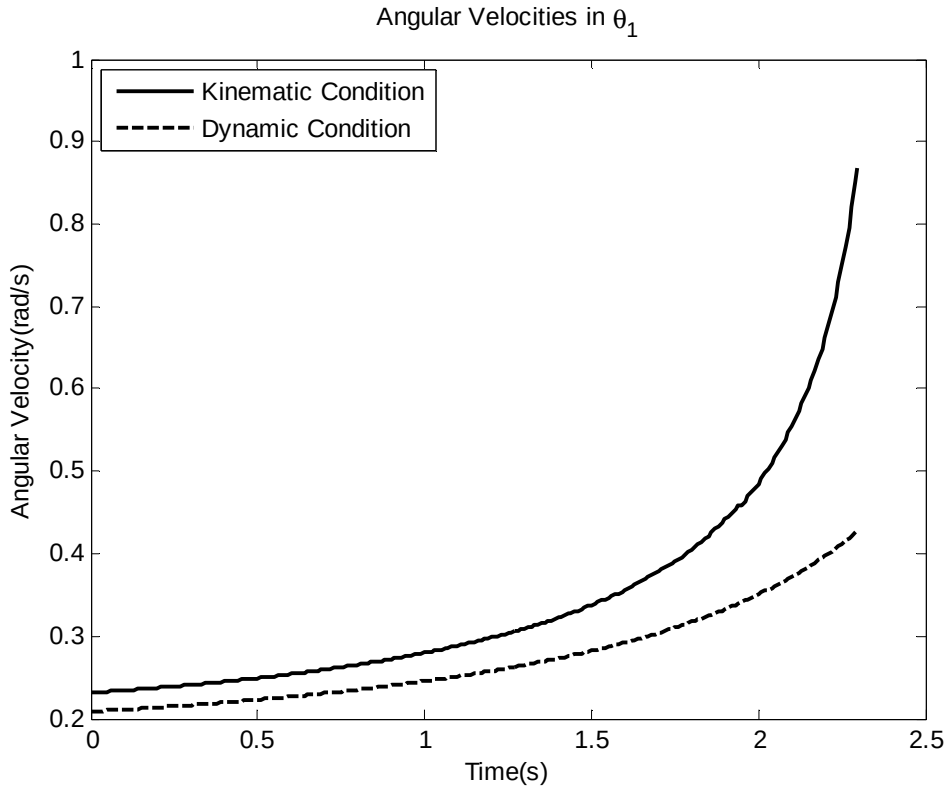

Fig. 2.4(d): Velocities of the Test Article in θ_1 Due to an Impulsive Force Applied at 90 Degrees in Kinematic and Dynamic Condition

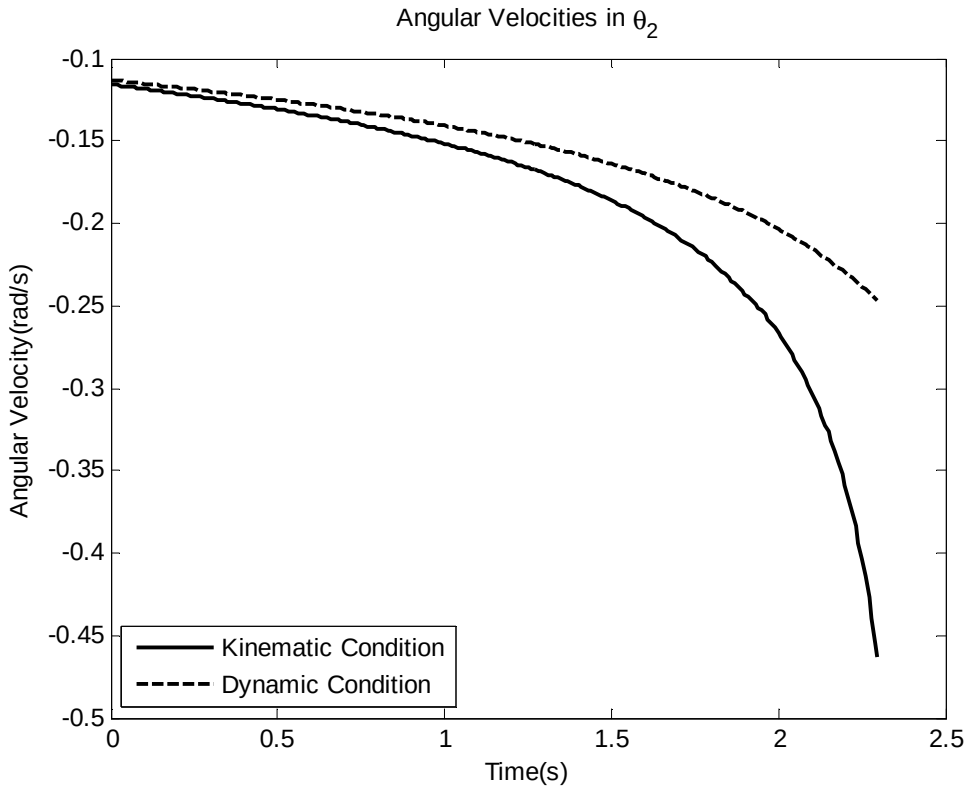

Fig. 2.4(e): Velocities of the Test Article in θ_2 Due to an Impulsive Force Applied at 90 Degrees in Kinematic and Dynamic Condition

Link #1 in kinematic mode hits the upper boundary, $\theta_1 = \frac{\pi}{2}$, after 2.29 seconds and the angle of motion in kinetic mode is 87.63 degree instead of 90 degree. In Fig. 2.4(d), it can be seen the small difference in the initial velocity of θ_1 which is due to the inertia of the parallelogram linkage absorbing some part of kinetic energy which is large enough to be reflected on the plot. In all the plots, it can be shown that how the inertia of the links compromises the performance of the device.

$(2)\alpha_P = \frac{3\pi}{4}$

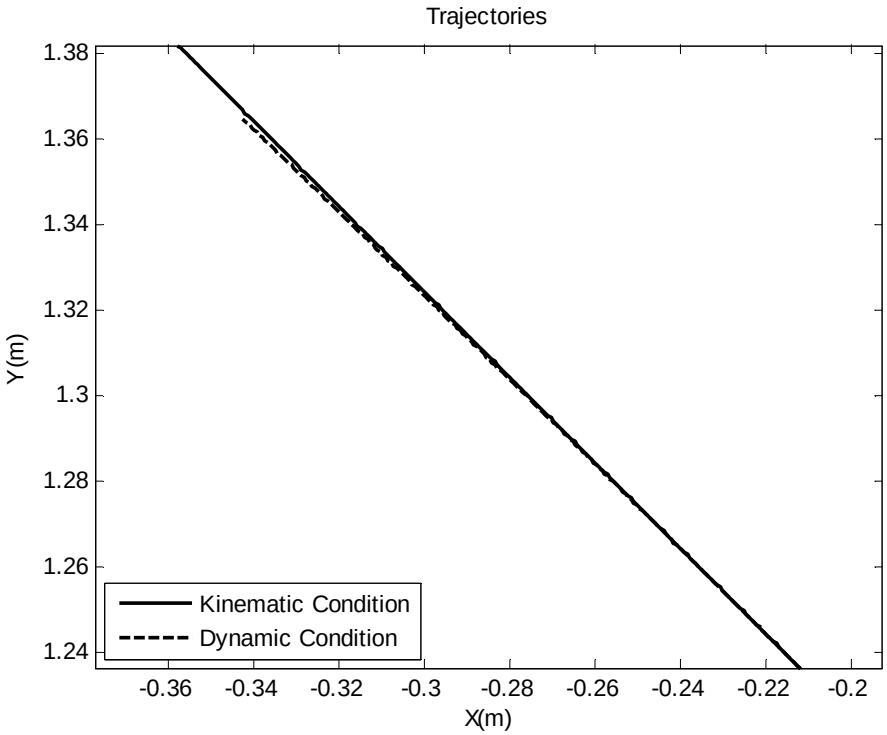

Fig. 2.5(a): Trajectories of the Test Article Due to an Impulsive Force Applied at 135 Degrees in Kinematic and Dynamic Condition

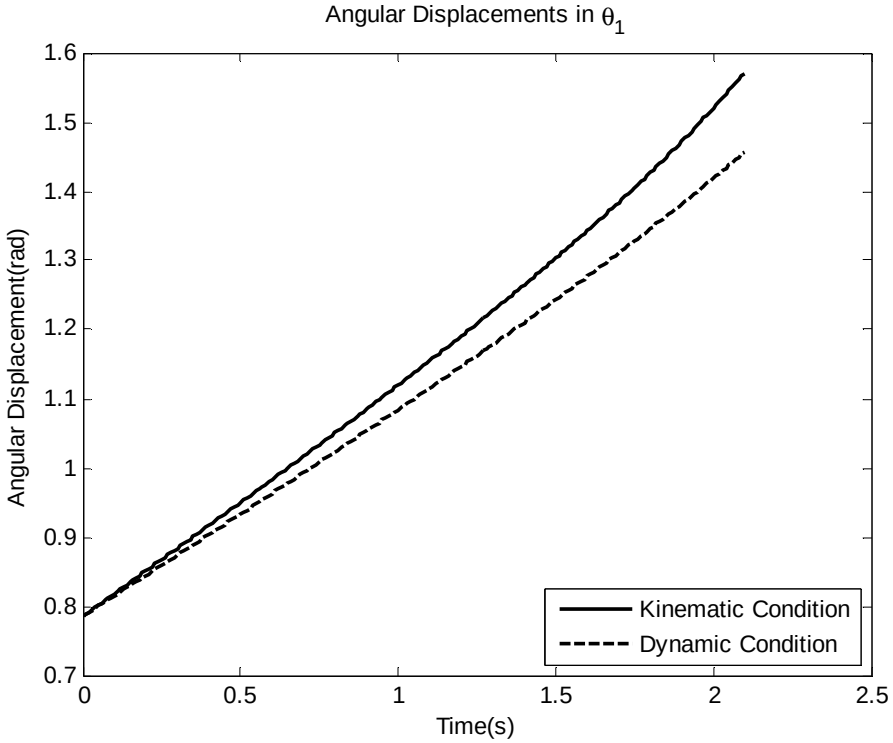

Fig. 2.5(b): Displacements of the Test Article in θ_1 Due to an Impulsive Force Applied at 135 Degrees in Kinematic and Dynamic Condition

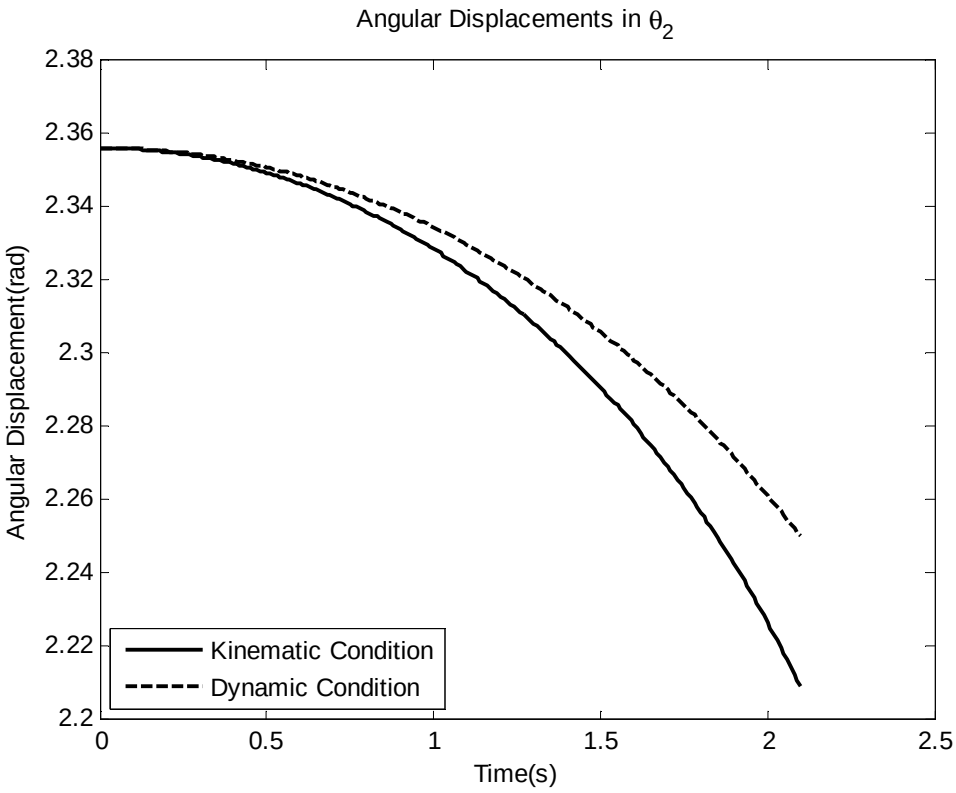

Fig. 2.5(c): Displacements of the Test Article in θ_2 Due to an Impulsive Force Applied at 135 Degrees in Kinematic and Dynamic Condition

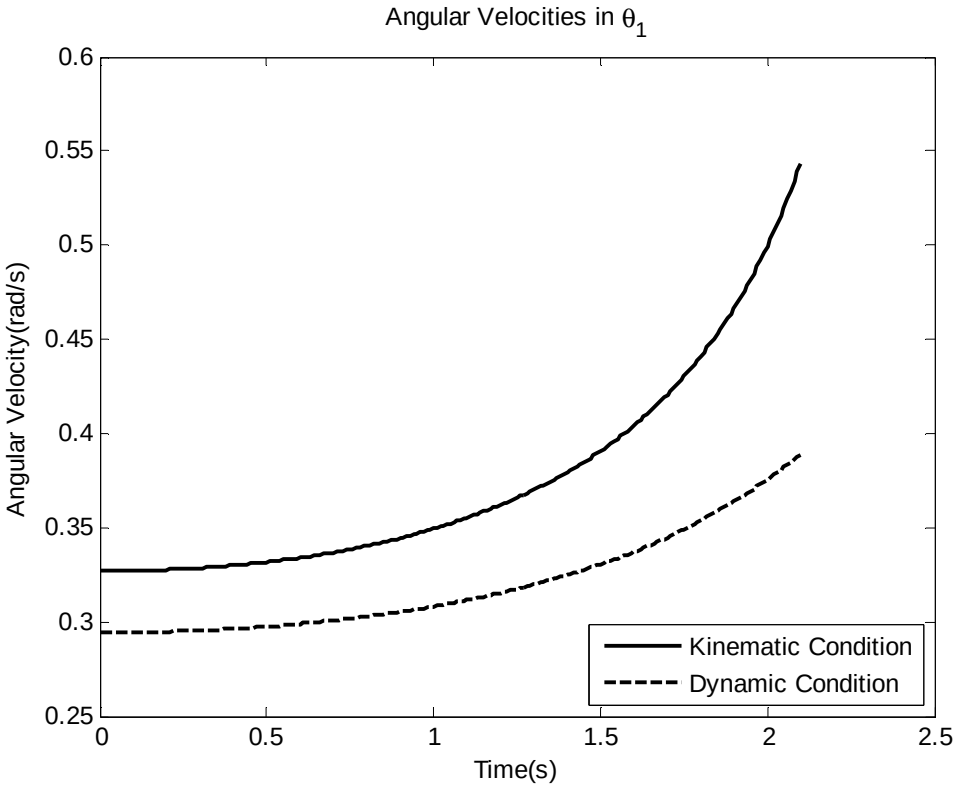

Fig. 2.5(d): Velocities of the Test Article in θ_1 Due to an Impulsive Force Applied at135 Degrees in Kinematic and Dynamic Condition

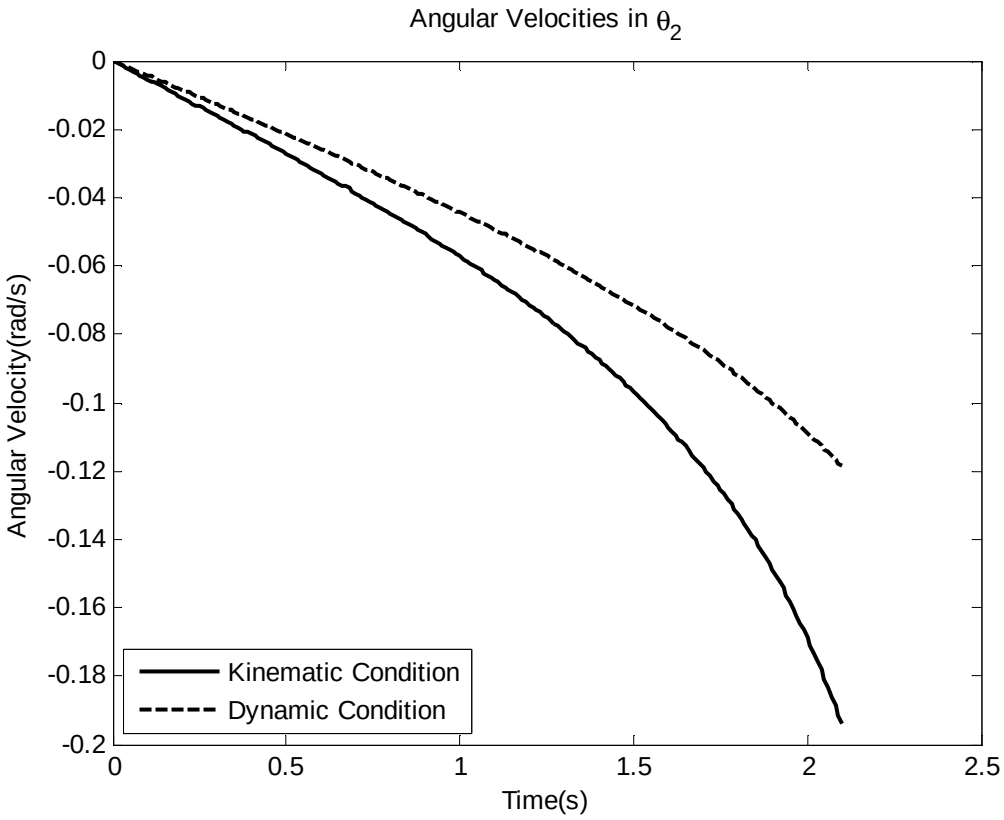

Fig. 2.5(e): Velocities of the Test Article in θ_2 Due to an Impulsive Force Applied at 135 Degrees in Kinematic and Dynamic Condition

Link #1 in kinematic mode hits the upper boundary, $\theta_1 = \frac{\pi}{2}$, after 2.10 seconds and the angle of motion in both modes are almost the same. In Fig. 2.5(d), the difference in the initial velocity of θ_1 gets larger compared with Fig 2.4(d). The reason is that applied impulse inclines with the parallelogram linkage at 45 degree and this makes more energy is absorbed.

$(3)\alpha_p = \pi$

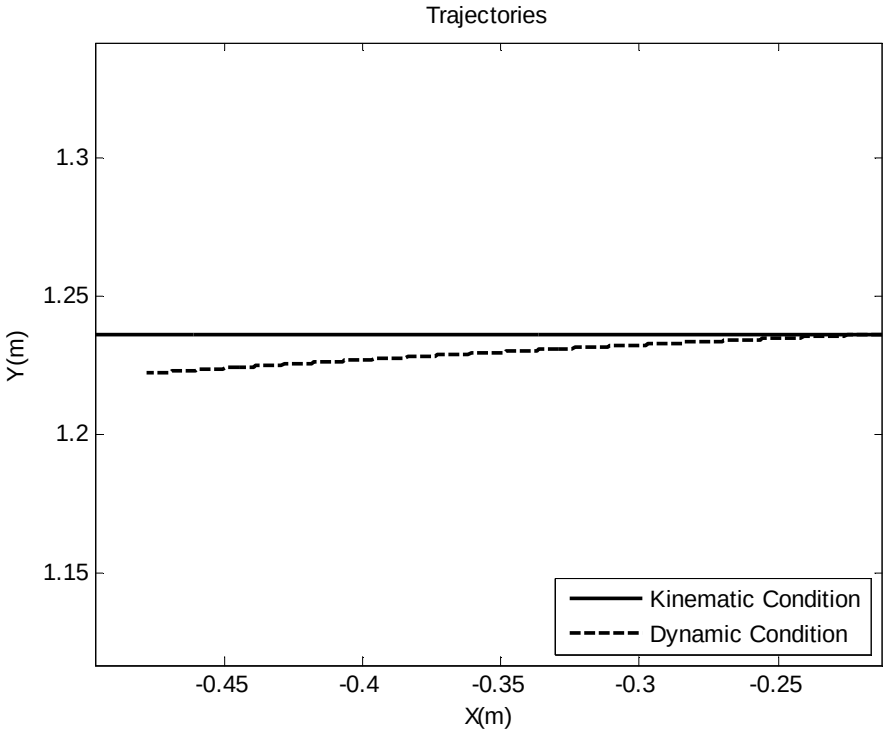

Fig. 2.6(a): Trajectories of the Test Article Due to an Impulsive Force Applied at 180 Degrees in Kinematic and Dynamic Condition

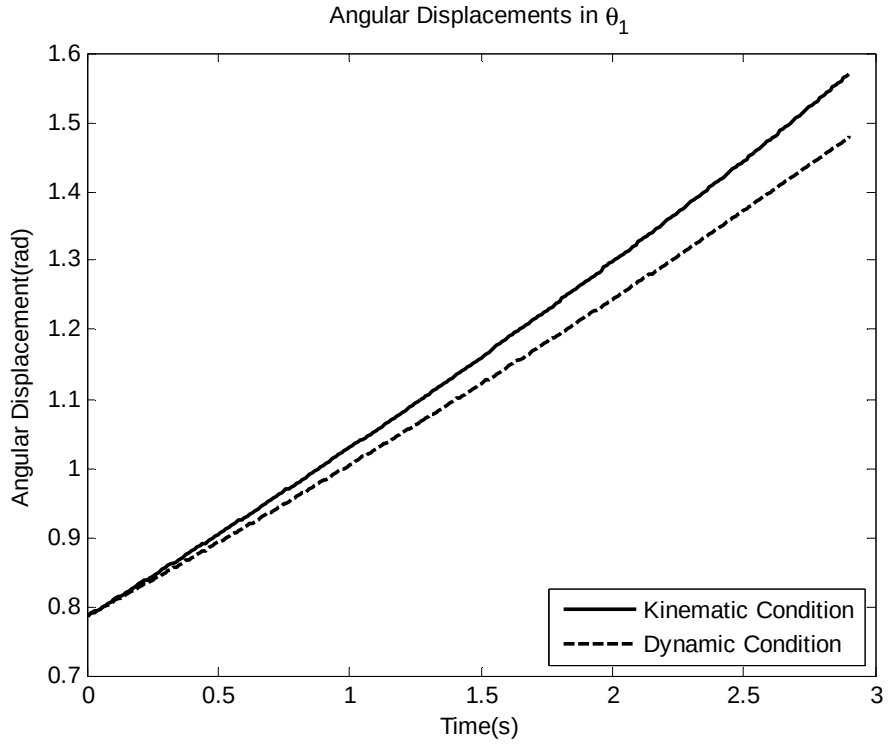

Fig. 2.6(b): Displacements of the Test Article in θ_1 Due to an Impulsive Force Applied at 180 Degrees in Kinematic and Dynamic Condition

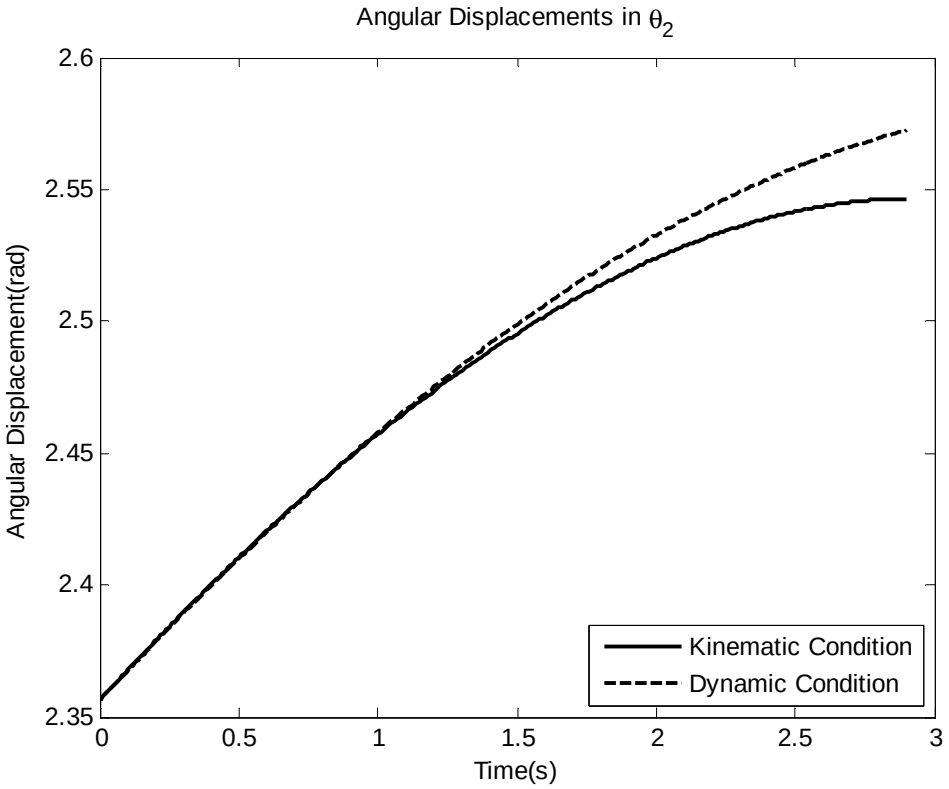

Fig. 2.6(c): Displacements of the Test Article in θ_2 Due to an Impulsive Force Applied at 180 Degrees in Kinematic and Dynamic Condition

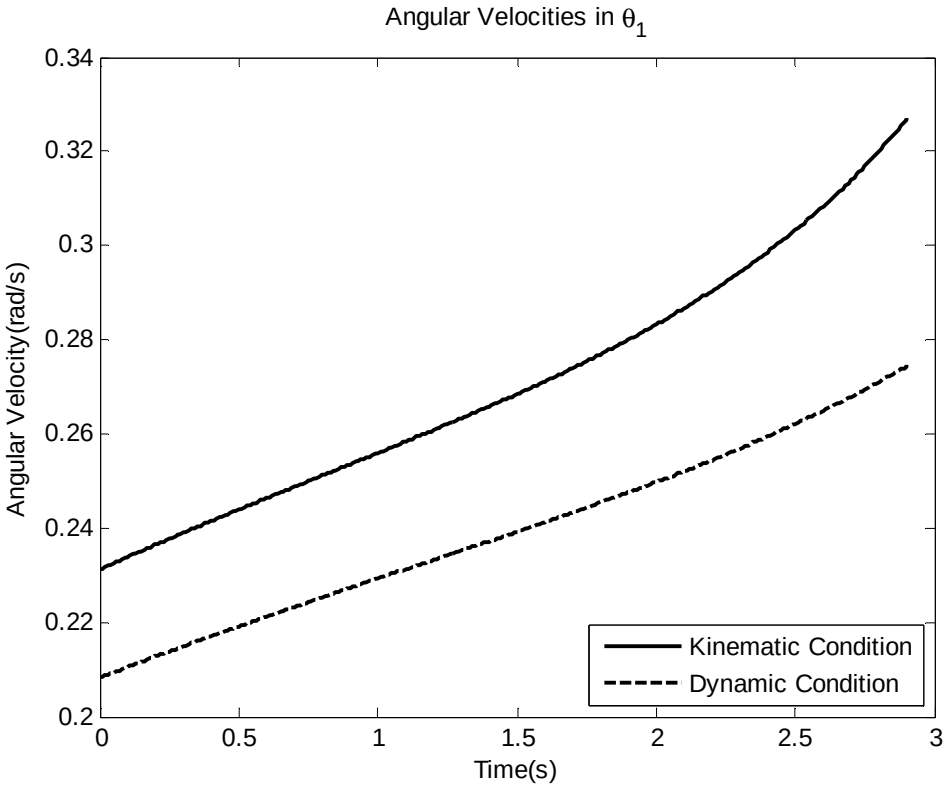

Fig. 2.6(d): Velocities of the Test Article in θ_1 Due to an Impulsive Force Applied at180 Degrees in Kinematic and Dynamic Condition

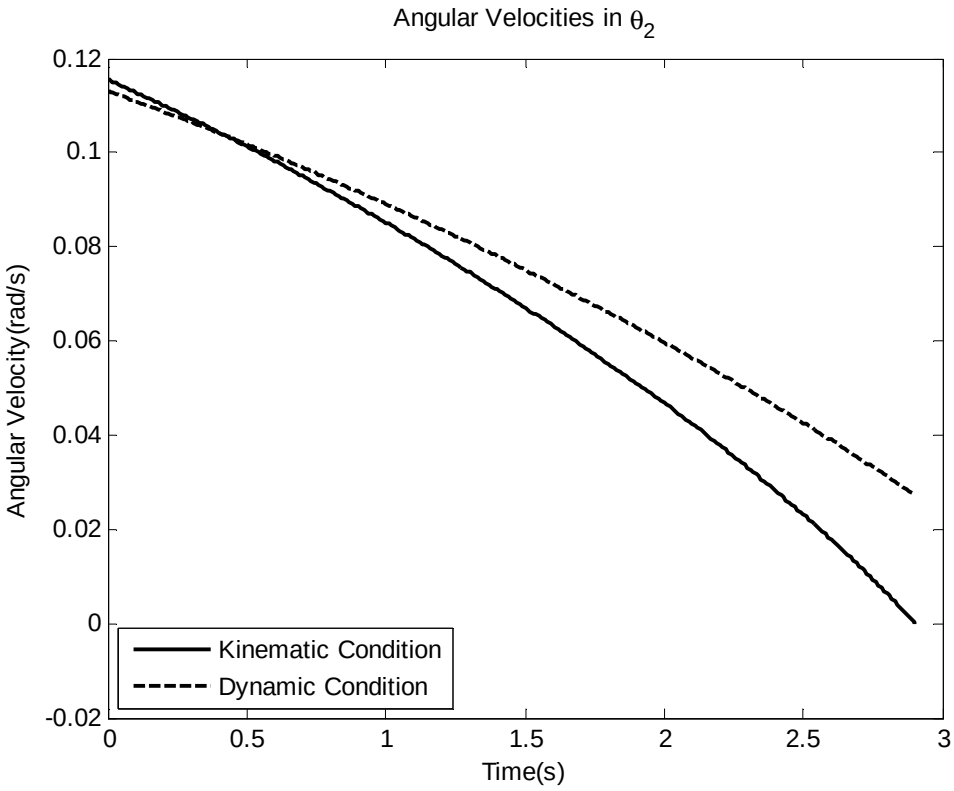

Fig. 2.6(e): Velocities of the Test Article in θ_2 Due to an Impulsive Force Applied at 180 Degrees in Kinematic and Dynamic Condition

Link #1 in kinematic mode hits the upper boundary, $\theta_1 = \frac{\pi}{2}$, after 2.90 seconds and the angle of motion in kinetic modes is 182.37 degree. In Fig. 2.6(d), the difference in the initial angular velocity can easily been seen. The motion in kinetic mode is slower then it in kinematic mode.

$(4)\,\alpha_P = \frac{5\pi}{4}$

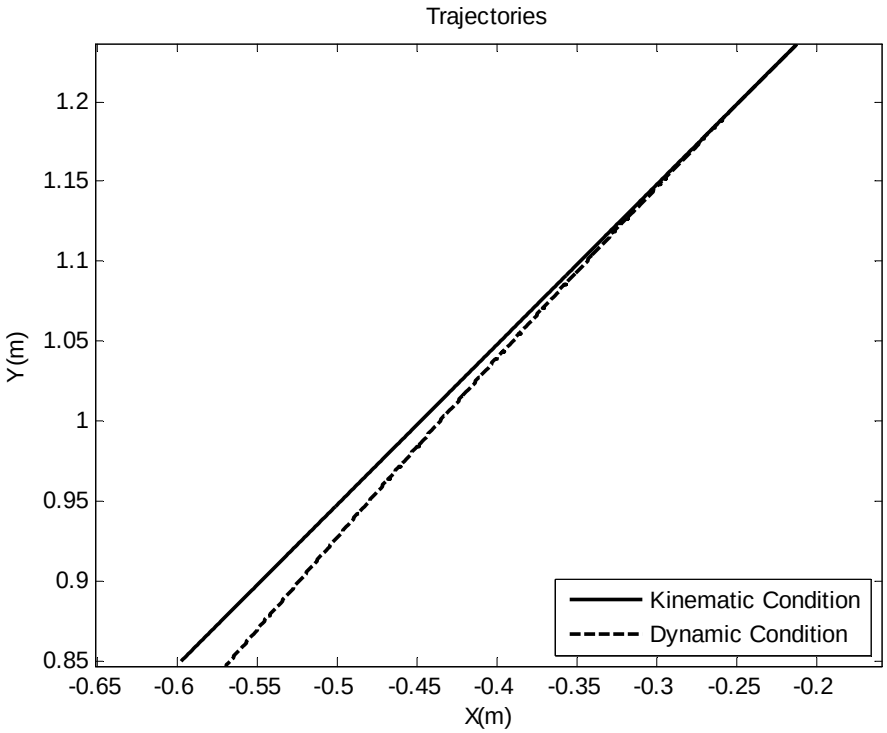

Fig. 2.7(a): Trajectories of the Test Article Due to an Impulsive Force Applied at 225 Degrees in Kinematic and Dynamic Condition

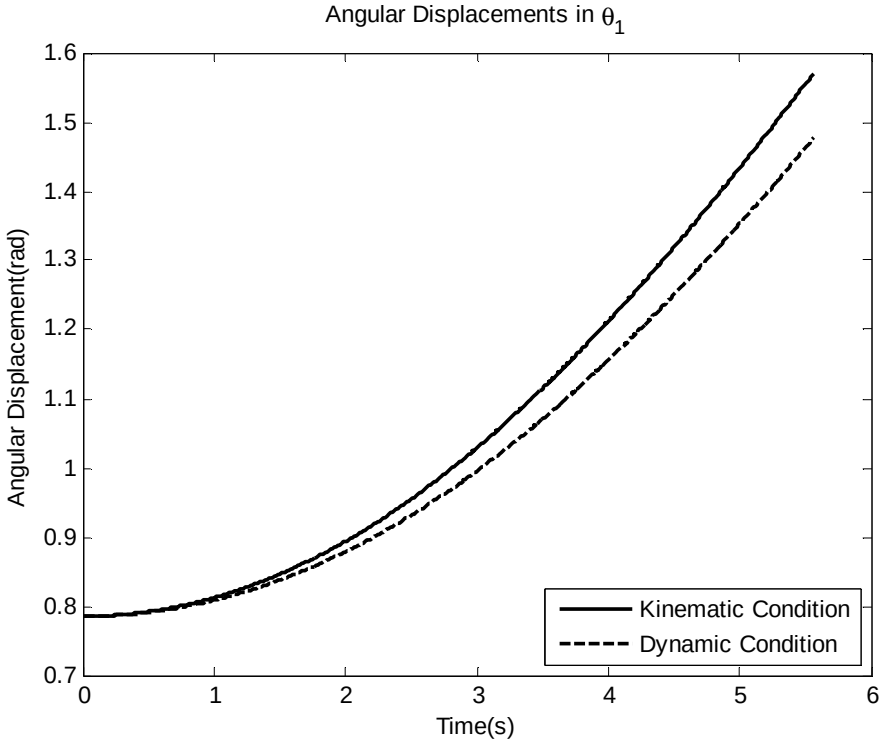

Fig. 2.7(b): Displacements of the Test article in θ_1 Due to an Impulsive Force Applied at 225 Degrees in Kinematic and Dynamic Condition

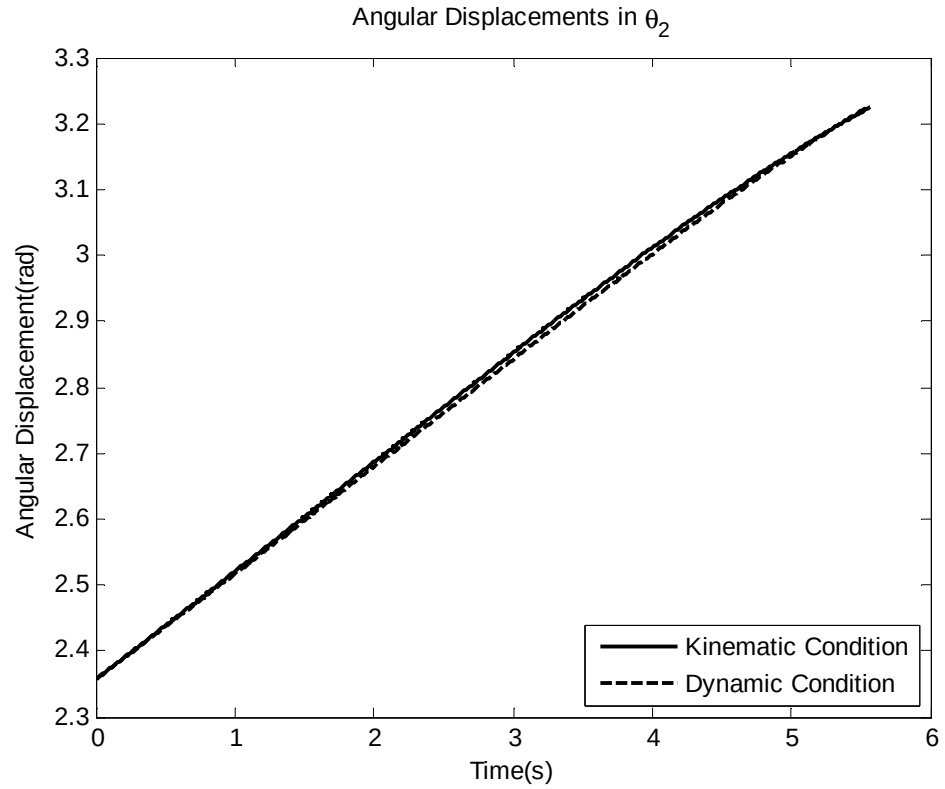

Fig. 2.7(c): Displacements of the Test Article in θ_2 Due to an Impulsive Force Applied at 225 Degrees in Kinematic and Dynamic Condition

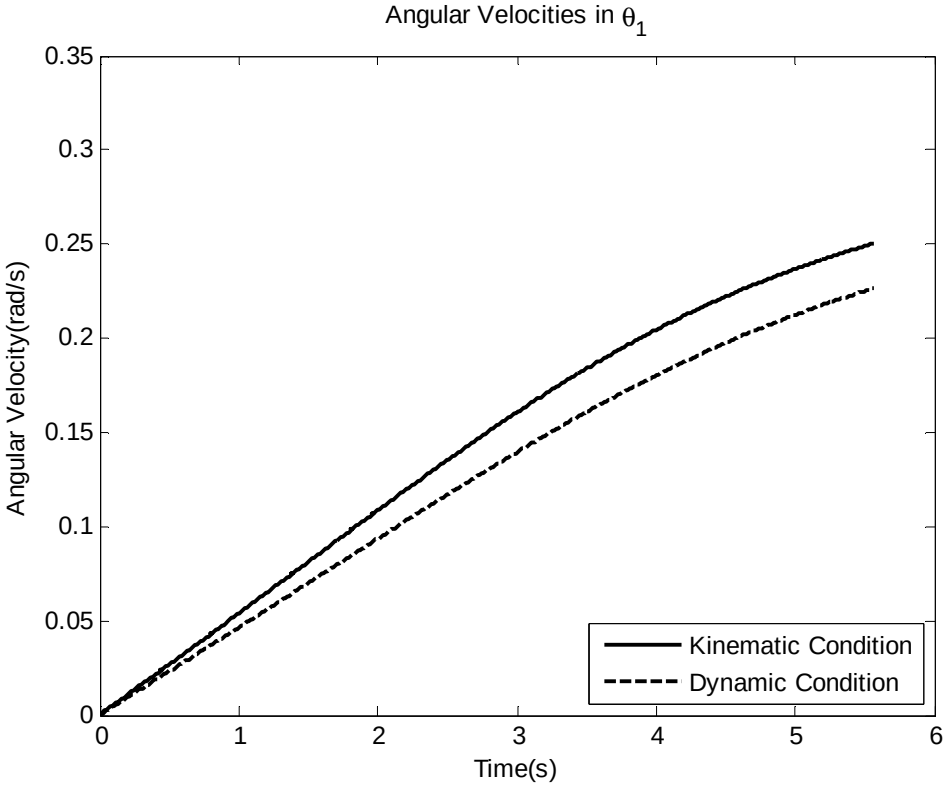

Fig. 2.7(d): Velocities of the Test Article in θ_1 Due to an Impulsive Force Applied at 225 Degrees in Kinematic and Dynamic Condition

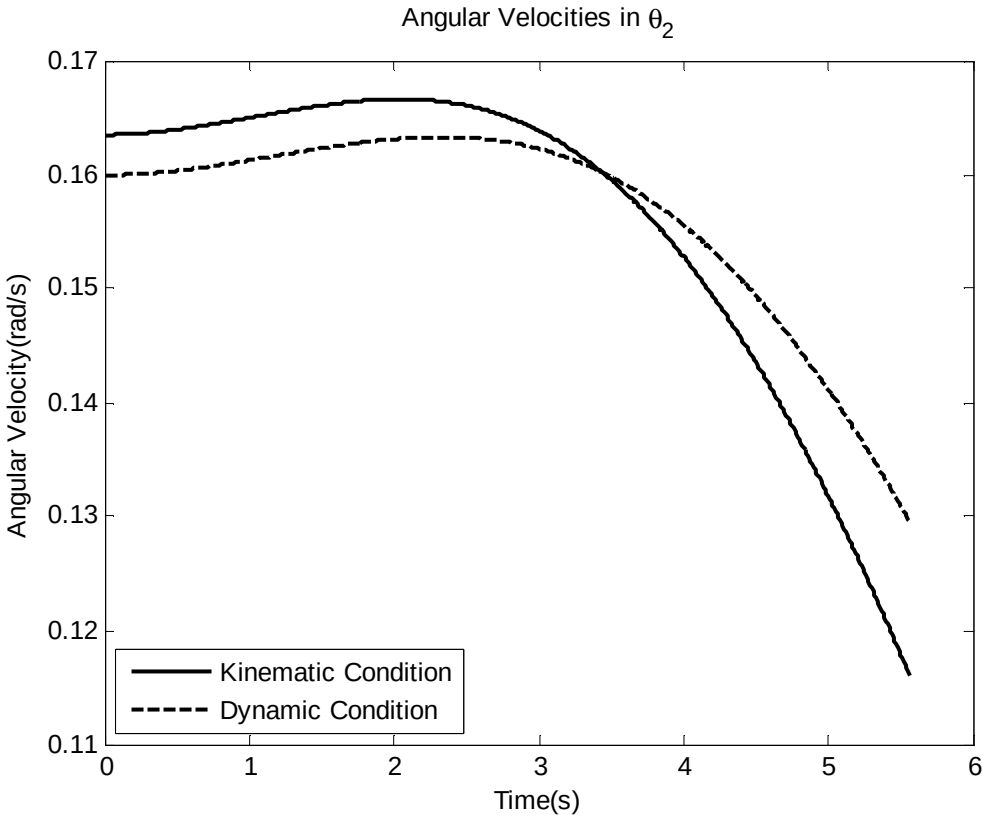

Fig. 2.7(e): Velocities of the Test Article in θ_2 Due to an Impulsive Force Applied at 225 Degrees in Kinematic and Dynamic Condition

Link #1 in kinematic mode hits the upper boundary, $\theta_1 = \frac{\pi}{2}$, after 5.56 seconds and the angle of motion after impact in both modes are almost the same. It is the longest stroke in the simulation that is why the position shift at the end is much more than the impulsive force applied in 135 degree. Considering the test article travels two times longer than in case #3, the position error at the end is half when compared with case #3.

$$(5)\ \alpha_P = \frac{3\pi}{2}$$

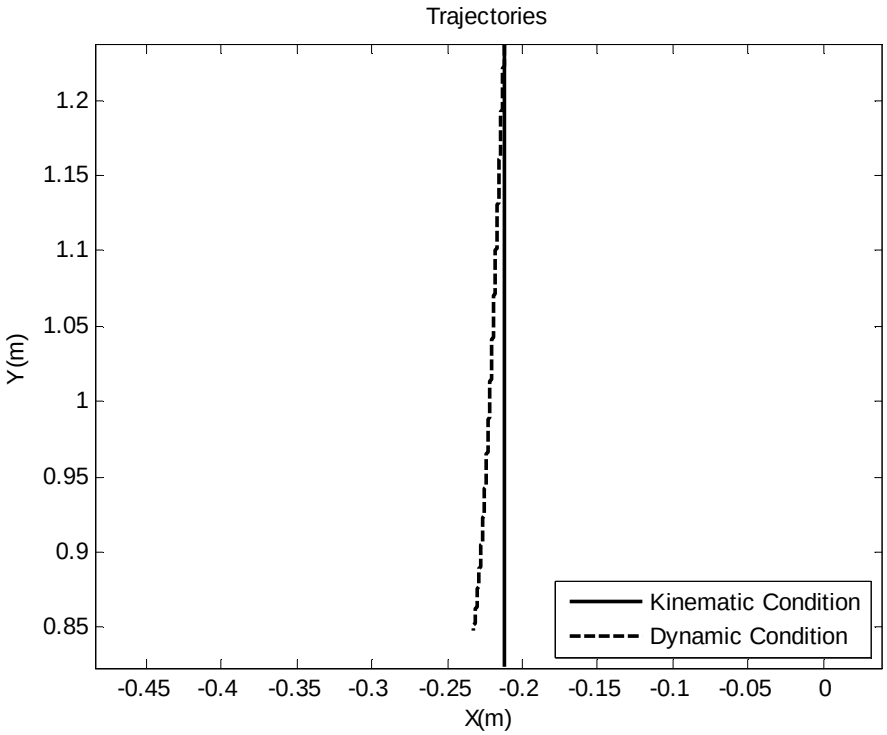

Fig. 2.8(a): Trajectories of the Test Article Due to an Impulsive Force Applied at 270 Degrees in Kinematic and Dynamic Condition

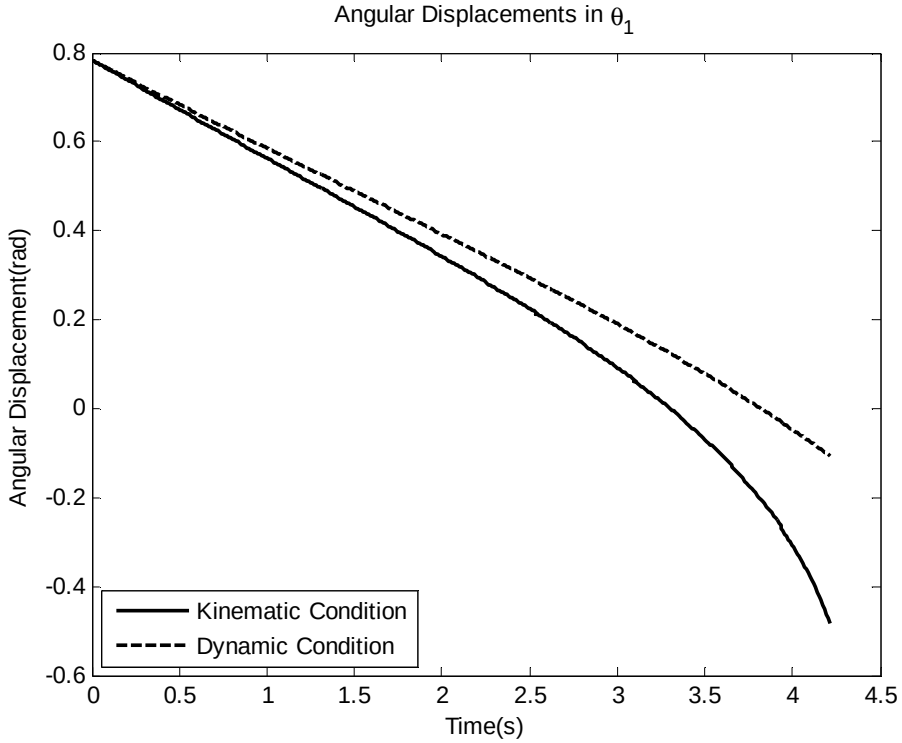

Fig. 2.8(b): Displacements of the Test Article in θ_1 Due to an Impulsive Force Applied at 270 Degrees in Kinematic and Dynamic Condition

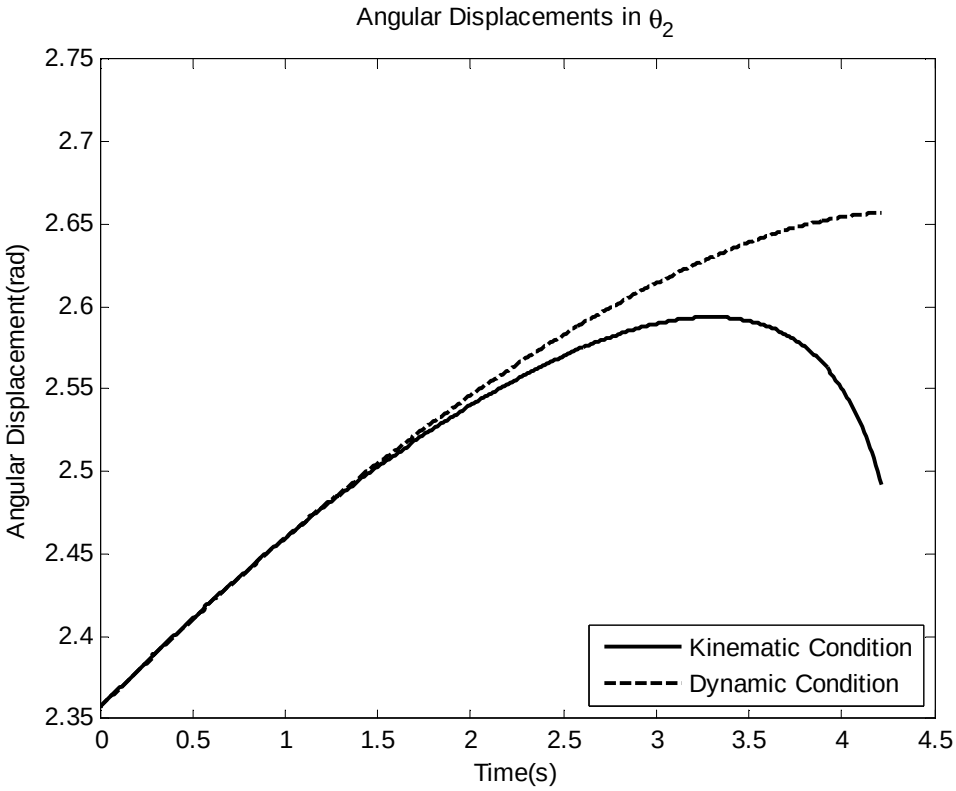

Fig. 2.8(c): Displacements of the Test Article in θ_2 Due to an Impulsive Force Applied at 270 dDegrees in Kinematic and Dynamic Condition

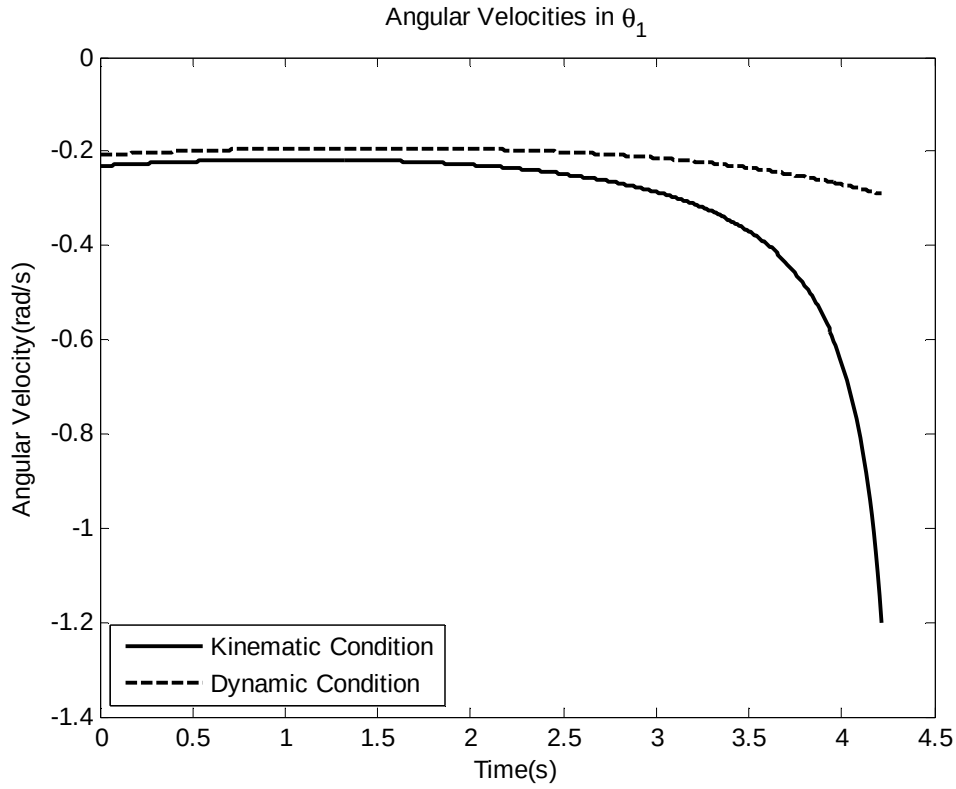

Fig. 2.8(d): Velocities of the Test Article in θ_1 Due to an Impulsive Force Applied at 270 Degrees in Kinematic and Dynamic Condition

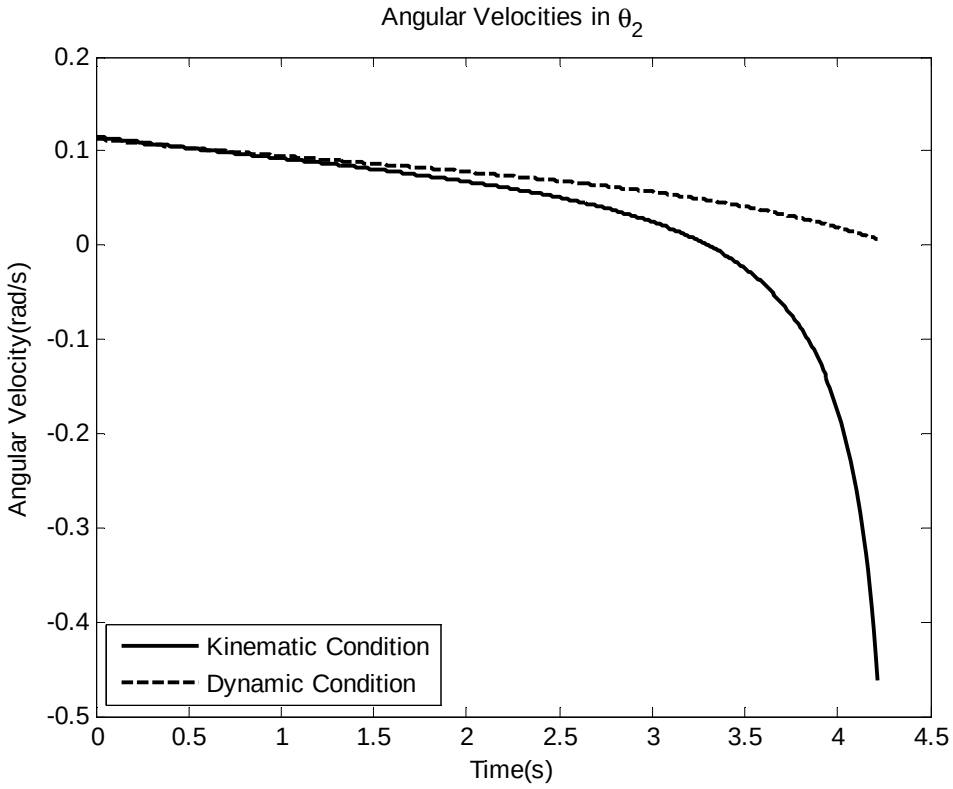

Fig. 2.8(e): Velocities of the Test Article in θ_2 Due to an Impulsive Force Applied at 270 Degrees in Kinematic and Dynamic Condition

Link #4 in kinetic mode hits the lower boundary, collision with link #2, after 4.21 seconds and the angle of motion in kinetic modes is 267.63 degree.

It can be seen that the trajectories shift more noticeably when the force is applied in vertical and horizontal directions. The angle of motion of the test article after impact, $\alpha_{Vimpact}$, and the angle of applied force are 2 to 3 degrees in difference. The reason is that linkage inertia takes away some part of kinetic energy for translation and rotation and how much is absorbed is dependent upon on the angle between the force and the links. When the force is vertical, it is inclined at an angle is 45 degree to every link except for link # 3. It means the rotations of links #1, #2, and #4 and the translation of link #3 absorb that energy of impact. When the impulsive force is in the direction parallel with any of the links, the links don't move and that means less kinetic energy is absorbed by them. For example, Fig. 2.7, the impulsive force is parallel with the links #1 and #2 and it means that they do not move after impact, since there is no moment acting on them. Link #3 does not move, either. Only the rotation of link #4 takes up that kinetic energy. That is the reason why the angle of the motion and the angle of the impact are almost identical in the simulations #2, #5.

2.3 Dynamics of the System under Force Applications

In this section, the system dynamics is going to be extended to a force system. The dynamic equations are derived from the Lagrange's equation. A constant force is applied in different direction on the test article instead of an impulsive force.

2.3.1 Lagrange's Equation for Force

Lagrange's equation for force system is given as:

$$\frac{d}{dt}\left(\frac{\partial L}{\partial \dot{q}_i}\right)-\frac{\partial L}{\partial q_i}=\sum_{n=1}^{q}\vec{F}_n\bullet\frac{\partial \vec{V}_n}{\partial \dot{q}_i}+\sum_{m=1}^{r}\vec{M}_m\frac{\partial \vec{\omega}_m}{\partial \dot{q}_i} \qquad q_1=\theta_1,\ \ q_2=\theta_2 \qquad L=T-V \tag{2.38}$$

$\vec{F}$ is the applied force and $\vec{M}$ is the applied moment. $\vec{V}$ is the velocity and $\vec{\omega}$ is the angular velocity.

The LHS of Eq. (2.38) is the same as the LHS of Eq. (2.16), so only the RHS of the equation need to be derived. In the simulation, there is only one force, $\vec{F}$, acting on the test article which can be denote as:

$$\vec{F}=F\bullet Cos\alpha_F\,\hat{i}+F\bullet Sin\alpha_F\,\hat{j}=F_x\hat{i}+F_y\hat{j} \tag{2.39}$$

Here the α_F is the angle of the force applied, similar to the α_P in impulse system.

From Eq. (2.14), the velocity of the test article is given as:

$$\vec{V}_a==\left(-l_1\dot{\theta}_1Sin\theta_1-l_{42}\dot{\theta}_2Sin\theta_2\right)\hat{i}+\left(l_1\dot{\theta}_1Cos\theta_1+l_{42}\dot{\theta}_2Cos\theta_2\right)\hat{j}$$

Since the applied torque, $\vec{M}$, is zero, the terms on the RHS of Eq. (2.38) can be shown as:

$$\begin{aligned}\vec{F}_a \bullet \frac{\partial \vec{V}_a}{\partial \dot{\theta}_1} &= -F_x l_1 Sin\theta_1 + F_y l_1 Cos\theta_1 \\ \vec{F}_a \bullet \frac{\partial \vec{V}_a}{\partial \dot{\theta}_2} &= -F_x l_{42} Sin\theta_2 + F_y l_{42} Cos\theta_2\end{aligned} \tag{2.40}$$

Using Eq. (2.23), (2.24), and (2.40), Lagrange's equation describing dynamics of the force system can be shown to be:

$$\begin{aligned}&\left(m_a + \frac{1}{3}m_1 + \frac{1}{3}m_2 + m_3 + m_4\right) l_1^{\,2}\ddot{\theta}_1 + m_a l_1 l_{42}\ddot{\theta}_2 Cos(\theta_1 - \theta_2) \\ &+ m_a l_1 l_{42}\dot{\theta}_2^{\,2} Sin(\theta_1 - \theta_2) + \left(\frac{1}{2}w_1 + \frac{1}{2}w_2 + w_3 + w_4 + w_a\right) l_1 Cos\theta_1 - k_1 l_{k1} l_1 Cos\theta_1 \\ &= -F_x l_1 Sin\theta_1 + F_y l_1 Cos\theta_1\end{aligned} \tag{2.41}$$

$$\begin{aligned}&\left(m_a + \frac{1}{3}m_4\right) l_{42}^{\,2}\ddot{\theta}_2 + m_a l_1 l_{41}\ddot{\theta}_1 Cos(\theta_1 - \theta_2) - m_a l_1 l_{42}\dot{\theta}_1^{\,2} Sin(\theta_1 - \theta_2) \\ &+ w_a l_{42} Cos\theta_2 - k_2 l_{k2} l_{42} Cos\theta_2 = -F_x l_{42} Sin\theta_2 + F_y l_{42} Cos\theta_2\end{aligned}$$

The equations can be expressed in the state space form:

$$\begin{bmatrix} A_{11} & A_{12} \\ A_{21} & A_{22} \end{bmatrix} \dot{X} = \begin{bmatrix} 0 & \mathrm{B}_{12} \\ \mathrm{B}_{21} & 0 \end{bmatrix} X^2 + \begin{bmatrix} D_1 \\ D_2 \end{bmatrix} \quad , \quad X = \begin{bmatrix} \dot{\theta}_1 \\ \dot{\theta}_2 \end{bmatrix} \quad , \quad \dot{X} = \begin{bmatrix} \ddot{\theta}_1 \\ \ddot{\theta}_2 \end{bmatrix} \tag{2.42}$$

Where:

$$\begin{aligned}A_{11} &= \left(m_a + \frac{1}{3}m_1 + \frac{1}{3}m_2 + m_3 + m_4\right) l_1^{\,2} \\ A_{12} &= m_a l_1 l_{41} Cos(\theta_1 - \theta_2) \\ A_{21} &= m_a l_1 l_{41} Cos(\theta_1 - \theta_2) \\ A_{22} &= \left(m_a + \frac{1}{3}m_4\right) l_{41}^{\,2} \\ \mathrm{B}_{12} &= -m_a l_1 l_{41} Sin(\theta_1 - \theta_2) \\ \mathrm{B}_{21} &= m_a l_1 l_{41} Sin(\theta_1 - \theta_2)\end{aligned}$$

$$D_1 = -\left(\frac{1}{2}w_1 + \frac{1}{2}w_2 + w_3 + w_4 + w_a\right) l_1 Cos\theta_1 + k_1 l_{k1} l_1 Cos\theta_1 - F_x l_1 Sin\theta_1 + F_y l_1 Cos\theta_1$$
$$D_2 = -w_a l_{42} Cos\theta_2 + k_2 l_{k2} l_{42} Cos\theta_2 - F_x l_{42} Sin\theta_2 + F_y l_{41} Cos\theta_2$$

If the links have no mass, the entries can be simplified into:

$$\begin{bmatrix} A_{11} & A_{12} \\ A_{21} & A_{22} \end{bmatrix} \dot{X} = \begin{bmatrix} 0 & \mathrm{B}_{12} \\ \mathrm{B}_{21} & 0 \end{bmatrix} X^2 + \begin{bmatrix} D_1 \\ D_2 \end{bmatrix}, \quad X = \begin{bmatrix} \dot{\theta}_1 \\ \dot{\theta}_2 \end{bmatrix}, \quad \dot{X} = \begin{bmatrix} \ddot{\theta}_1 \\ \ddot{\theta}_2 \end{bmatrix} \tag{2.43}$$

Where:

$$A_{11} = m_a l_1^2$$
$$A_{12} = m_a l_1 l_{41} Cos(\theta_1 - \theta_2)$$
$$A_{21} = m_a l_1 l_{41} Cos(\theta_1 - \theta_2)$$
$$A_{22} = m_a l_{41}^2$$
$$\mathrm{B}_{12} = -m_a l_1 l_{41} Sin(\theta_1 - \theta_2)$$
$$\mathrm{B}_{21} = m_a l_1 l_{41} Sin(\theta_1 - \theta_2)$$
$$D_1 = -w_a l_1 Cos\theta_1 + k_1 l_{k1} l_1 Cos\theta_1 - F_x l_1 Sin\theta_1 + F_y l_1 Cos\theta_1$$
$$D_2 = -w_a l_{42} Cos\theta_2 + k_2 l_{k2} l_{42} Cos\theta_2 - F_x l_{42} Sin\theta_2 + F_y l_{41} Cos\theta_2$$

The matrix in Eq. (2.42) is referred to as the kinematic equations of the test article. When the mass of the linkage is introduced, the matrix equation (2.43) is used and will be referred to as kinetic equations.

2.3.2 Simulation under Force Applications

In the simulation, t_s indicates the simulation time as was used in a previous simulation. The criteria of stopping and the parameters setting remain the same, except that the magnitude of the applied force is 10 newton. The force is applied in various angles, α_F , from 90 degree to 270 degree in steps of 45 degree. More details of the system parameters setup for simulation are listed in the Table A.2.

(1) $\alpha_F = \frac{\pi}{2}$

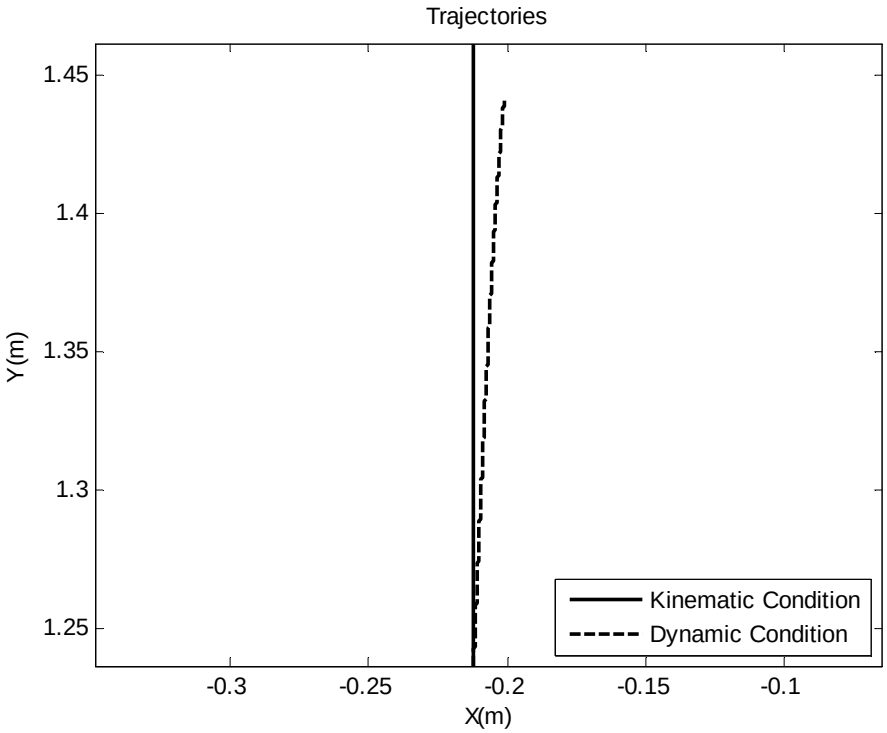

Fig. 2.9(a): Trajectories of the test article due to a force applied at 90 degrees in kinematic and dynamic condition

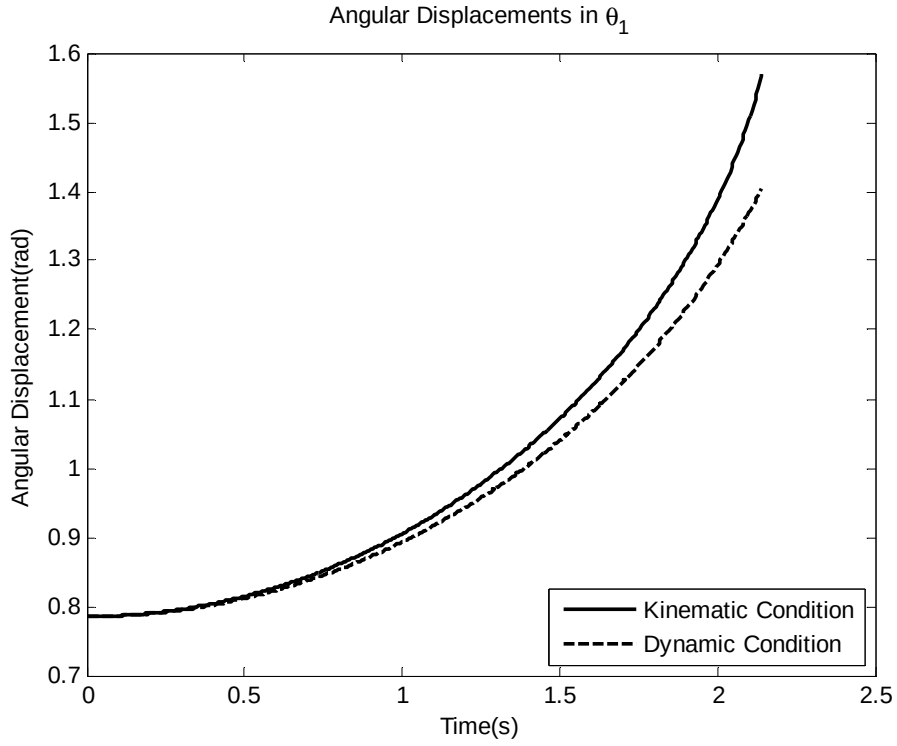

Fig. 2.9(b): Displacements of the Test Article in θ_1 Due to a Force Applied at 90 Degrees in Kinematic and Dynamic Condition

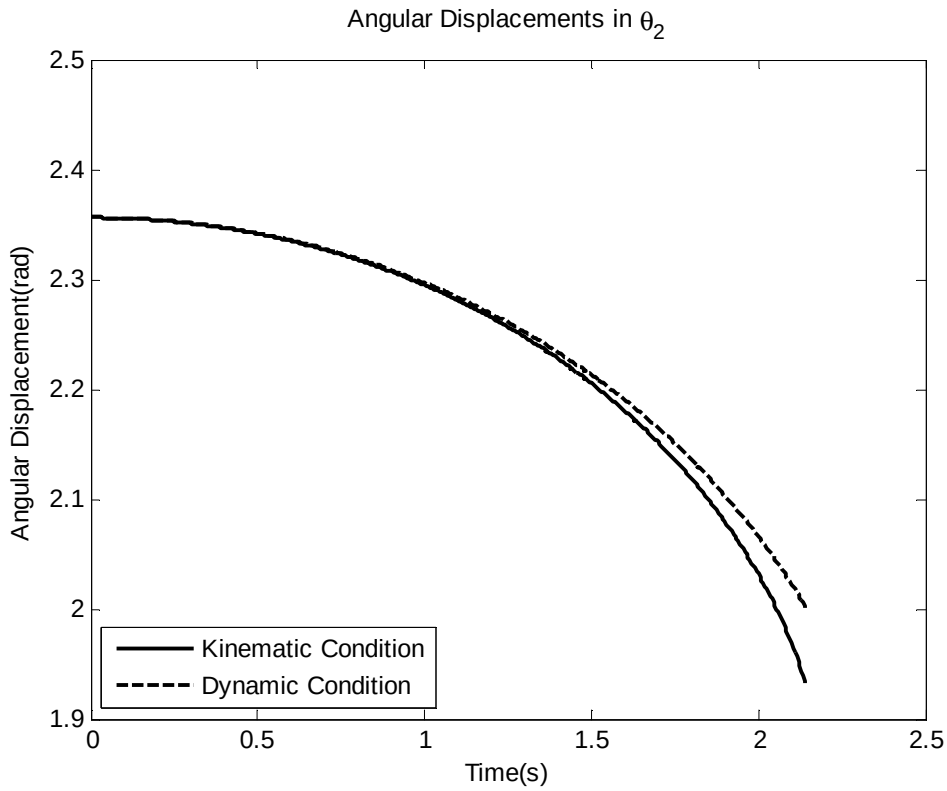

Fig. 2.9(c): Displacements of the Test Article in θ_2 Due to a Force Applied at 90 Degrees in Kinematic and Dynamic Condition

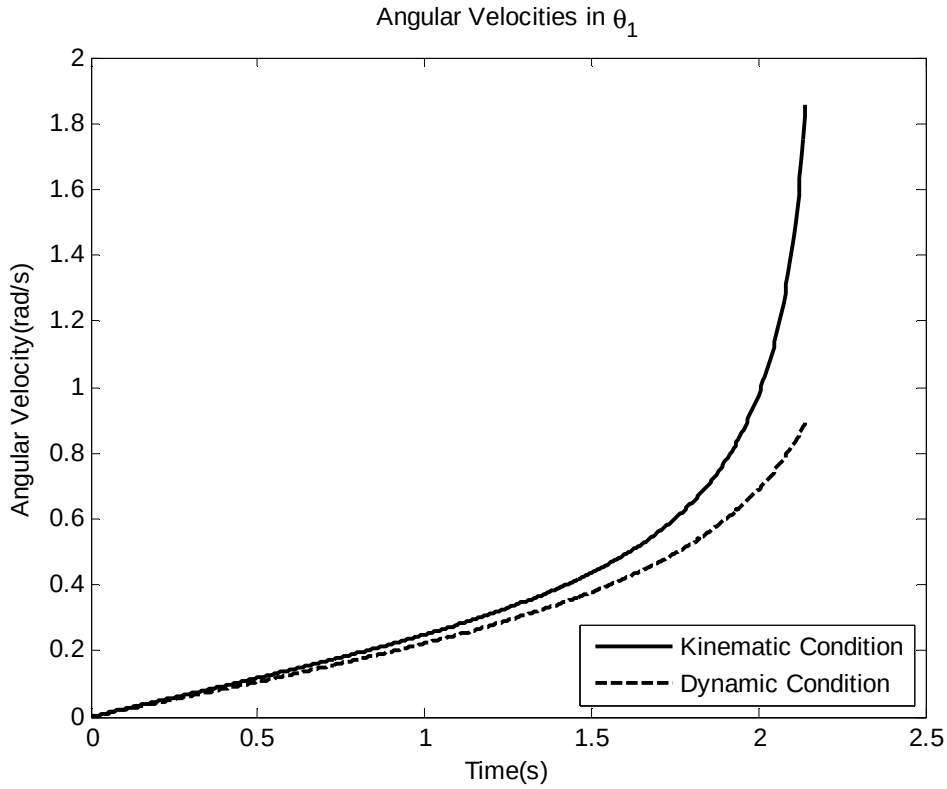

Fig. 2.9(d): Velocities of the Test Article in θ_1 Due to a Force Applied at 90 Degrees in Kinematic and Dynamic Condition

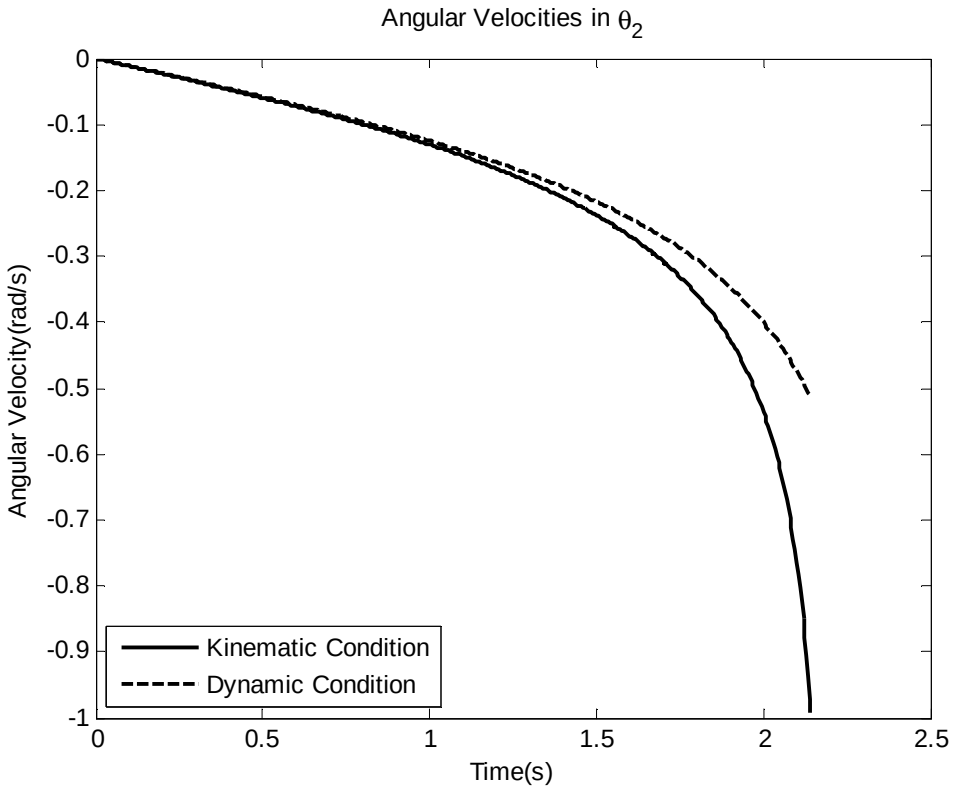

Fig. 2.9(e): Velocities of the Test Article in θ_2 Due to a Force Applied at 90 Degrees in Kinematic and Dynamic Condition

Link #1 in kinematic mode hits the upper boundary, $\theta_1 = \frac{\pi}{2}$, after 2.14 seconds. Since it's a force system, there is no difference in initial velocity, but the slower system response no matter in angular displacement or velocity to the applied force is obviously can be told in the figures.

$(2)\alpha_F = \frac{3\pi}{4}$

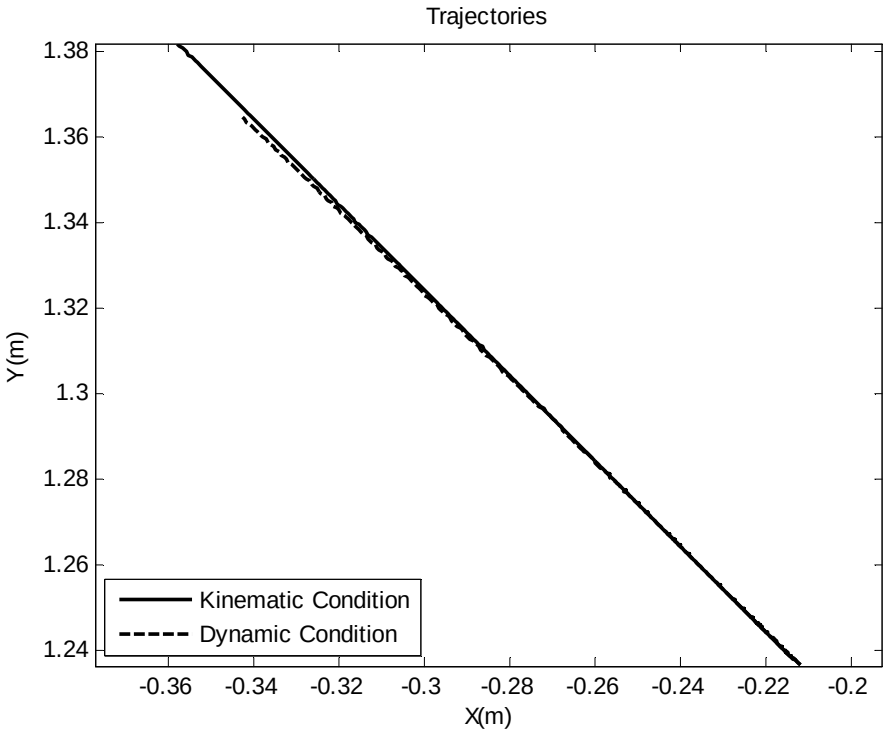

Fig. 2.10(a): Trajectories of the Test Article Due to a Force Applied at 135 Degrees in Kinematic and Dynamic Condition

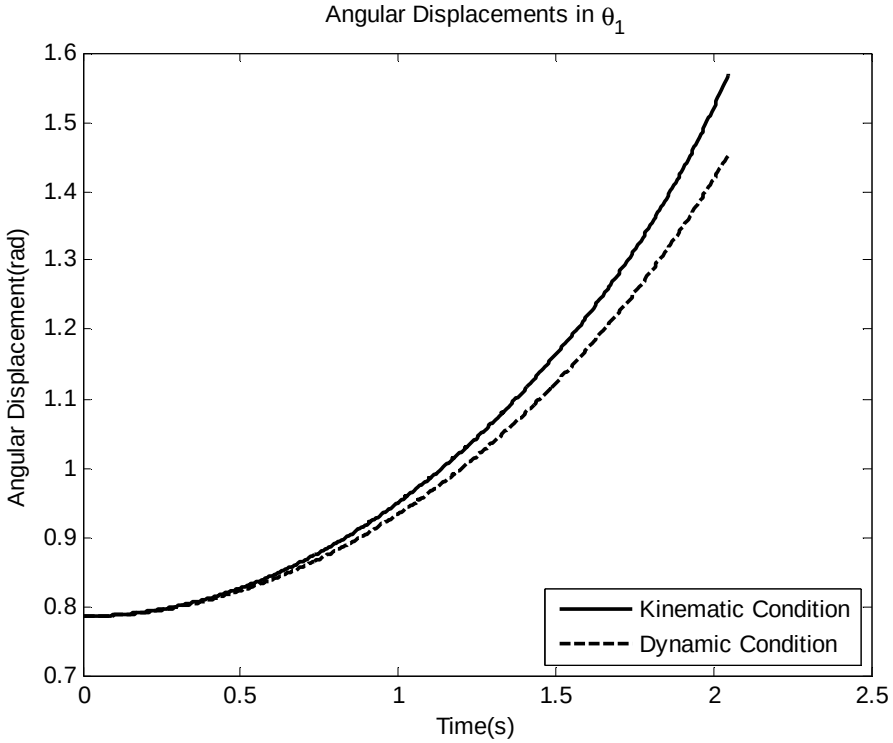

Fig. 2.10(b): Displacements of the Test Article in θ_1 Due to a Force Applied at 135 Degrees in Kinematic and Dynamic Condition

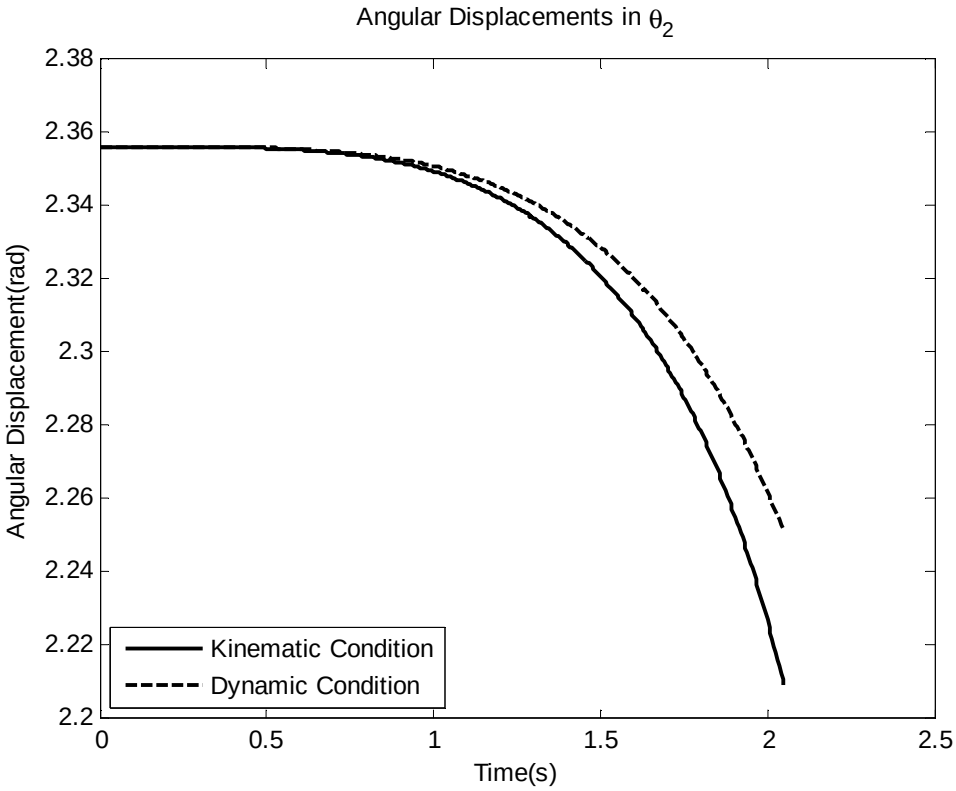

Fig. 2.10(c): Displacements of the Test Article in θ_2 Due to a Force Applied at 135 Degrees in Kinematic and Dynamic Condition

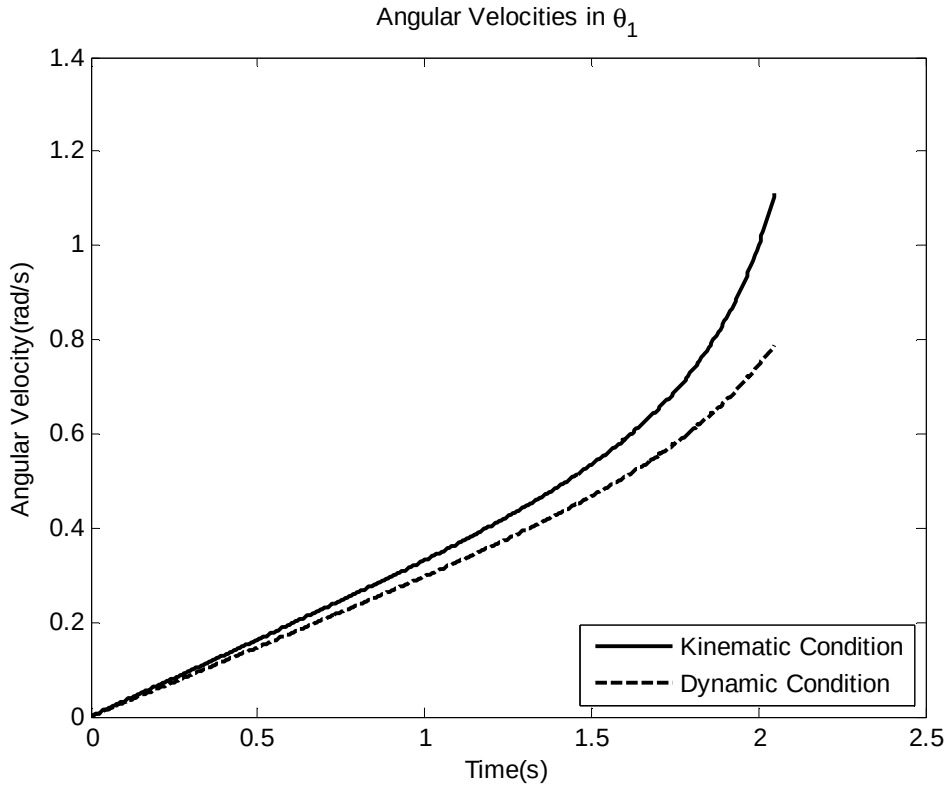

Fig. 2.10(d): Velocities of the Test Article in θ_1 Due to a Force Applied at 135 Degrees in Kinematic and Dynamic Condition

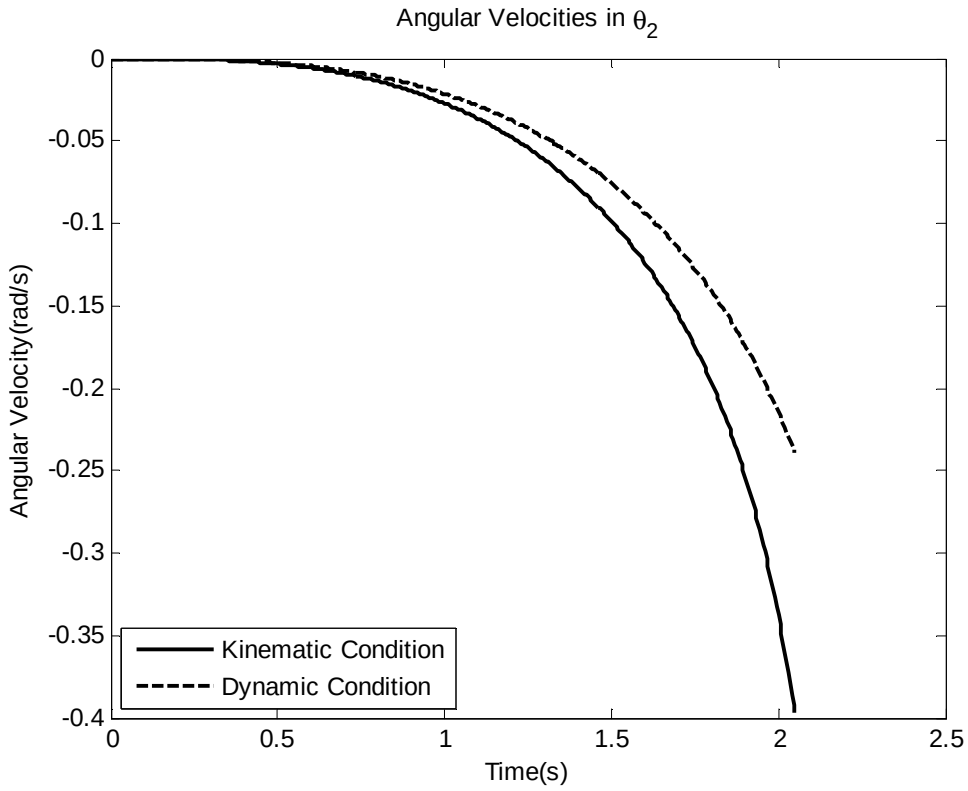

Fig. 2.10(e): Velocities of the Test Article in θ_2 Due to a Force Applied at 135 Degrees in Kinematic and Dynamic Condition

Link #1 in kinematic mode hits the upper boundary, $\theta_1 = \frac{\pi}{2}$, after 2.05 seconds. The difference becomes more obvious when the test article is closer to the boundary of working space.

$(3)\alpha_F = \pi$

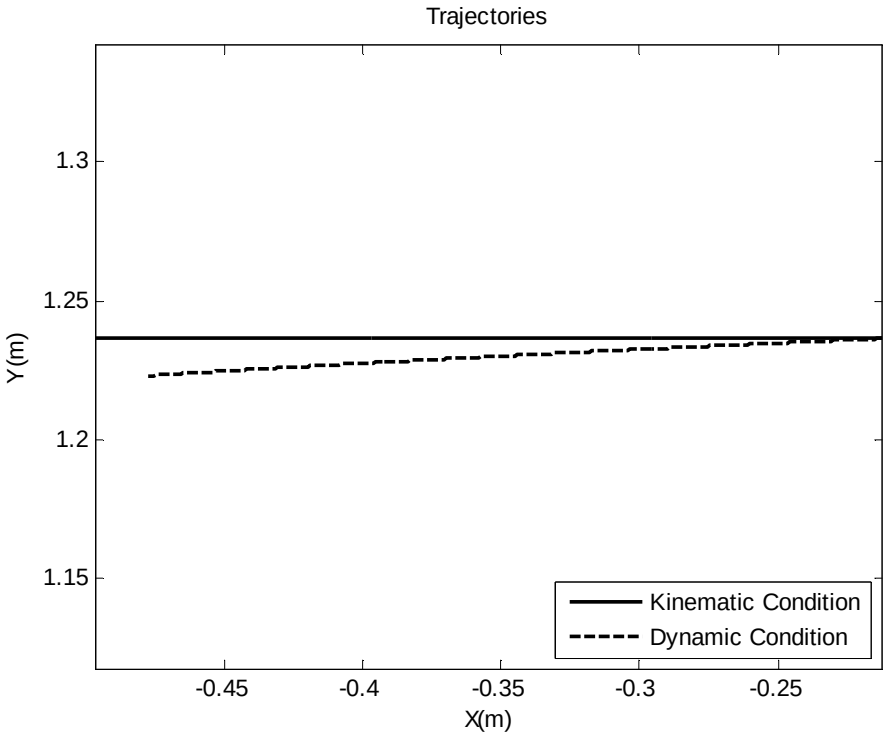

Fig. 2.11(a): Trajectories of the Test Article Due to a Force Applied at 180 Degrees in Kinematic and Dynamic Condition

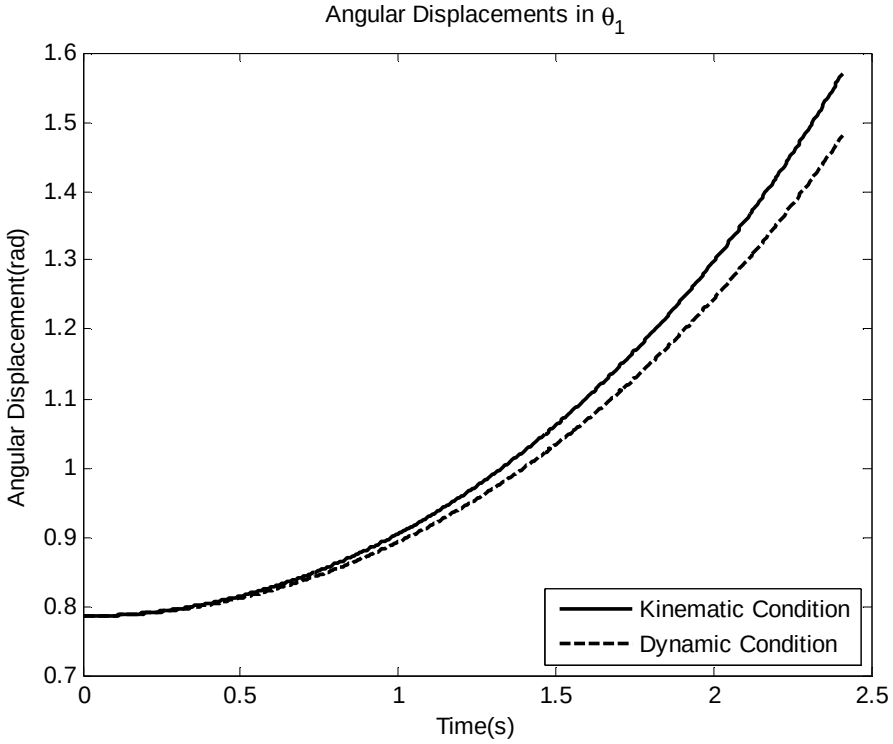

Fig. 2.11(b): Displacements of the Test Article in θ_1 Due to a Force Applied at 180 Degrees in Kinematic and Dynamic Condition

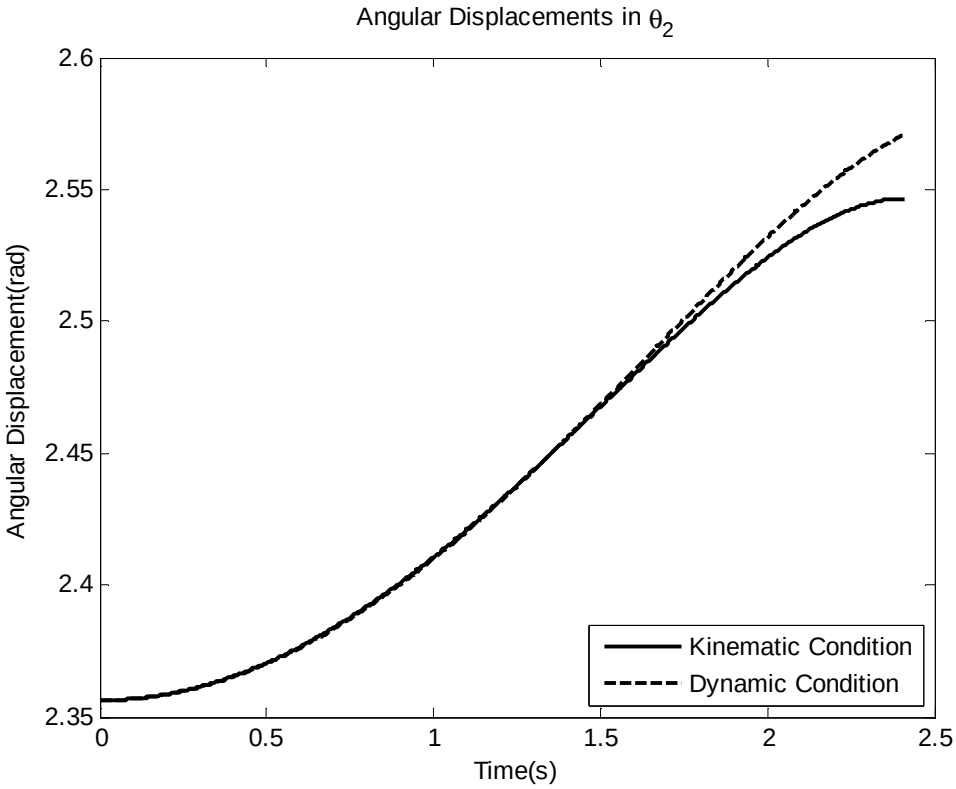

Fig. 2.11(c): Displacements of the Test Article in θ_2 Due to a Force Applied at 180 Degrees in Kinematic and Dynamic Condition

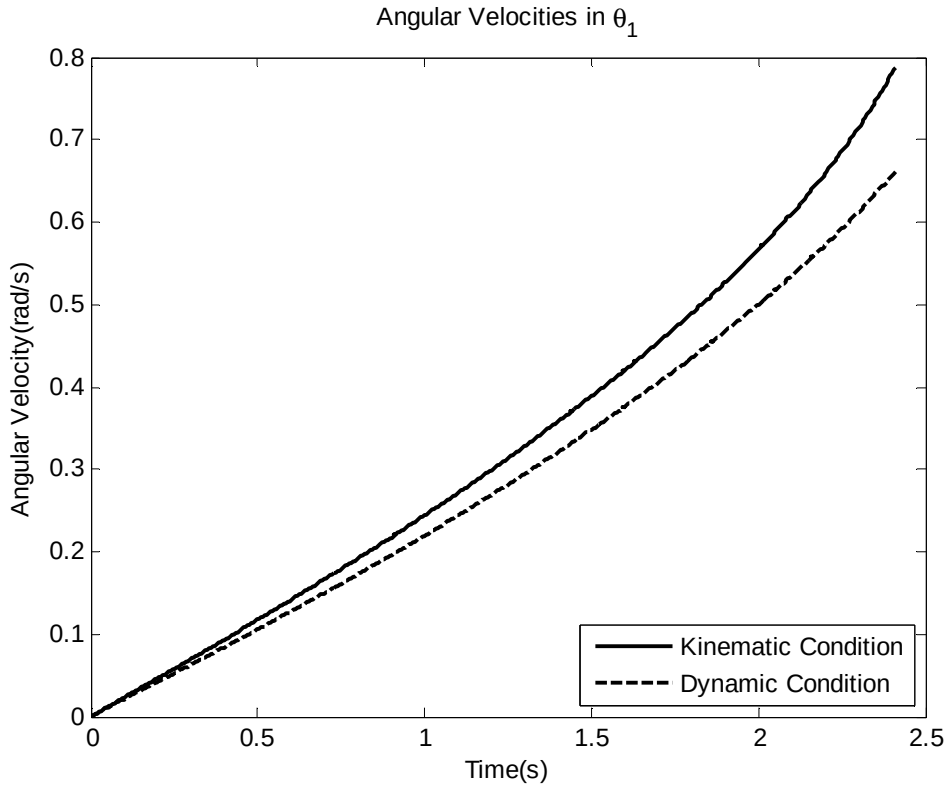

Fig. 2.11(d): Velocities of the Test Article in θ_1 Due to a Force Applied at 180 Degrees in Kinematic and Dynamic Condition

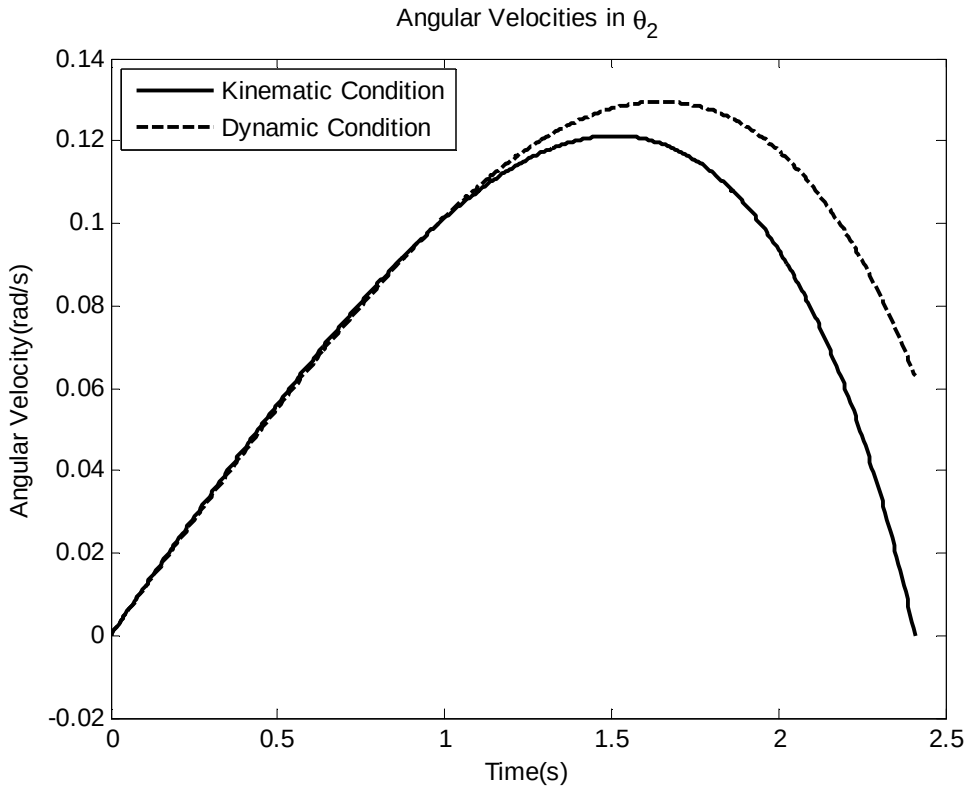

Fig. 2.11(e): Velocities of the Test Article in θ_2 Due to a Force Applied at 180 Degrees in Kinematic and Dynamic Condition

Link #1 in kinematic mode hits the upper boundary, $\theta_1 = \frac{\pi}{2}$, after 2.41 seconds. The way system reacted to the applied force is the same as to impulsive force.

$(4)\alpha_F = \frac{5\pi}{4}$

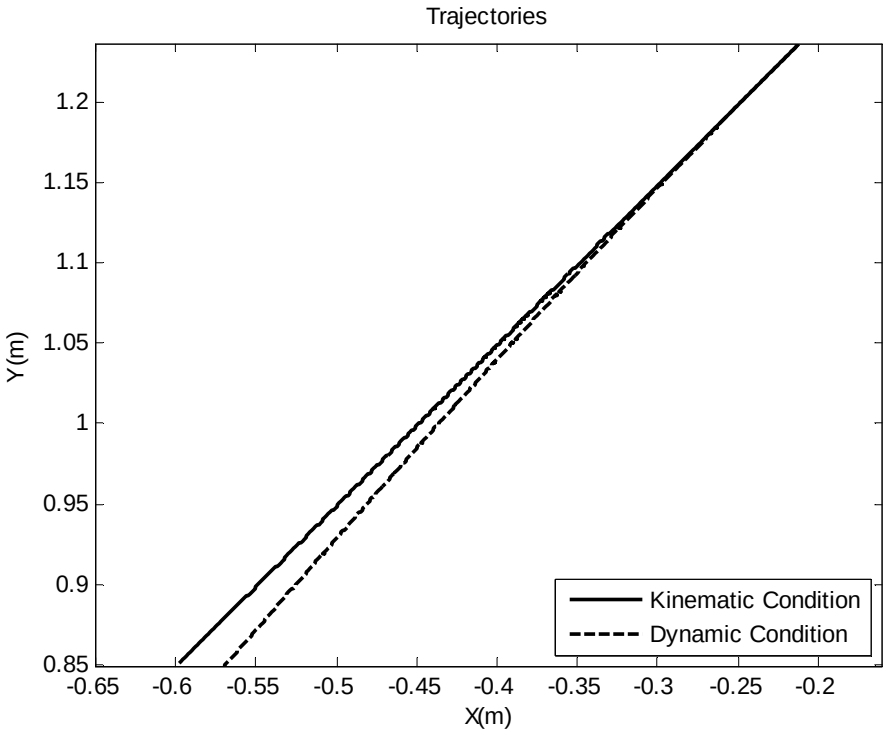

Fig. 2.12(a): Trajectories of the Test Article Due to a Force Applied at 225 Degrees in Kinematic and Dynamic Condition

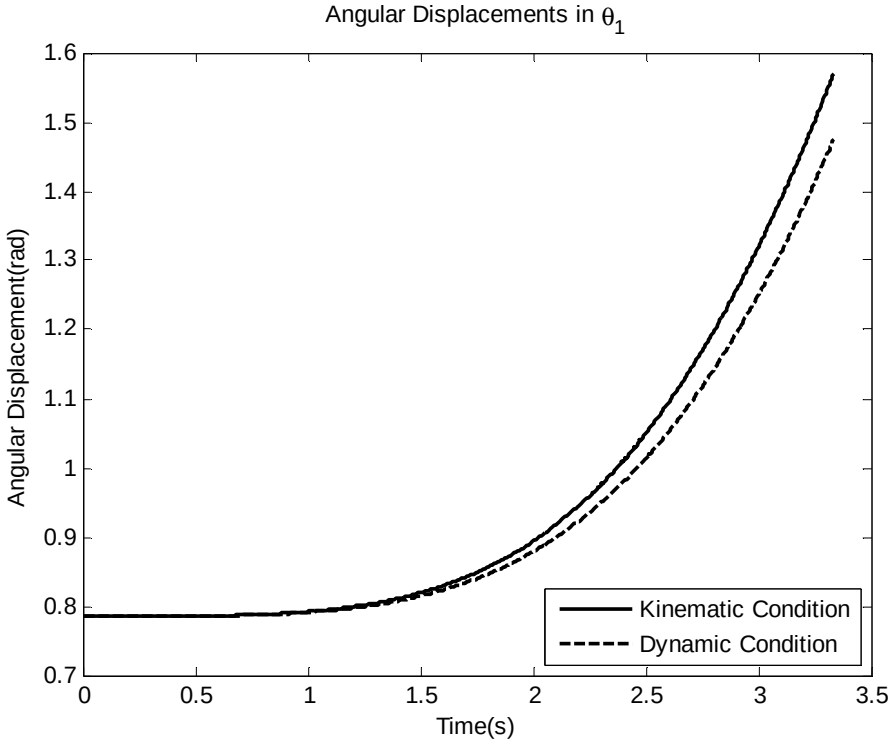

Fig. 2.12(b): Displacements of the Test Article in θ_1 Due to a Force Applied at 225 Degrees in Kinematic and Dynamic Condition

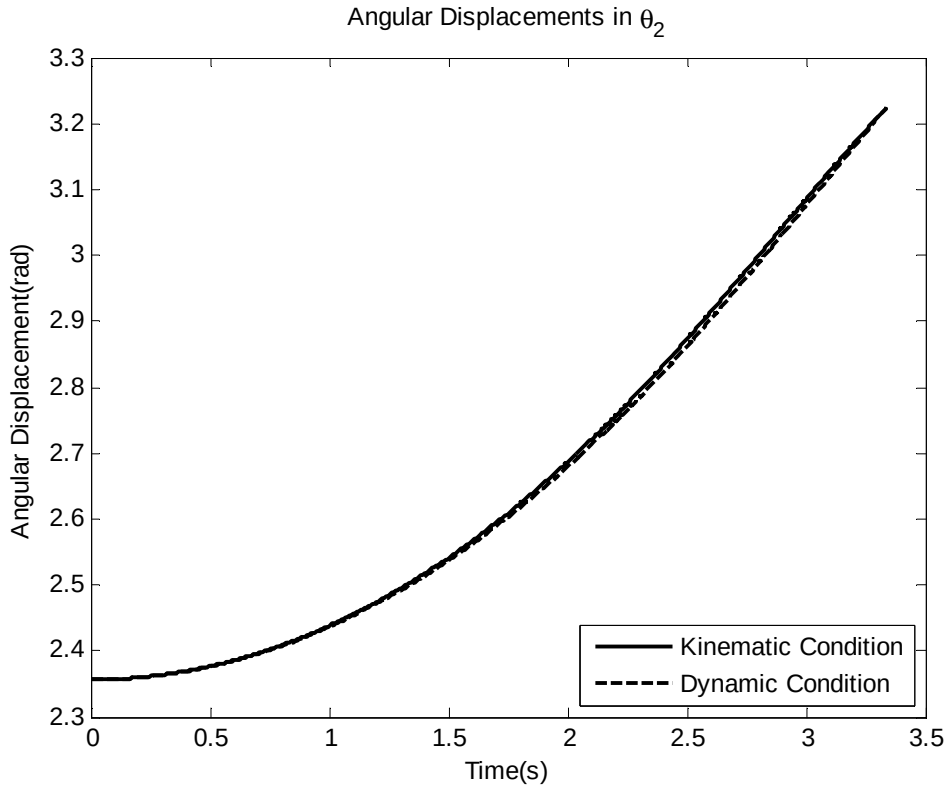

Fig. 2.12(c): Displacements of the Test Article in θ_2 Due to a Force Applied at 225 Degrees in Kinematic and Dynamic Condition

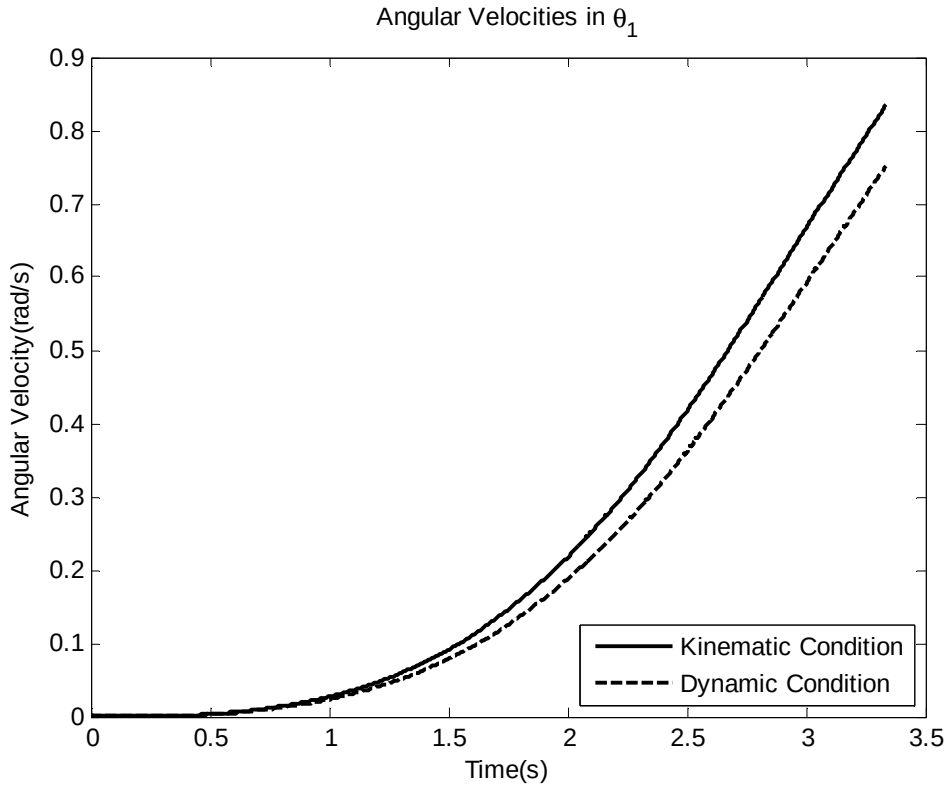

Fig. 2.12(d): Velocities of the Test Article in θ_1 Due to a Force Applied at 225 Degrees in Kinematic and Dynamic Condition

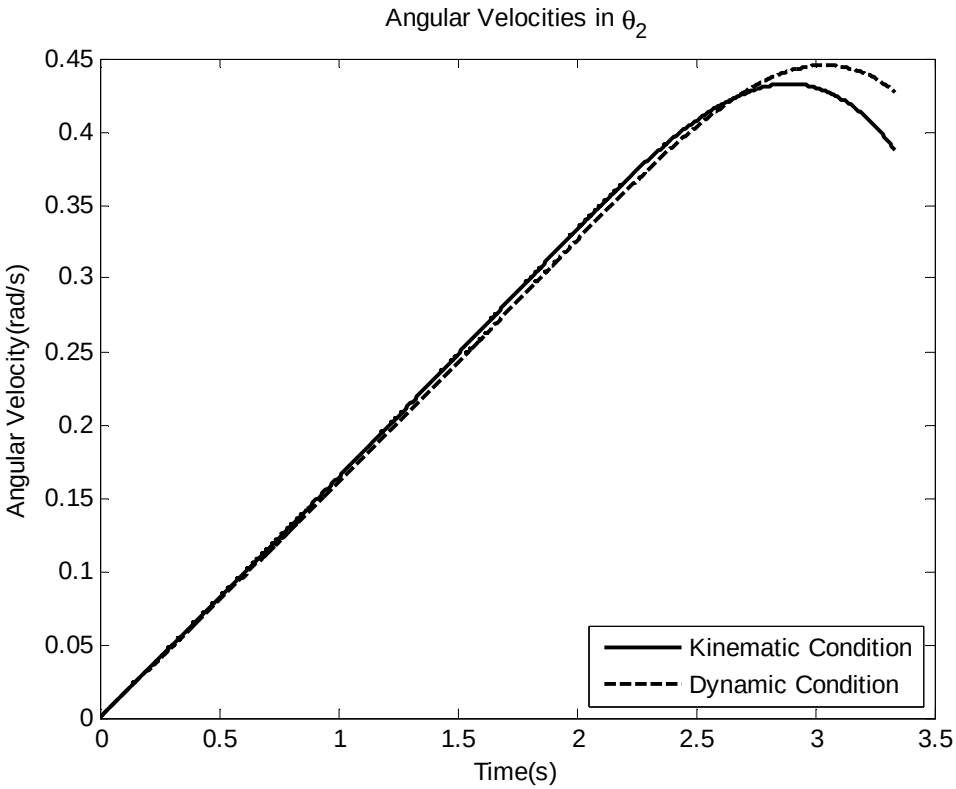

Fig. 2.12(e): Velocities of the Test Article in θ_2 Due to a Force Applied at 225 Degrees in Kinematic and Dynamic Condition

Link #1 in kinematic mode hits the upper boundary, $\theta_1 = \frac{\pi}{2}$, after 3.34 seconds. Because of the direction of the force applied, the trajectory shift is relatively small compared with other cases.

$$(5)\,\alpha_F = \frac{3\pi}{2}$$

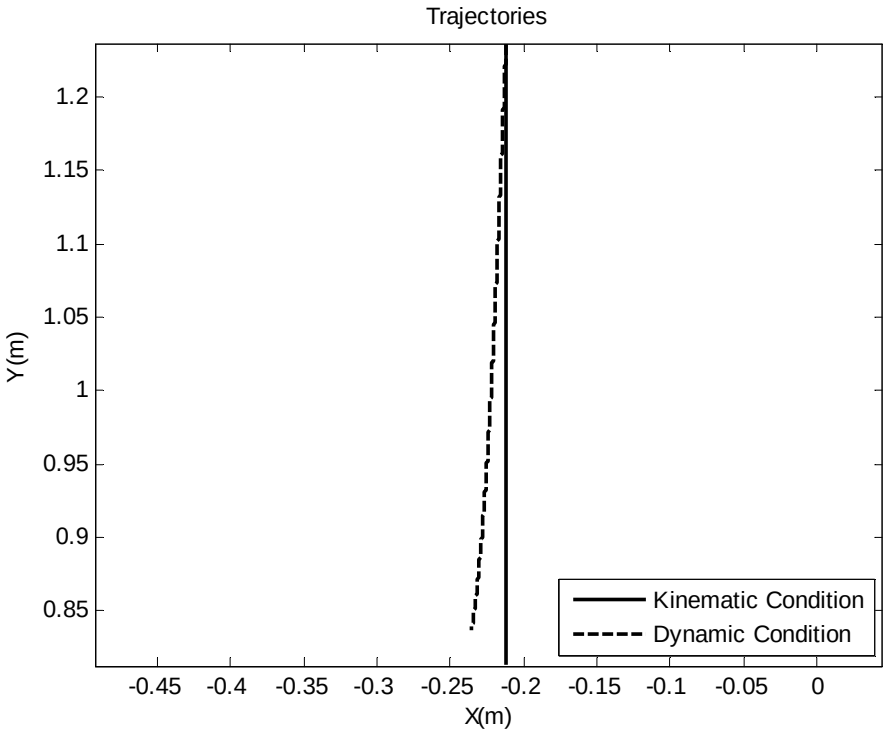

Fig. 2.13(a): Trajectories of the Test Article Due to a Force Applied at 270 Degrees in Kinematic and Dynamic Condition

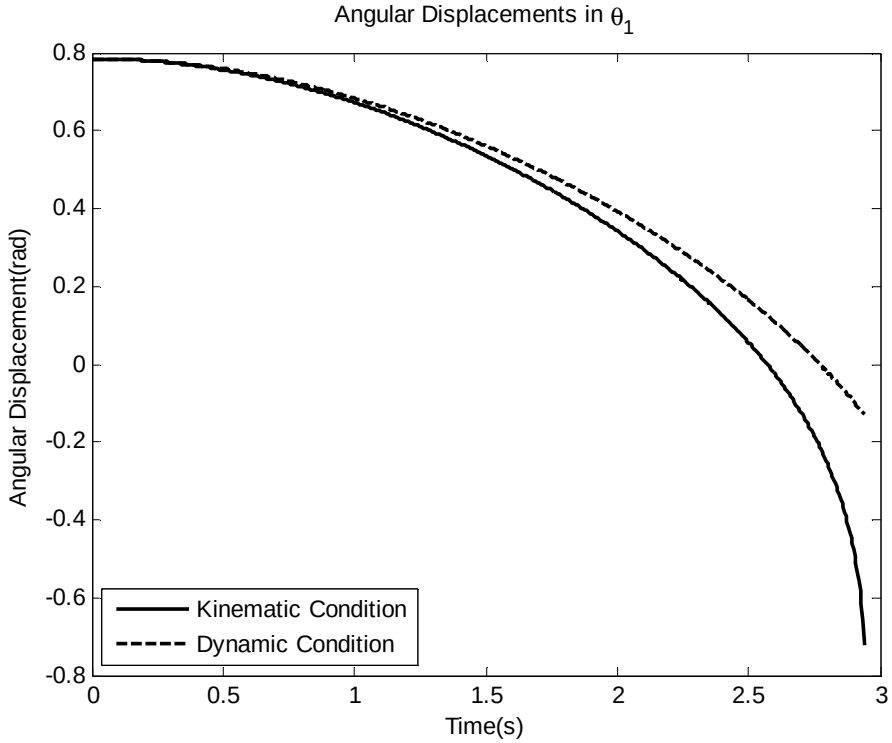

Fig. 2.13(b): Displacements of the Test Article in θ_1 Due to a Force Applied at 270 Degrees in Kinematic and Dynamic Condition

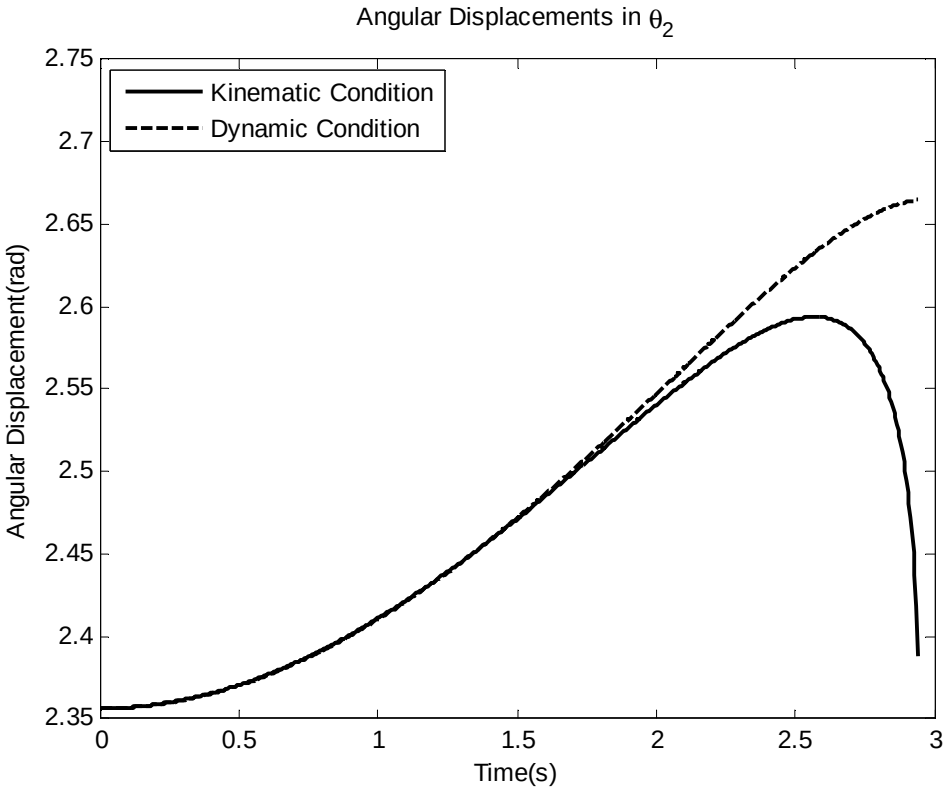

Fig. 2.13(c): Displacements of the Test Article in θ_2 due to a Force Applied at 270 Degrees in Kinematic and Dynamic Condition

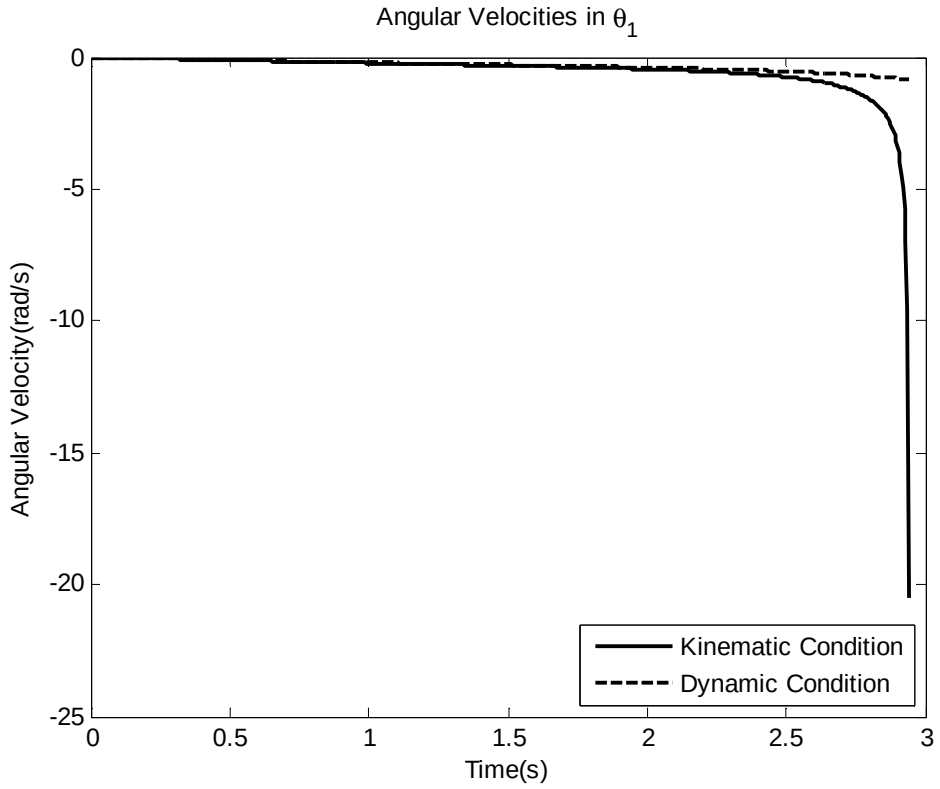

Fig. 2.13(d): Velocities of the Test Article in θ_1 Due to a Force Applied at 270 Degrees in Kinematic and Dynamic Condition

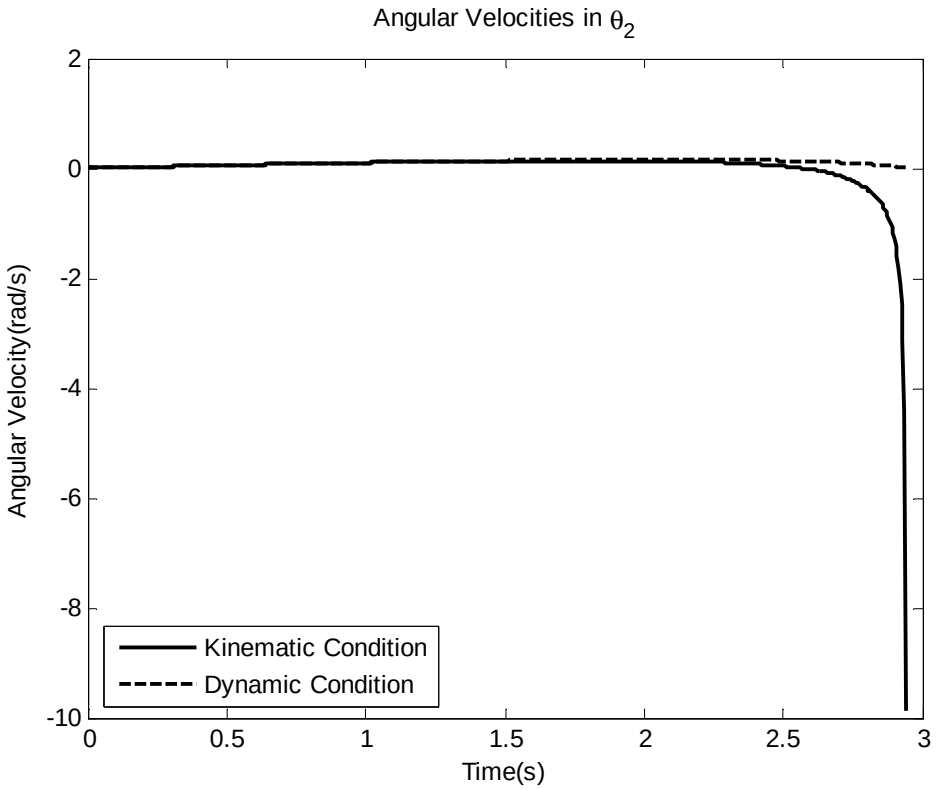

Fig. 2.13(e): Velocities of the Test Article in θ_2 Due to a Force Applied at 270 Degrees in Kinematic and Dynamic Condition

The simulation lasts for 2.94 seconds and is terminated by the program due to the value of the velocities increasing drastically when the test article gets really close to the boundary of working space. Since the linear motion on the device is in fact a combination of rotation of links, the sudden angular acceleration near the boundary can be anticipated.

The same tendency of system response to the force applied in different direction can be observed in Fig. (2.10) to the Fig. (2.16). The trajectory shifts directions is are explained and discussed in subsection 2.2.2. The trajectory shift due to the inertia of the links is even larger than it in the previous simulation.

Chapter 3

Adaptive Control Method

In previous chapter, how the inertia of the links limit the performance of the suspension system has already been demonstrated. It is can be shown that removing the gravitational effect would significantly decrease the actuator power requirement when the ratio of the total mass of the linkage and the mass of suspended object gets smaller. To deal with this situation, control methods need to be applied. Since the dynamic equations of the system, Eq. (2.25) and Eq. (2.42) are nonlinear, the traditional linear control methods, such as PID control and state space control, are not applicable. The linearization of the equations at certain operating points is not practical either. Based on these considerations, adaptive control is introduced to compensate the undesirable effect due to the inertia of the links.

Adaptive control is widely used in nonlinear control, especially when the system is highly nonlinear or the parameters of the system are too many or even unknown. For instance, when guided missile is flying, the weight of missile is decreasing because of fuel consumption and the surrounding air flow field is almost unpredictable. In old days, to deal with this kind of problem needs to build a huge data base after a lot of experiments and to install many sensors on the controlled object, so the controller can process the data measured by the sensor, refer them to the data base, and then adjust the controllable parameters. However, adaptive control provides an easy way to achieve this. By using adaptive control, all the parameters are not

necessary to be known a priori, only the measurement of the desired output is needed. This means that such a control method is more feasible and efficient for nonlinear systems. In particular feed-forward adaptive control method is well known as being very effective in tracking time-varying signal as long as the output signal can be correctly measured. In the following, feed-forward adaptive control method will be introduced and applied to the suspension system to see how it works.

3.1 Concept of Adaptive Control Method

The original idea to eliminate the inertia effect of the links is forcing the motion of the kinetic system to track the motion of the kinematic system. The method is to install one electric motor, assigned #1, at the joint of link#1 and ground link and one at the joint located at the middle of link#4, assigned #2, and use those motors to offset the deviation in displacement and velocity. The controller must be capable of handling different weights of the suspended mass and be robust enough to adapt to highly nonlinear system. Therefore, feed-forward model reference adaptive control is particularly well suited to serve for this purpose. The whole steps can be simplified as follows:

1. Choosing the reference model.
2. Setting up adjustment mechanism.
3. Generating output for compensation based on the reference model against the

measurement performance of the system by the controller.

The overall control scheme is shown in Fig. 3.1

The more specific procedure scheme for each motor is shown in the Fig. 3.2. e is the voltage output from the controller to drive the motor for the torque, τ, which compensate the inertia effect of the linkage. θ_d is the desired angular displacement from reference model against θ which is the angular displacement of the device in practical application. $\varepsilon(t)$ and $\varepsilon(\dot{t})$ are the difference between θ_d and θ, $\dot{\theta}_d$ and $\dot{\theta}$, respectively. Once $\varepsilon(t)$ and $\varepsilon(\dot{t})$ are determined, the adjustment mechanism will find out how much torque is needed for compensation.

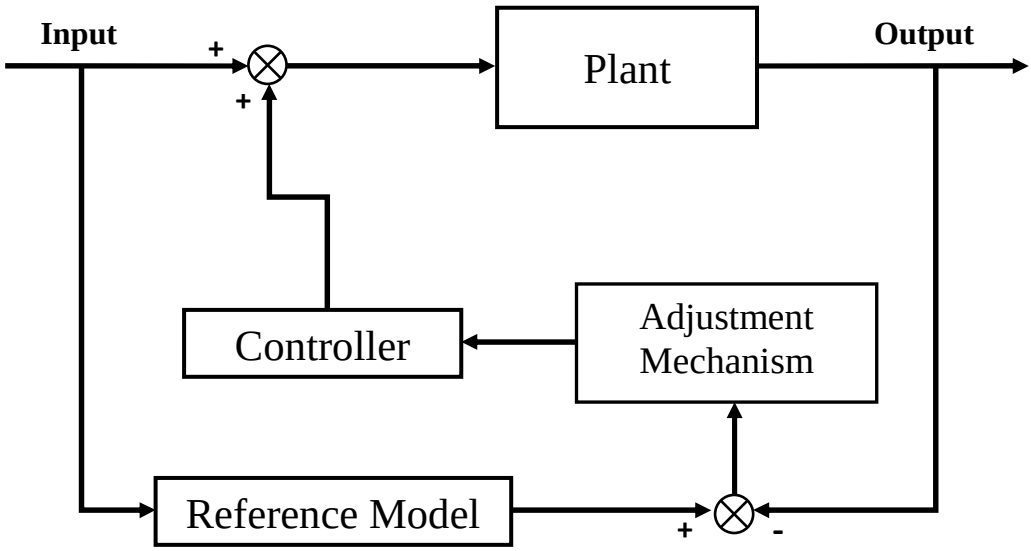

Fig. 3.1: Scheme of Feed-Forward Model Reference Adaptive Control

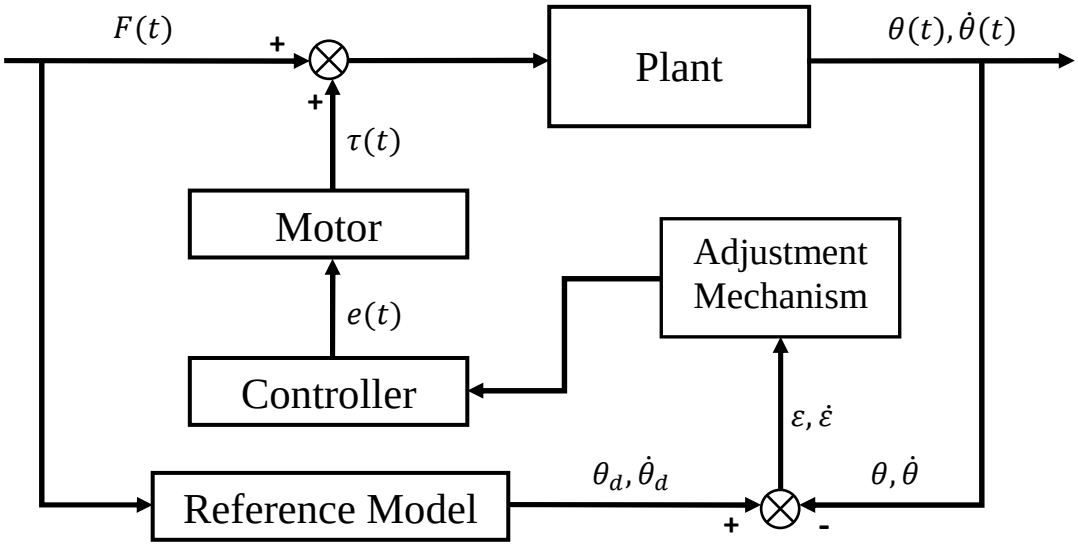

Fig. 3.2: The Control Scheme for Each Motor

3.2 Dynamic Equations with Motors

Before deriving the dynamic equations with motors, the behavior of the motors needs to be considered first. For an armature-controlled DC motor, the torque, T_m, is directly proportional to the armature current, i_a, so that:

$$T_m = K_m i_a \tag{3.1}$$

K_m is the motor torque constant.

The armature-controlled DC motor is driven by the armature voltage, e_a. The voltage equation of the motor is given as:

$$L_a \dot{i}_a + i_a R_a + e_b = e_a \tag{3.2}$$

The induced voltage, e_b, is proportional to the angular velocity, $\dot{\theta}_m$. It takes the form:

$$e_b = K_b \dot{\theta}_m \tag{3.3}$$

K_b is the induced voltage constant.

Since the armature-winding inductance, L_a, can be negligible. From Eq. (3.3) and Eq. (3.4), the armature current, i_a, can be written as:

$$i_a = \frac{e_a}{R_a} - \frac{K_b \dot{\theta}_m}{R_a} \tag{3.4}$$

Thus, the relation between the motor torque and the armature voltage can be found substituting Eq. (3.5) into Eq. (3.1):

$$T_m = K_m \left(\frac{e_a}{R_a} - \frac{K_b \dot{\theta}_m}{R_a} \right) \tag{3.5}$$

The torque equilibrium equation of the motor is given as:

$$I_m\ddot{\theta}_m + c_V\dot{\theta}_m + T_L = T_m \tag{3.6}$$

T_L is the loading torque to the motor.

Substitute Eq. (3.5) into Eq. (3.6) and rearrange the equation:

$$I_m\ddot{\theta}_m + \left(c_V + \frac{K_m K_b}{R_a}\right)\dot{\theta}_m + T_L = K_m\frac{e_a}{R_a} \tag{3.7}$$

There is a reduction gear which step-down ratio is N_g between the motor and the link and the torque output applied on the link is T_O , so that:

$$N_g T_L = T_O \quad \text{and} \quad N_g\theta_m = \theta \tag{3.8}$$

With Eq. (3.7) and Eq. (3.8), the equation can be shown as:

$$T_O = \frac{I_m}{N_g^2}\ddot{\theta} + \left(\frac{c_V + \frac{K_m K_b}{R_a}}{N_g^2}\right)\dot{\theta}_m + \frac{K_m}{R_a N_g}e_a \tag{3.9}$$

Recalled the dynamic equation for force system, Eq. (2.38), the second term, $\vec{\omega}\bullet\frac{\partial\vec{\omega}}{\partial q_i}$, on the RHS now is considered. The angular velocities are given as:

$$\begin{aligned}\vec{\omega}_1 &= \dot{\theta}_1\hat{k}\\ \vec{\omega}_2 &= \dot{\theta}_2\hat{k}\end{aligned} \tag{3.10}$$

The output torque, $\vec{\tau}_1$ and $\vec{\tau}_2$, are from the controlling motors, so the term, $\vec{\omega}\bullet\frac{\partial\vec{\omega}}{\partial q_i}$, is given as:

$$\begin{aligned}\vec{\tau}_1\bullet\frac{\partial\vec{\omega}}{\partial\dot{\theta}_1} &= \tau_1\\ \vec{\tau}_2\bullet\frac{\partial\vec{\omega}}{\partial\dot{\theta}_2} &= \tau_2\end{aligned} \tag{3.11}$$

Combined Eq. (3.11) and Eq. (2.42), the dynamic equation for the system now becomes:

$$\begin{bmatrix} A_{11} & A_{12} \\ A_{21} & A_{22} \end{bmatrix} \dot{X} = \begin{bmatrix} 0 & \mathrm{B}_{12} \\ \mathrm{B}_{21} & 0 \end{bmatrix} X^2 + \begin{bmatrix} D_1 \\ D_2 \end{bmatrix} \quad , \quad X = \begin{bmatrix} \dot{\theta}_1 \\ \dot{\theta}_2 \end{bmatrix} \quad , \quad \dot{X} = \begin{bmatrix} \ddot{\theta}_1 \\ \ddot{\theta}_2 \end{bmatrix} \tag{3.12}$$

Where:

$$A_{11} = \left(m_a + \frac{1}{3} m_1 + \frac{1}{3} m_2 + m_3 + m_4 \right) l_1^{\,2}$$
$$A_{12} = m_a l_1 l_{41} Cos\left(\theta_1 - \theta_2\right)$$
$$A_{21} = m_a l_1 l_{41} Cos\left(\theta_1 - \theta_2\right)$$
$$A_{22} = \left(m_a + \frac{1}{3} m_4 \right) l_{41}^{\,2}$$
$$\mathrm{B}_{12} = -m_a l_1 l_{41} Sin\left(\theta_1 - \theta_2\right)$$
$$\mathrm{B}_{21} = m_a l_1 l_{41} Sin\left(\theta_1 - \theta_2\right)$$
$$D_1 = -\left(\frac{1}{2} w_1 + \frac{1}{2} w_2 + w_3 + w_4 + w_a \right) l_1 Cos\theta_1 + k_1 l_{k1} l_1 Cos\theta_1 - F_x l_1 Sin\theta_1 + F_y l_1 Cos\theta_1 + \tau_1$$
$$D_2 = -w_a l_{42} Cos\theta_2 + k_2 l_{k2} l_{42} Cos\theta_2 - F_x l_{42} Sin\theta_2 + F_y l_{41} Cos\theta_2 + \tau_2$$

Substitute applied torque shown in Eq. (3.9) and rearrange into state space form. The dynamic equation is now given as:

$$\begin{bmatrix} A_{11} & A_{12} \\ A_{21} & A_{22} \end{bmatrix} \dot{X} = \begin{bmatrix} C_{11} & 0 \\ 0 & C_{22} \end{bmatrix} X + \begin{bmatrix} 0 & \mathrm{B}_{12} \\ \mathrm{B}_{21} & 0 \end{bmatrix} X^2 + \begin{bmatrix} D_1 \\ D_2 \end{bmatrix} + \begin{bmatrix} E_1 & 0 \\ 0 & E_2 \end{bmatrix} \begin{bmatrix} e_{a1} \\ e_{a2} \end{bmatrix} \tag{3.13}$$

$$A_{11} = \left(m_a + \frac{1}{3} m_1 + \frac{1}{3} m_2 + m_3 + m_4 \right) l_1^{\,2} + \frac{I_{m1}}{N_{g1}^{\,2}}$$
$$A_{12} = m_a l_1 l_{42} Cos\left(\theta_1 - \theta_2\right)$$
$$A_{21} = m_a l_1 l_{42} Cos\left(\theta_1 - \theta_2\right)$$
$$A_{22} = \left(m_a + \frac{1}{3} m_4 \right) l_{42}^{\,2} + \frac{I_{m2}}{N_{g2}^{\,2}}$$
$$\mathrm{B}_{12} = -m_a l_1 l_{41} Sin\left(\theta_1 - \theta_2\right)$$
$$\mathrm{B}_{21} = m_a l_1 l_{41} Sin\left(\theta_1 - \theta_2\right)$$

$$C_{11} = \frac{c_{v1} + \frac{k_{t1}k_{b1}}{R_{a1}}}{N_{g1}^{\ 2}}$$

$$C_{22} = \frac{c_{v2} + \frac{k_{t2}k_{b2}}{R_{a2}}}{N_{g2}^{\ 2}}$$

$$D_1 = -\left(\frac{1}{2}w_1 + \frac{1}{2}w_2 + w_3 + w_4 + w_A\right)l_1 Cos\theta_1 + k_1 l_{k1} l_1 Cos\theta_1 - F_x l_1 Sin\theta_1 + F_y l_1 Cos\theta_1$$

$$D_2 = -w_A l_{41} Cos\theta_2 + k_2 l_{k2} l_{42} Cos\theta_2 - F_x l_{42} Sin\theta_2 + F_y l_{42} Cos\theta_2$$

$$E_1 = \frac{k_{t1}}{R_{a1}N_{g1}}$$

$$E_2 = \frac{k_{t2}}{R_{a2}N_{g2}}$$

3.3Establishment of a Reference Model

Since the goal is let the device act as if the links have no mass, the kinematic equations for impulsive force and force, Eq. (2.26) and Eq. (2.43) respectively, are the best choice for use as a reference model. In the following subsection, the reference model for impulsive force and force system is going to be derived.

3.3.1 Reference Model of Impulsive Force System

From Eq. (2.26), the matrices equation is given as:

$$\begin{bmatrix} A_{11} & A_{12} \\ A_{21} & A_{22} \end{bmatrix} \dot{X} = \begin{bmatrix} 0 & \mathrm{B}_{12} \\ \mathrm{B}_{21} & 0 \end{bmatrix} X^2 + \begin{bmatrix} D_1 \\ D_2 \end{bmatrix}, \quad X = \begin{bmatrix} \dot{\theta}_1 \\ \dot{\theta}_2 \end{bmatrix}, \quad \dot{X} = \begin{bmatrix} \ddot{\theta}_1 \\ \ddot{\theta}_2 \end{bmatrix} \tag{3.14}$$

Where:

$$A_{11} = m_a l_1^{\,2}$$
$$A_{12} = m_a l_1 l_{42} Cos(\theta_1 - \theta_2)$$
$$A_{21} = m_a l_1 l_{42} Cos(\theta_1 - \theta_2)$$
$$A_{22} = m_a l_{42}^{\,2}$$
$$\mathrm{B}_{12} = -m_a l_1 l_{41} Sin(\theta_1 - \theta_2)$$
$$\mathrm{B}_{21} = m_a l_1 l_{41} Sin(\theta_1 - \theta_2)$$
$$D_1 = -w_a l_1 Cos\theta_1 + k_1 l_{k1} l_1 Cos\theta_1$$
$$D_2 = -w_a l_{42} Cos\theta_2 + k_2 l_{k2} l_{42} Cos\theta_2$$

The equation can be more simplified by substituting Eq. (2.4) and Eq. (2.9), $w_A = k_1 l_{k1} = k_2 l_{k2}$, into the entries D_1 and D_2. The entries become zero, so the equations can be shown as:

$$\begin{aligned} m_a l_1^{\,2}\ddot{\theta}_1 + m_a l_1 l_{42}\ddot{\theta}_2 Cos(\theta_1 - \theta_2) + m_a l_1 l_{42}\dot{\theta}_2^{\,2} Sin(\theta_1 - \theta_2) = 0 \\ m_a l_{41}^{\,2}\ddot{\theta}_2 + m_a l_1 l_{42}\ddot{\theta}_1 Cos(\theta_1 - \theta_2) - m_a l_1 l_{42}\dot{\theta}_1^{\,2} Sin(\theta_1 - \theta_2) = 0 \end{aligned} \tag{3.15}$$

After simplification, they become:

$$\begin{aligned} l_1\ddot{\theta}_1 + l_{42}\ddot{\theta}_2 Cos(\theta_1 - \theta_2) + l_{42}\dot{\theta}_2^{\,2} Sin(\theta_1 - \theta_2) = 0 \\ l_{42}\ddot{\theta}_2 + l_1\ddot{\theta}_1 Cos(\theta_1 - \theta_2) - l_1\dot{\theta}_1^{\,2} Sin(\theta_1 - \theta_2) = 0 \end{aligned} \tag{3.16}$$

Express in state space form:

$$\begin{bmatrix} l_1 & l_{42}Cos(\theta_1 - \theta_2) \\ l_1 Cos(\theta_1 - \theta_2) & l_{42} \end{bmatrix} \begin{bmatrix} \ddot{\theta}_1 \\ \ddot{\theta}_2 \end{bmatrix} = \begin{bmatrix} 0 & -l_{42}Sin(\theta_1 - \theta_2) \\ l_1 Sin(\theta_1 - \theta_2) & 0 \end{bmatrix} \begin{bmatrix} \dot{\theta}_1^2 \\ \dot{\theta}_2^2 \end{bmatrix} \tag{3.17}$$

Considering the dimension of link #1 and #4, $2l_1 = l_{42}$, the equation (3.3) is shown as:

$$\begin{bmatrix} 1 & 2Cos(\theta_1 - \theta_2) \\ Cos(\theta_1 - \theta_2) & 2 \end{bmatrix} \begin{bmatrix} \ddot{\theta}_1 \\ \ddot{\theta}_2 \end{bmatrix} = \begin{bmatrix} 0 & -2Sin(\theta_1 - \theta_2) \\ Sin(\theta_1 - \theta_2) & 0 \end{bmatrix} \begin{bmatrix} \dot{\theta}_1^2 \\ \dot{\theta}_2^2 \end{bmatrix} \tag{3.18}$$

The Eq. (3.18) is the reference model for impulsive force system. It is noticeable there is only variables of generalized coordinates in the equation which means the equation kinematic equation. The $\theta(t)$ here is the angle of motion that is desired. To prevent being confusing to the reader with the angle of kinetic motion, the angle of the reference model is referred to as $\theta_d(t)$. Thus, equation (3.18) is expressed as:

$$\begin{bmatrix} 1 & 2Cos(\theta_{d1}-\theta_{d2}) \\ Cos(\theta_{d1}-\theta_{d2}) & 2 \end{bmatrix}\begin{bmatrix} \ddot{\theta}_{d1} \\ \ddot{\theta}_{d2} \end{bmatrix} = \begin{bmatrix} 0 & -2Sin(\theta_{d1}-\theta_{d2}) \\ Sin(\theta_{d1}-\theta_{d2}) & 0 \end{bmatrix}\begin{bmatrix} \dot{\theta}_{d1}^2 \\ \dot{\theta}_{d2}^2 \end{bmatrix} \quad (3.19)$$

3.3.2 Reference Model of Force System

Next, the reference model of force system is concerned. It can be found through similar procedure. From Eq. (2.43), the matrices equation is given as:

$$\begin{bmatrix} A_{11} & A_{12} \\ A_{21} & A_{22} \end{bmatrix}\dot{X} = \begin{bmatrix} 0 & \mathrm{B}_{12} \\ \mathrm{B}_{21} & 0 \end{bmatrix}X^2 + \begin{bmatrix} D_1 \\ D_2 \end{bmatrix}, \quad X = \begin{bmatrix} \dot{\theta}_1 \\ \dot{\theta}_2 \end{bmatrix}, \quad \dot{X} = \begin{bmatrix} \ddot{\theta}_1 \\ \ddot{\theta}_2 \end{bmatrix} \quad (3.20)$$

$$A_{11} = m_a l_1^{\,2}$$
$$A_{12} = m_a l_1 l_{42} Cos(\theta_1 - \theta_2)$$
$$A_{21} = m_a l_1 l_{42} Cos(\theta_1 - \theta_2)$$
$$A_{22} = m_a l_{42}^{\,2}$$
$$\mathrm{B}_{12} = -m_a l_1 l_{42} Sin(\theta_1 - \theta_2)$$
$$\mathrm{B}_{21} = m_a l_1 l_{42} Sin(\theta_1 - \theta_2)$$
$$D_1 = -w_a l_1 Cos\theta_1 + k_1 l_{k1} l_1 Cos\theta_1 - F_x l_1 Sin\theta_1 + F_y l_1 Cos\theta_1$$
$$D_2 = -w_a l_{42} Cos\theta_2 + k_2 l_{k2} l_{42} Cos\theta_2 - F_x l_{42} Sin\theta_2 + F_y l_{42} Cos\theta_2$$

The equation can be more simplified by substituting Eq. (2.4) and Eq. (2.9), $w_A = k_1 l_{k1} = k_2 l_{k2}$, into the entries D_1 and D_2. The entries become:

$$D_1 = -F_x l_1 Sin\theta_1 + F_y l_1 Cos\theta_1$$
$$D_2 = -F_x l_{42} Sin\theta_2 + F_y l_{42} Cos\theta_2 \tag{3.21}$$

Thus, the equations can be shown as:

$$m_a {l_1}^2 \ddot{\theta}_1 + m_a l_1 l_{42} \ddot{\theta}_2 Cos(\theta_1 - \theta_2) + m_a l_1 l_{42} \dot{\theta}_2^2 Sin(\theta_1 - \theta_2) + F_x l_1 Sin\theta_1 - F_y l_1 Cos\theta_1 = 0$$
$$m_a {l_{42}}^2 \ddot{\theta}_2 + m_a l_1 l_{42} \ddot{\theta}_1 Cos(\theta_1 - \theta_2) - m_a l_1 l_{42} \dot{\theta}_1^2 Sin(\theta_1 - \theta_2) + F_x l_{42} Sin\theta_2 - F_y l_{42} Cos\theta_2 = 0 \tag{3.22}$$

After simplification, they become:

$$l_1 \ddot{\theta}_1 + l_{42} \ddot{\theta}_2 Cos(\theta_1 - \theta_2) + l_{42} \dot{\theta}_2^2 Sin(\theta_1 - \theta_2) + \frac{F_x Sin\theta_1 - F_y Cos\theta_1}{m_a} = 0$$
$$l_{42} \ddot{\theta}_2 + l_1 \ddot{\theta}_1 Cos(\theta_1 - \theta_2) - l_1 \dot{\theta}_1^2 Sin(\theta_1 - \theta_2) + \frac{F_x Sin\theta_2 - F_y Cos\theta_2}{m_a} = 0 \tag{3.23}$$

Recall that $2l_1 = l_{42}$ and expressed in the state space form:

$$\begin{bmatrix} 1 & 2Cos(\theta_1 - \theta_2) \\ Cos(\theta_1 - \theta_2) & 2 \end{bmatrix} \begin{bmatrix} \ddot{\theta}_1 \\ \ddot{\theta}_2 \end{bmatrix} = \begin{bmatrix} 0 & -2Sin(\theta_1 - \theta_2) \\ Sin(\theta_1 - \theta_2) & 0 \end{bmatrix} \begin{bmatrix} \dot{\theta}_1^2 \\ \dot{\theta}_2^2 \end{bmatrix} + \begin{bmatrix} \frac{-F_x Sin\theta_1 + F_y Cos\theta_1}{m_a l_1} \\ \frac{-F_x Sin\theta_2 + F_y Cos\theta_2}{m_a l_1} \end{bmatrix} \tag{3.24}$$

For the same reason, denote kinematic angle as$\theta_d(t)$. The equation (3.24) can be shown as:

$$\begin{bmatrix} 1 & 2Cos(\theta_{d1} - \theta_{d2}) \\ Cos(\theta_{d1} - \theta_{d2}) & 2 \end{bmatrix} \begin{bmatrix} \ddot{\theta}_{d1} \\ \ddot{\theta}_{d2} \end{bmatrix} = \begin{bmatrix} 0 & -2Sin(\theta_{d1} - \theta_{d2}) \\ Sin(\theta_{d1} - \theta_{d2}) & 0 \end{bmatrix} \begin{bmatrix} \dot{\theta}_{d1}^2 \\ \dot{\theta}_{d2}^2 \end{bmatrix} + \begin{bmatrix} \frac{-F_x Sin\theta_{d1} + F_y Cos\theta_{d1}}{m_a l_1} \\ \frac{-F_x Sin\theta_{d2} + F_y Cos\theta_{d2}}{m_a l_1} \end{bmatrix} \tag{3.25}$$

3.4 Adjustment Mechanism

The adjustment mechanism takes the form:

$$e_a = \begin{bmatrix} e_{a1} \\ e_{a2} \end{bmatrix} = \begin{bmatrix} \varepsilon_1 & \dot{\varepsilon}_1 \\ \varepsilon_2 & \dot{\varepsilon}_2 \end{bmatrix} \begin{bmatrix} g_s \\ g_v \end{bmatrix} + \begin{bmatrix} e_{f1} \\ e_{f2} \end{bmatrix} \tag{3.26}$$

The number in the subscript indicates the variables related to the number of motors and the g_s and g_v are the selected gain for the error in angular displacements and angular velocities respectively.

It is a combination of a regulator and an adaptation tuner. The first term is the regulator which is a vector product of the selected fixed gain and $\varepsilon(t)$, $\varepsilon(\dot{t})$. The function of the regulator is let the output voltage converge to a certain value which is zero in this case. The second term is the adaptation tuner which is derived from the gradient of the deviation function, $J = \frac{1}{2}\left(\varepsilon^2 + \dot{\varepsilon}^2\right)$, and it tends to adjust the chosen parameter, w, which is proportional to the gradient of the error, $\varepsilon(t)$ or $\varepsilon(\dot{t})$, but in opposite direction and minimize the deviation function. The method is so called MIT rule. The adaptation tuner for each motor takes the form:

$$e_f = \left[w_{s1} + w_{s2}\right]\theta_d(t) + \left[w_{v1} + w_{v2}\right]\dot{\theta}_d(t) + \left[w_{a1} + w_{a2}\right]\ddot{\theta}_d(t) \tag{3.27}$$

The parameter, w, can be regarded as the sensitivity of the system error to itself and its derivative, $\dot{w}$, represents the sensitivity derivative of the system error which shows how error is influenced by the parameter. The *s*, *v*, and *a* in the subscript is corresponding to θ_d, $\dot{\theta}_d$, and $\ddot{\theta}_d$. For w_{s1}, it is given as:

$$\dot{w}_{s1} = -\gamma \frac{\partial \varepsilon}{\partial w_{s1}} \varepsilon \tag{3.28}$$

γ is the selected fixed gain. According to MIT rule, the gradient of the error with respect to the adjusting parameters is given as:

$$-\frac{\partial \varepsilon}{\partial w_{\mathrm{sn}}} = \theta_d \,, \quad -\frac{\partial \dot{\varepsilon}}{\partial w_{vn}} = \dot{\theta}_d \,, \quad -\frac{\partial \ddot{\varepsilon}}{\partial w_{an}} = \ddot{\theta}_d \,, \quad \text{n=1,2} \tag{3.29}$$

Then the equation becomes:

$$\dot{w}_{s1} = -\gamma \frac{\partial \varepsilon}{\partial w_{s1}} \varepsilon = \gamma \theta_d \varepsilon \tag{3.30}$$

For all the parameters, they can be shown as:

$$\begin{aligned} &\dot{w}_{s1} = \gamma \theta_d \varepsilon \;;\; \dot{w}_{s2} = \gamma \theta_d \dot{\varepsilon} \\ &\dot{w}_{v1} = \gamma \dot{\theta}_d \varepsilon \;;\; \dot{w}_{s2} = \gamma \dot{\theta}_d \dot{\varepsilon} \\ &\dot{w}_{a1} = \gamma \ddot{\theta}_d \varepsilon \;;\; \dot{w}_{a2} = \gamma \ddot{\theta}_d \dot{\varepsilon} \end{aligned} \tag{3.31}$$

The number in the subscript indicates it is related to the error of angular displacements or angular velocities. Since there are two motors in the system, one more number is added in the subscript at the front to specify the number of motors.

$$\begin{aligned} e_{1f} &= \left[w_{1s1} + w_{1s2} \right] \theta_{1d}(t) + \left[w_{1v1} + w_{1v2} \right] \dot{\theta}_{1d}(t) + \left[w_{1a1} + w_{1a2} \right] \ddot{\theta}_{1d}(t) \\ e_{2f} &= \left[w_{2s1} + w_{2s2} \right] \theta_{2d}(t) + \left[w_{2v1} + w_{2v2} \right] \dot{\theta}_{2d}(t) + \left[w_{2a1} + w_{2a2} \right] \ddot{\theta}_{2d}(t) \end{aligned} \tag{3.32}$$

3.5 Simulation of System Dynamics with Adaptive Control

The effectiveness of the feed-forward adaptive control will be shown in the following simulation, so the most deviated cases are chosen: the impulsive force or force applied in vertical and horizontal direction. α_P and α_F denote the angle which impulsive force and force is applied with respect to the horizontal line. The initial condition is the same for each

case in same force applied direction with or without adaptive control. The system parameters setup is listed in the Table B.1 for impulsive force system and Table B.2 for force system. To generalize the simulation and let the result could be more instinctively perceived by the reader. The output shown in the results is the torque directly exerting on the links instead of the output voltage to motors.

3.5.1 Trajectory of Impulsive Force System

$(1)\,\alpha_P = \dfrac{\pi}{2}$

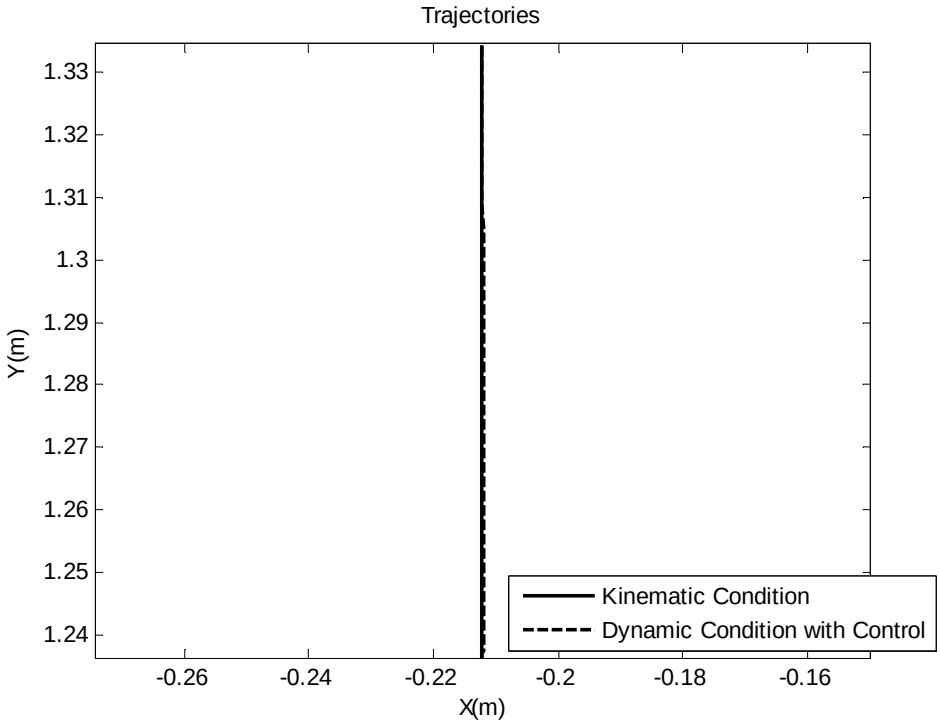

Fig. 3.3(a): Trajectories of the Test Article with and without Feed-Forward Adaptive Control Due to an Impulsive Force Applied at 90 Degrees

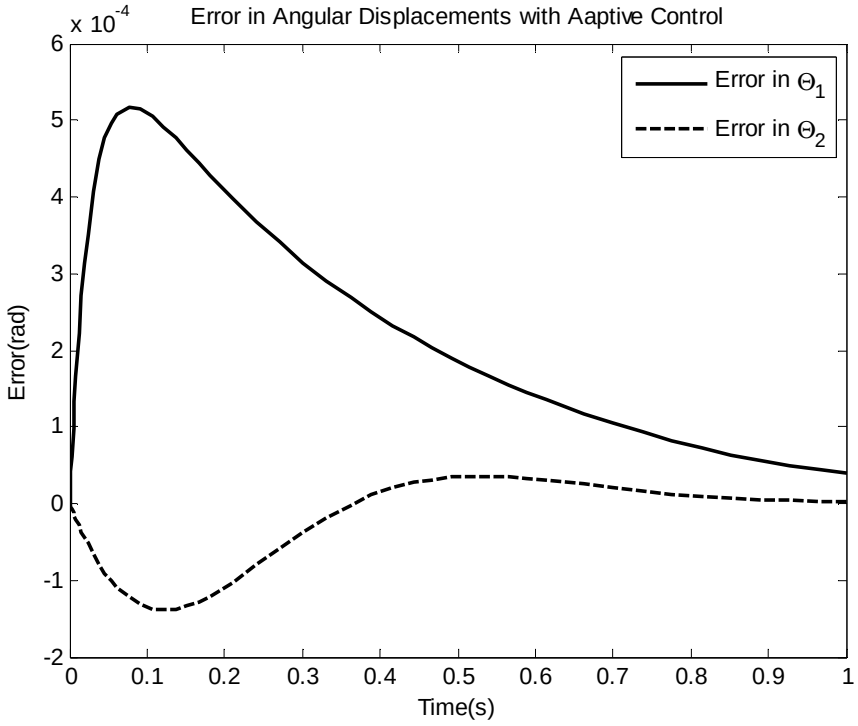

Fig. 3.3(b): Displacements of the Test Article with and without Feed-Forward Adaptive Control in θ_1 Due to an Impulsive Force Applied at 90 Degrees

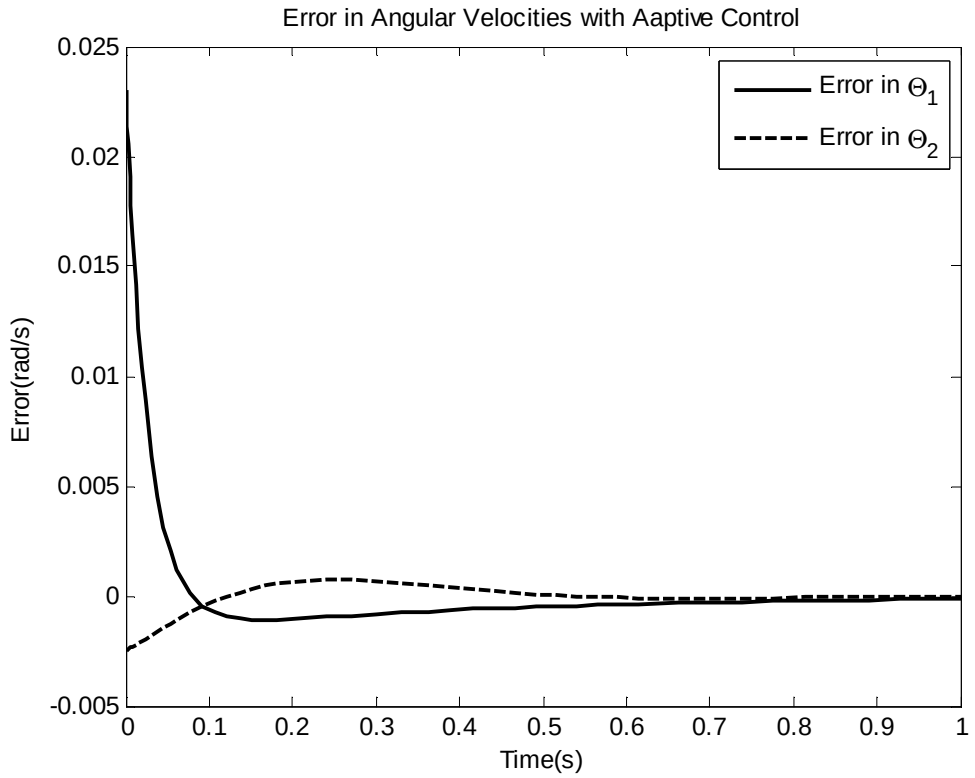

Fig. 3.3(c): Displacements of the Test Article with and without Feed-Forward Adaptive Control in θ_2 Due to an Impulsive Force Applied at 90 Degrees

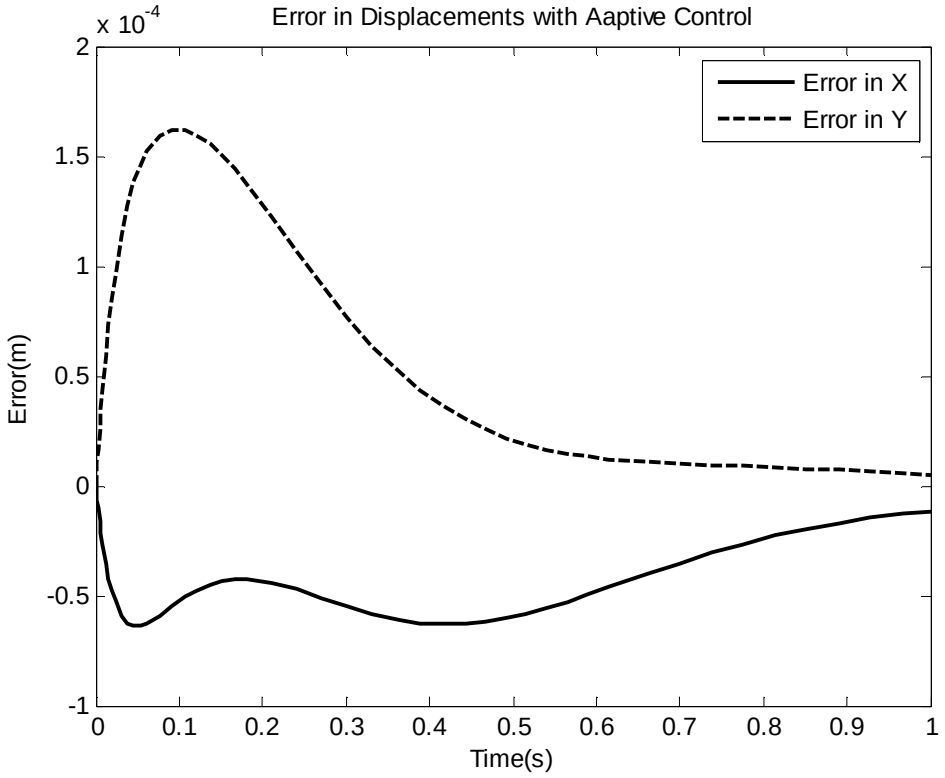

Fig. 3.3(d): Velocities of the Test Article with and without Feed-Forward Adaptive Control in θ_1 Due to an Impulsive Force Applied at 90 Degrees

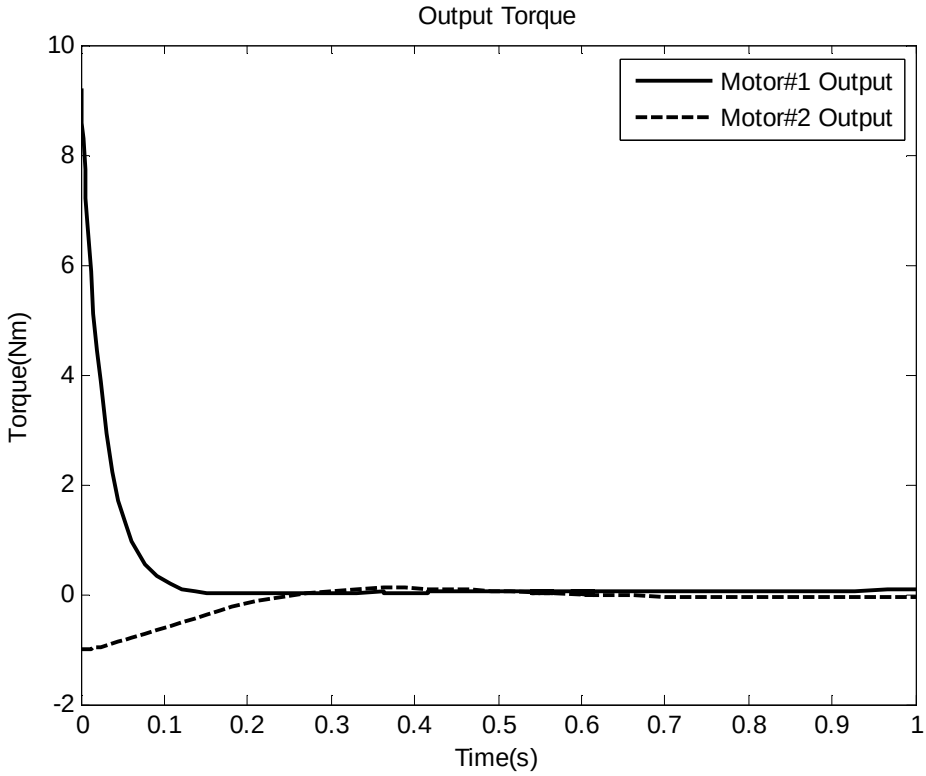

Fig. 3.3(e): Velocities of the Test Article with and without Feed-Forward Adaptive Control in θ_2 Due to an Impulsive Force Applied at 90 Degrees

Considering the Fig. 3.3(a), the test article moves upward and it is obvious that the trajectory with adaptive control is almost overlapping with the kinematic trajectory near the end of simulation. Fig. 3.3(b) and Fig. 3.3(c) demonstrate the error in angular displacements and velocities converge to zero. Then check it with Fig. 3.3(d), both the displacement error in X, Y direction are successfully reduced to less than 10^{-5} m. Compared to the diameter of hair, 0.1 mm, this means the control method nearly eliminated the downgrade effect of the inertia of the links. Furthermore, the output torque for both motors, Fig. 3.3(e), is continuous and the maximum value of output is 8 Nm. These all show the control method and the mechanism design is applicable and practical. The two springs support the weight of the whole device and the motors just need to take care of the inertia of the links while moving.

$(2)\alpha_p = \pi$

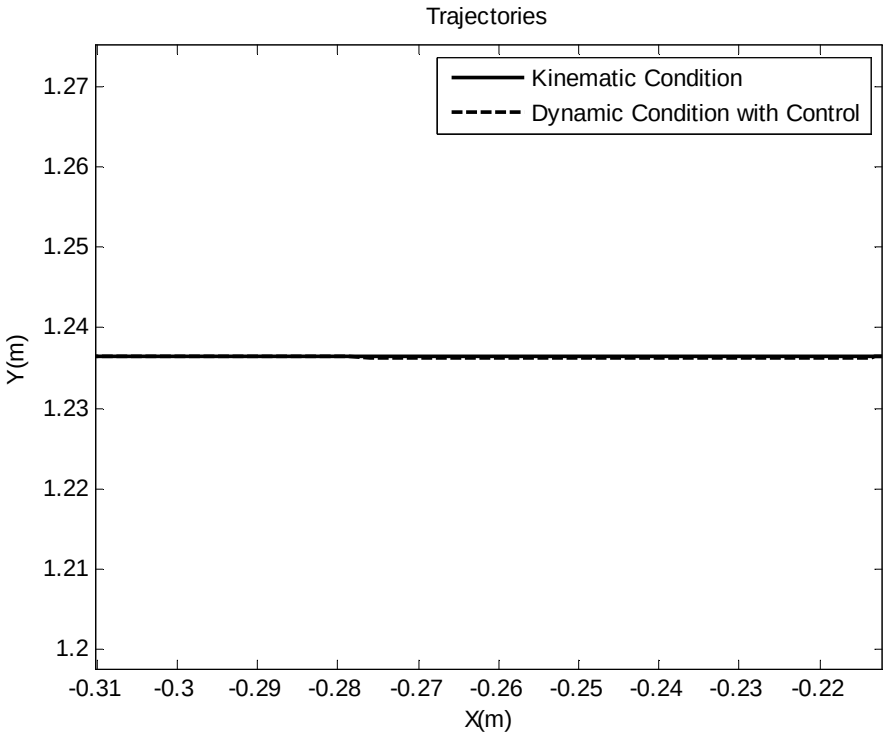

Fig. 3.4(a): Trajectories of the Test Article with and without Feed-Forward Adaptive Control Due to an Impulsive Force Applied at180 Degrees

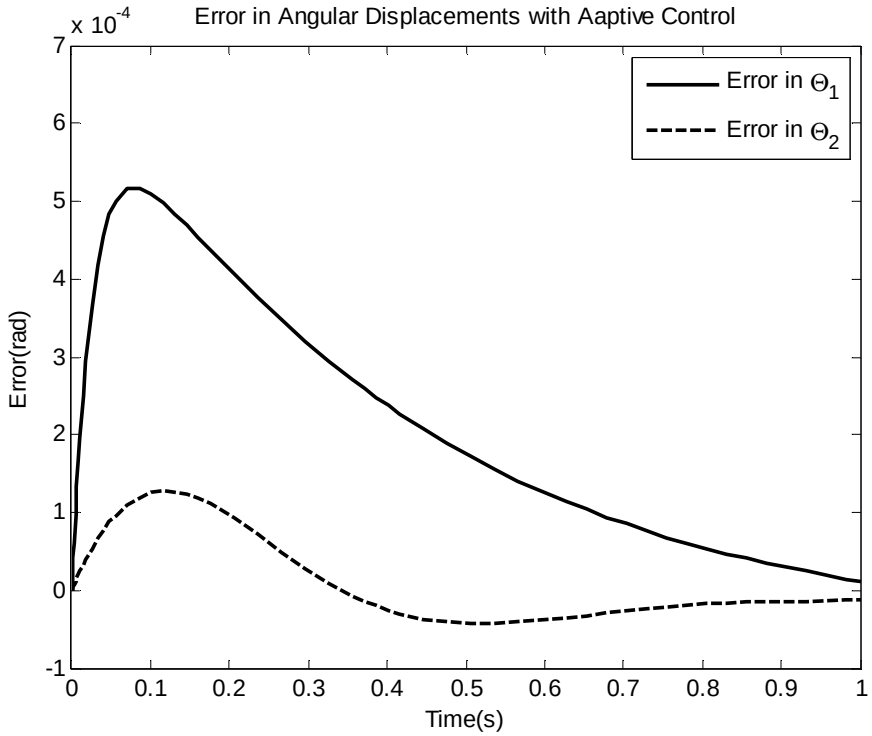

Fig. 3.4(b): Displacements of the Test Article with and without Feed-Forward Adaptive Control in θ_1 Due to an Impulsive Force Applied at 180 Degrees

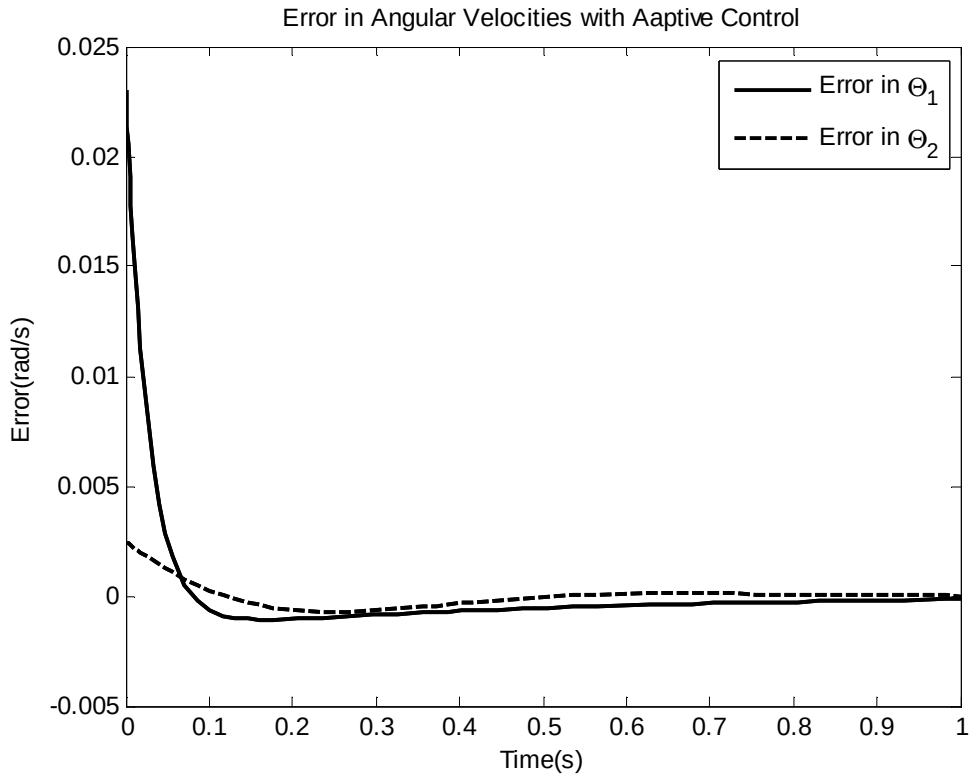

Fig. 3.4(c): Displacements of the Test Article with and without Feed-Forward Adaptive Control in θ_2 Due to an Impulsive Force Applied at 180 Degrees

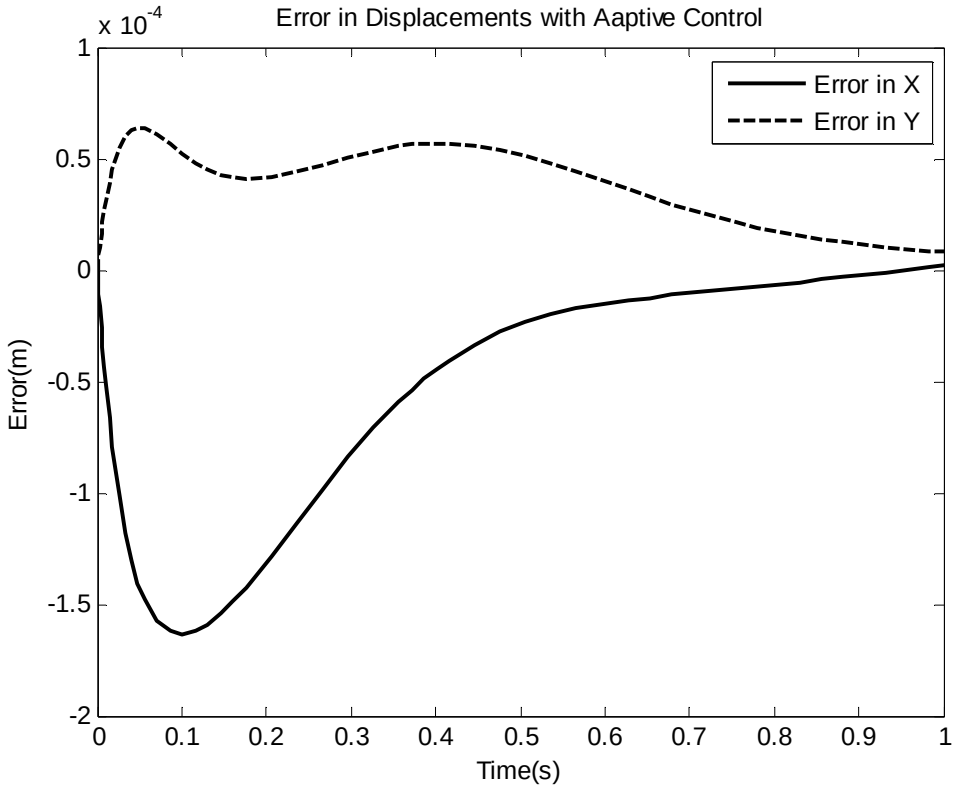

Fig. 3.4(d): Velocities of the Test Article with and without Feed-Forward Adaptive Control in θ_1 Due to an Impulsive Force Applied at 180 Degrees

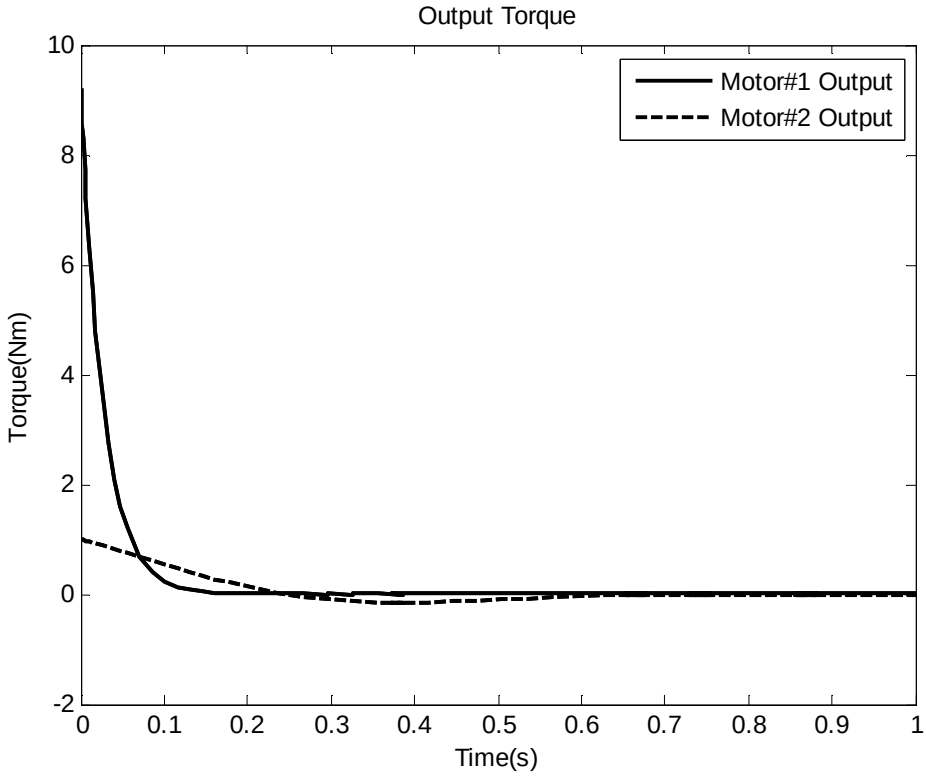

Fig. 3.4(e): Velocities of the Test Article with and without Feed-Forward Adaptive Control in θ_2 Due to an Impulsive Force Applied at 180 Degrees

In the Fig. 3.4(a) and Fig. 3.4(d), the error of the displacement is well controlled and converges to zero. It has been shown in Fig. 3.4(b) and Fig. 3.4(c) that both the error of angular displacement and velocity decrease to zero. The maximum output is nearly 8.5 Nm which is applicable.

3.5.2 Trajectory of Force System

$(1)\alpha_F = \frac{\pi}{2}$

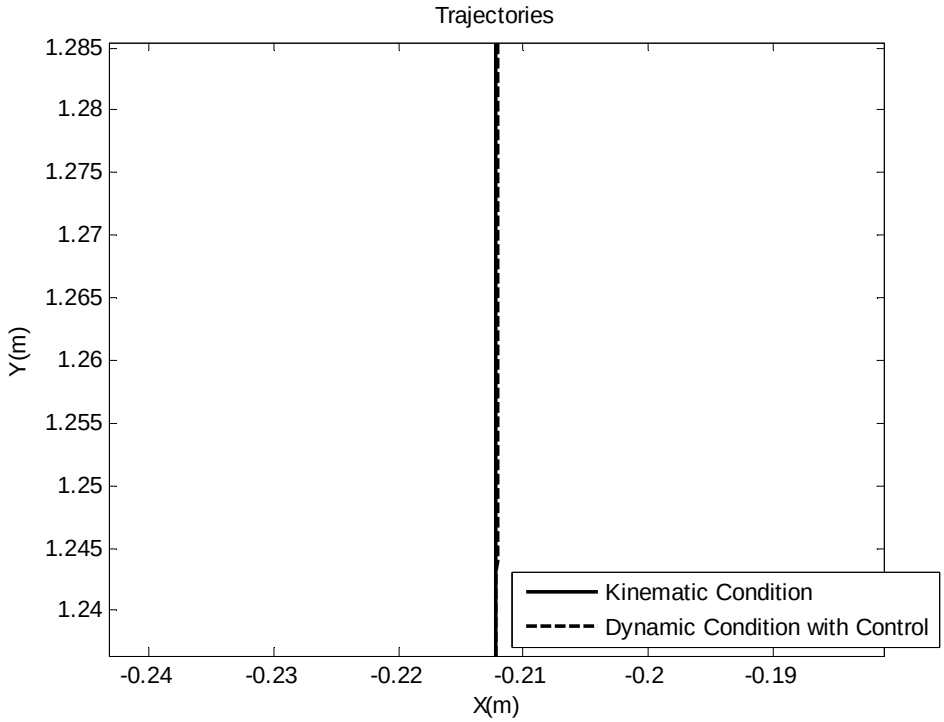

Fig. 3.5(a): Trajectories of the Test Article with and without Feed-Forward Adaptive Control Due to a Force Applied at 90 Degrees

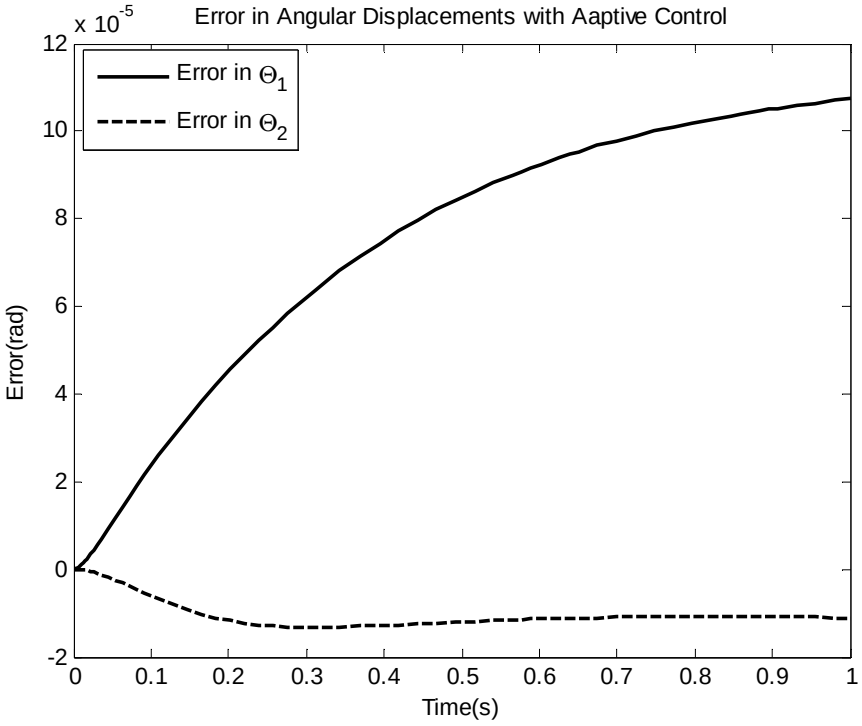

Fig. 3.5(b): Displacements of the Test Article with and without Feed-Forward Adaptive Control in θ_1 Due to a Force Applied at 90 Degrees

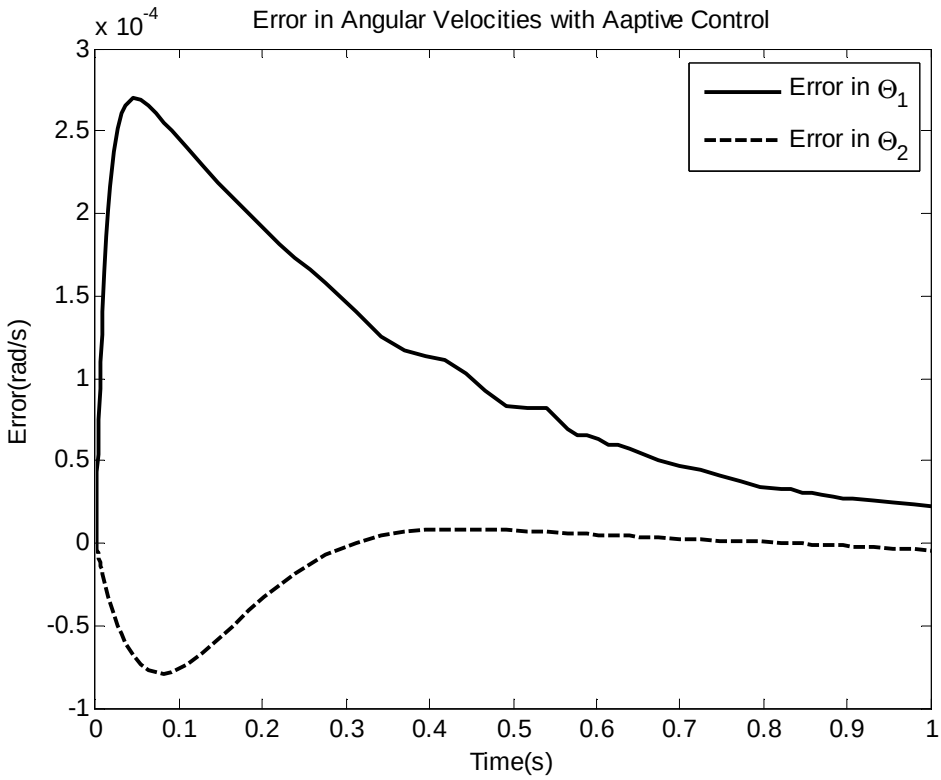

Fig. 3.5(c): Displacements of the Test Article with and without Feed-Forward Adaptive Control in θ_2 Due to a Force Applied at 90 Degrees

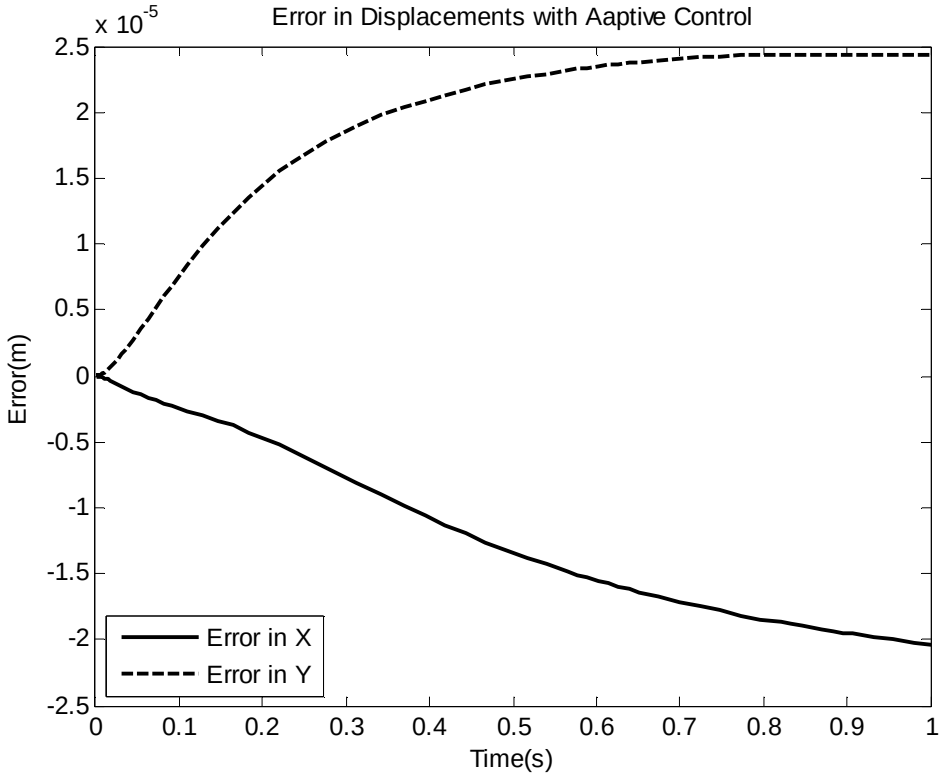

Fig. 3.5(d) : Velocities of the Test Article with and without Feed-Forward Adaptive Control in θ_1 Due to a Force Applied at 90 Degrees

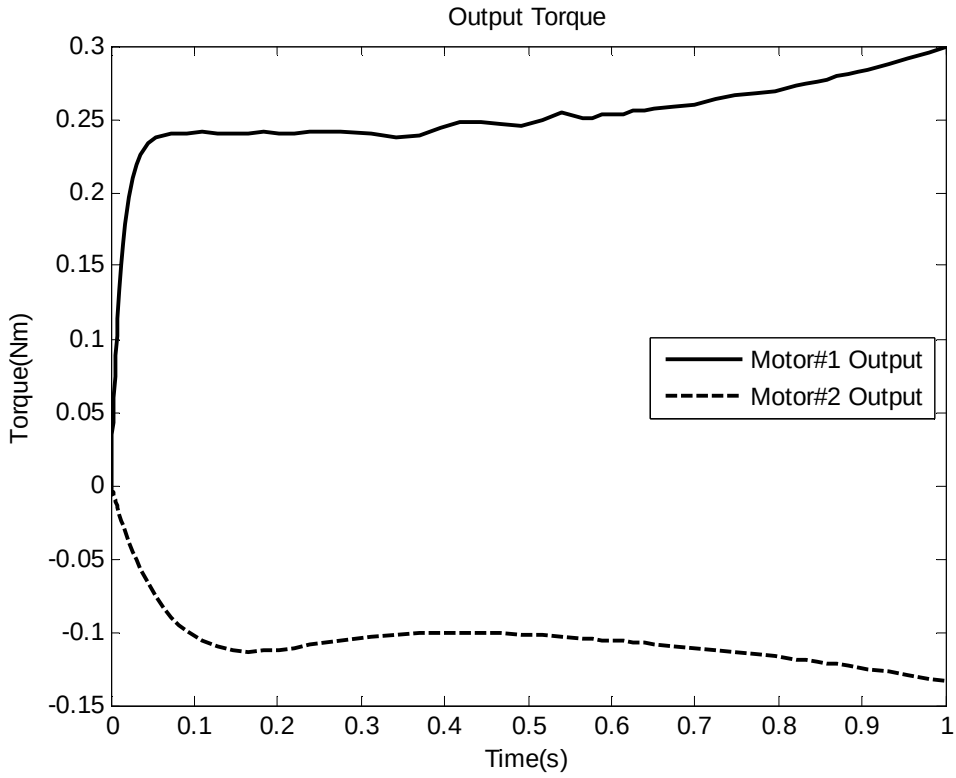

Fig. 3.5(e): Velocities of the Test Article with and without Feed-Forward Adaptive Control in θ_2 Due to a Force Applied at 90 Degrees

It is shown in Fig. 3.5(a) the trajectory is well controlled. Even though the error in Fig. 3.4(b) and Fig. 3.5(c) do not converge to zero, the errors approach to a fixed value which is less than 10^{-4} in unit. The results have already proven the control method still works pretty well in the force system, even the angular acceleration is disregarded in the adjustment mechanism setup which helps reduce the torque needed in control to avoid the needed torque becomes too large to be applicable. It is also noticeable the torque needed in force system is much more less than the one in impulsive force system. It results in the initial angular velocity of impulsive system is different from the kinematic one. Though the difference is small, the motors still have to drive the links with larger torque to make the compensation in a short period of time.

$(2)\alpha_F = \pi$

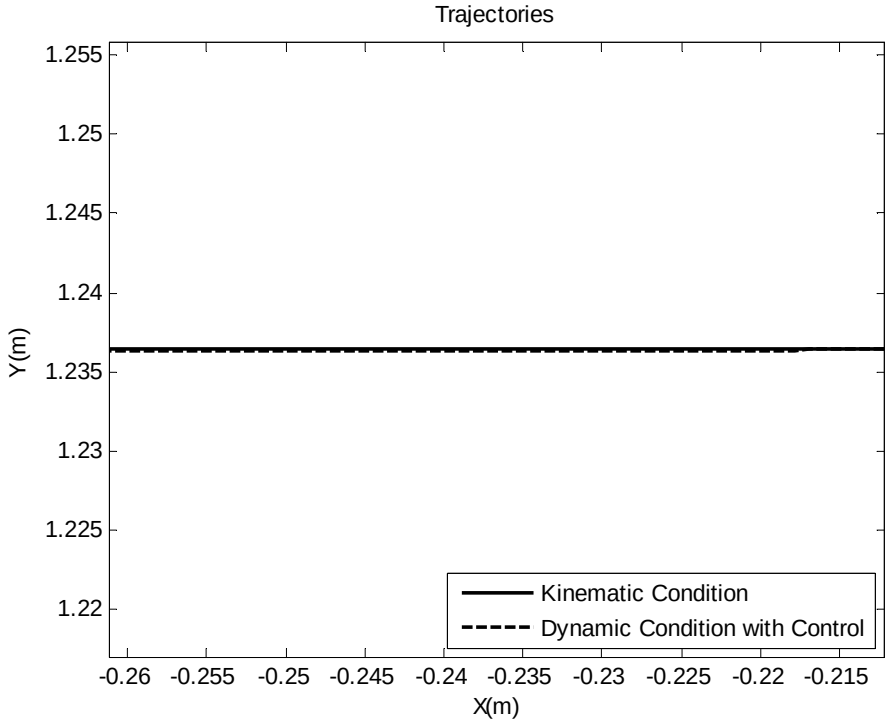

Fig. 3.6(a): Trajectories of the Test Article with and without Feed-Forward Adaptive Control Due to a Force Applied at 180 Degrees

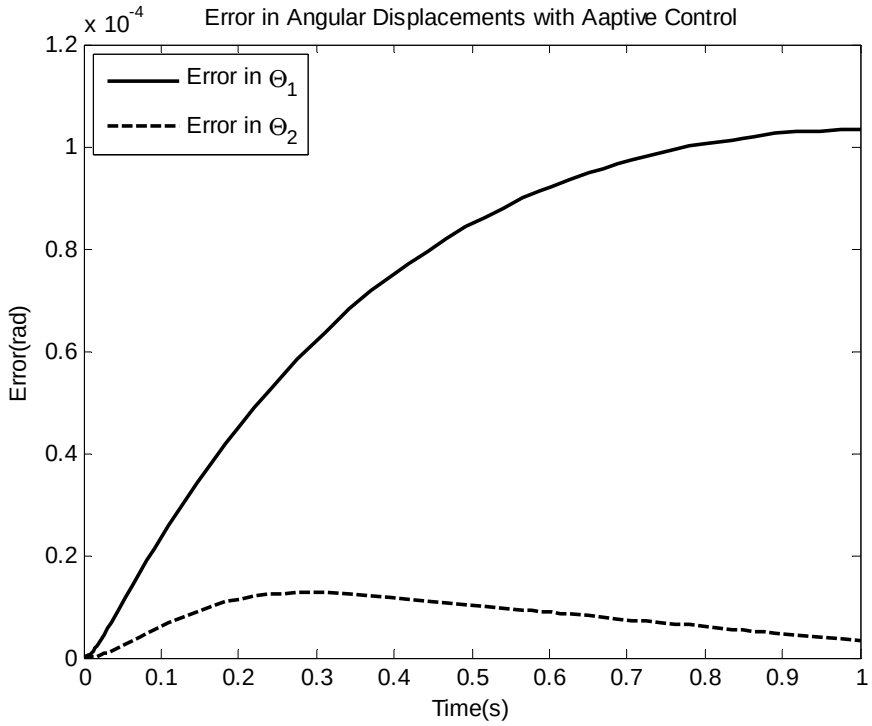

Fig. 3.6(b): Displacements of the Test Article with and without Feed-Forward Adaptive Control in θ_1 Due to a Force Applied at 180 Degrees

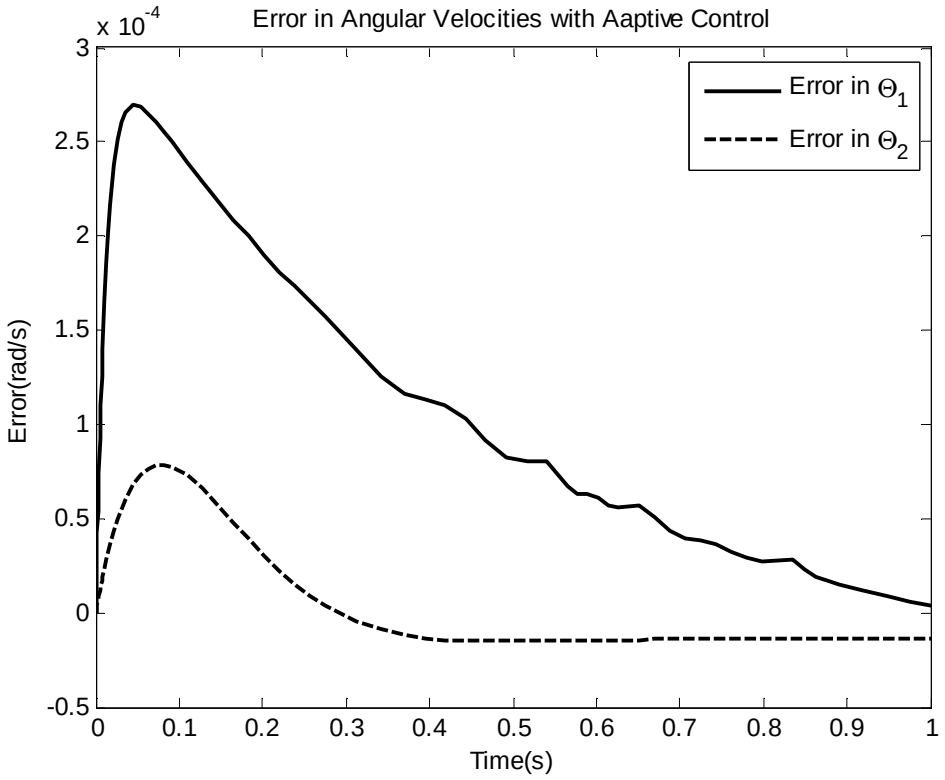

Fig. 3.6(c): Displacements of the Test Article with and without Feed-Forward Adaptive Control in θ_2 Due to a Force Applied at 180 Degrees

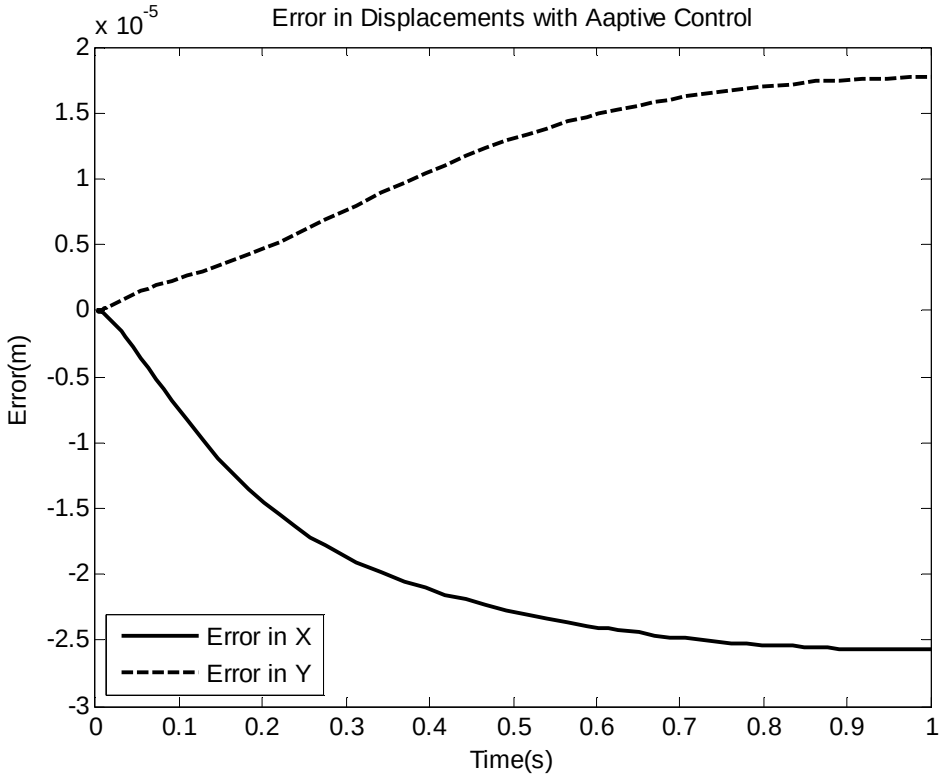

Fig. 3.6(d): Velocities of the Test Article with and without Feed-Forward Adaptive Control in θ_1 Due to a Force Applied at 180 Degrees

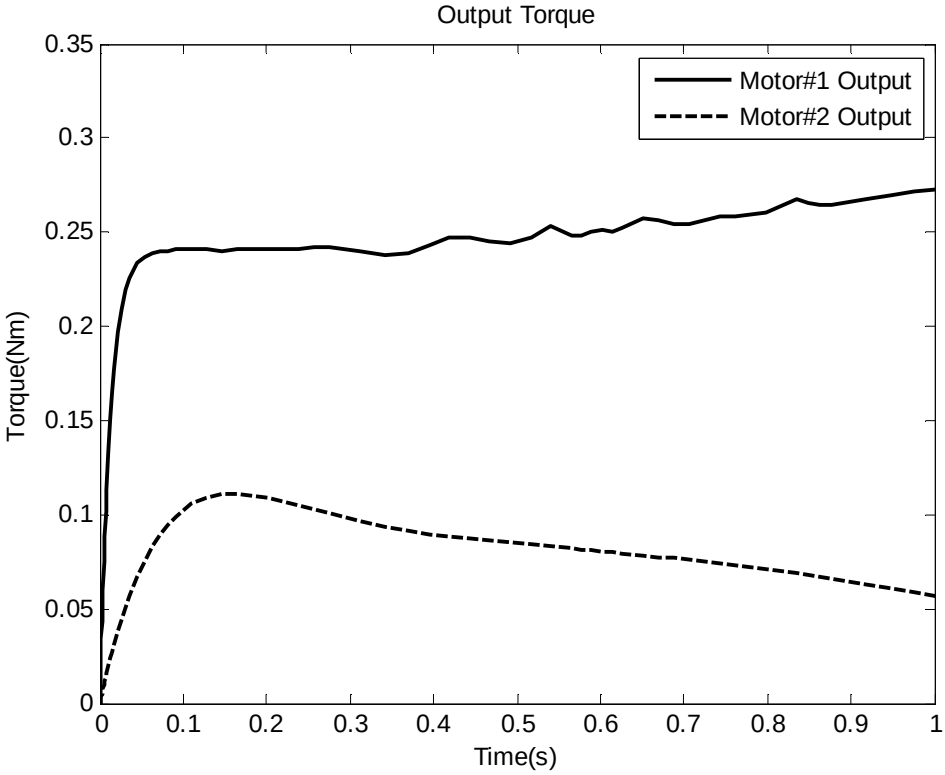

Fig. 3.6(e): Velocities of the Test Article with and without Feed-Forward Adaptive Control in θ_2 Due to a Force Applied at 180 Degrees

In the Fig. 3.6(a) and Fig. 3.6(d), the error of the displacement is negligible and the system response is nearly identical to the kinematic trajectory. Although it has been shown in Fig. 3.4(b) and Fig. 3.4(d) that the error don't decrease to zero, the error do converge to a fixed value less than 10^{-4} in unit which is still an outstanding performance for the controller. The maximum output is nearly 2.75 Nm which is applicable.

Chapter 4

Application to Lower-limb Rehabilitation

The major application of this kind of the gravity compensation devices is just creating a zero gravity environment for lab experiments to simulate the environment in space and this is indeed what the devices are built for at first. However, people now start looking for new possibility on the devices. It is not news that the system is used as a rehabilitation device. In 2004, the team in the Mechanical Systems Lab in University of Delaware created a gravity balancing mechanism to directly reduce the load on the lower limb while walking [8,9].

Here the function of the device is providing constant support to ease the load on the lower limb for those who need to train their weakened muscle after injury. The traditional solution is hooked patient on one side of the leverage and adding the counter-weight on the other side. Imaging that if a 90 kg man was suspended, there are 180kg actually loading on the machine! The device is definitely bulky and heavy. Besides, the patients can only be allowed walking on the treadmill. The only advantage is the supporting force is always constant without any control.

In our design, to avoid the complicated and various from person to person leg motion analysis, the patient is suspended on the waist and hip, near the center of mass(CoM) of the body. Through this method, only the CoM of human gait is need to be concerned and the device won’t interfere the leg motion and the support is valid for both legs. Since the spring

takes the load, the device will be much lighter than the counter-weight design and can let patient walk around like walking aid. If the trajectory shift was the major issues, the control method discussed before is handy to cope with.

4.1 Walking Pattern Analysis

The most tricky point is, unlike an applied force in previous system, the system is actually constrained by the displacement of CoM of the body. The force can still be used to achieve an approximation result of control in simulation. More details will be discussed later in this section. However, according to the paper published by Alan Crowe [7] in1995, the motion of CoM while walking in Z direction can be nearly described by trigonometric function, sine or cosine with phase shift and the amplitude is varied from person to person. The trajectory of CoM versus gait phase is given as:

$$d_y = A \bullet Cos\left(2\pi ft + \frac{5}{6}\pi\right) \qquad (4.1)$$

d_y d is the vertical displacement of CoM. A denotes the maximum amplitude of the shift and the f represents the frequency of walking pace. Now assuming the maximum CoM shift is 0.02 m, the trajectory versus gait phase can be shown in Fig. (4.1)

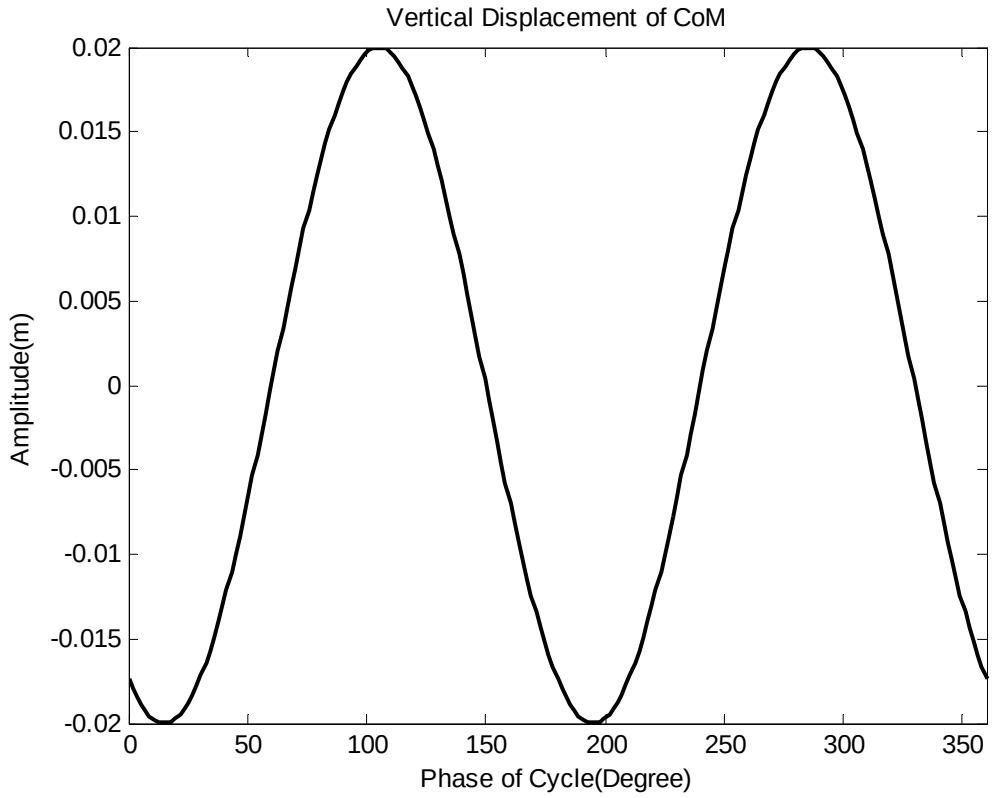

Fig. (4.1): The Vertical Displacement of CoM of a Human Body While Walking

One should notice that this turns out to be a simple harmonic motion. Therefore, the velocity and acceleration can be given as:

$$v_y = -2\pi f \bullet A \bullet Sin\left(2\pi ft + \frac{5}{6}\pi\right) \tag{4.2}$$

$$a_y = -\left(2\pi f\right)^2 \bullet A \bullet C\,\mathrm{os}\left(2\pi ft + \frac{5}{6}\pi\right) \tag{4.3}$$

Since the system is constrained by the displacement of CoM, the force becomes an unknown variable. For the system which links are massless (kinematic mode), the force can be found directly by:

$$F_{leg} = F_d + m_a \bullet a_y \quad , \quad F_d = w_a - F_{LF} \tag{4.4}$$

Where F_{leg} is the force supported by the leg and F_{LF} is the lifting force provided by the device.

Eq. (4.4) does not work for the case which links has mass (kinetic mode). It is also need to be clarified that the force discuss here and in simulation is the force provided by the leg to drive the mass moving on the assigned trajectory instead of suspension force.

To find out how the force varies through time, it is need to convert the generalized coordinates from x, y to θ_1, θ_2. Using Eq. (2.14), three sets of equations derived from displacement, velocity, and acceleration is shown to be:

$$\begin{cases} l_1 Cos\theta_1 + l_{42} Cos\theta_2 = 0 \\ l_1 Sin\theta_1 + l_3 + l_{42} Sin\theta_2 = A \bullet Cos\left(2\pi ft + \frac{5}{6}\pi\right) \end{cases} \tag{4.5}$$

$$\begin{cases} -l_1\dot{\theta}_1 Sin\theta_1 - l_{42}\dot{\theta}_2 Sin\theta_2 = 0 \\ l_1\dot{\theta}_1 Cos\theta_1 + l_{42}\dot{\theta}_2 Cos\theta_2 = -2\pi f \bullet A \bullet Sin\left(2\pi ft + \frac{5}{6}\pi\right) \end{cases} \tag{4.6}$$

$$\begin{cases} -l_1\ddot{\theta}_1 Sin\theta_1 - l_{42}\ddot{\theta}_2 Sin\theta_2 - l_1\dot{\theta}_1^2 Cos\theta_1 - l_{42}\dot{\theta}_2^2 Cos\theta_2 = 0 \\ l_1\ddot{\theta}_1 Cos\theta_1 + l_{42}\ddot{\theta}_2 Cos\theta_2 - l_1\dot{\theta}_1^2 Sin\theta_1 - l_{42}\dot{\theta}_2^2 Sin\theta_2 = -\left(2\pi f\right)^2 \bullet A \bullet C\,\mathrm{os}\left(2\pi ft + \frac{5}{6}\pi\right) \end{cases} \tag{4.7}$$

Because of the nonlinearity of the first set of equation, it is impossible to find unique solution for conversion. Only thing can be done is converting the numerical value of motion from x, y coordinates to θ_1, θ_2 coordinates. To solve these sets of equations, the first set of equation, Eq. (4.5), needs to be solved by the nonlinear solver in Matlab to find the angular displacements. Then substitute them back in to Eq. (4.6), the Eq. (4.6) become linear equations and can be solved by linear solver. Repeating the same procedure in solving Eq. (4.7), all the value of variables can be found. Then substitute all the value of variables into Eq. (2.42) and Eq. (2.43). The force needed in both kinetic mode and kinematic mode can be found.

To exam the accuracy of this method, the force directly derived from Eq. (4.4) in kinematic mode is compared with the results. In the simulation, the suspended mass is 100 kg and supporting force by the device is 800 newton. Consult Table C.1 for more details in parameter setup. In Fig. 4.2 and Fig. 4.3, it is can be seen that the error in x direction is negligible and the force in y direction is overlapping with each other. All of these prove the method is correct and feasible.

Next, the force needed in x, y directions in kinetic mode is concerned. In Fig. 4.4, it is noticeable that the force in x direction is not zero anymore due to the influence of the inertia of the links. On the other hand, it shows the force in y direction in kinetic mode in dash line comparing with the force in kinematic mode in solid line in Fig. 4.5. One could find the force in kinetic mode is larger which can be anticipated, since there is an effect of inertia of the links. To be more insightful, the error shows in Fig. 4.6 indicates that the upper part and the lower part divided by the center line, F=200 N in Fig. 4.5, of the force in the kinetic mode is not symmetric which also contributes to the inertia effect. However, considering the magnitude of the differences, it is one fiftieth less than the total force supported by the leg no matter in which direction. This means the device works pretty well even without control. If the force in the y direction is real concerned, the adaptive control method is readily to be applied.

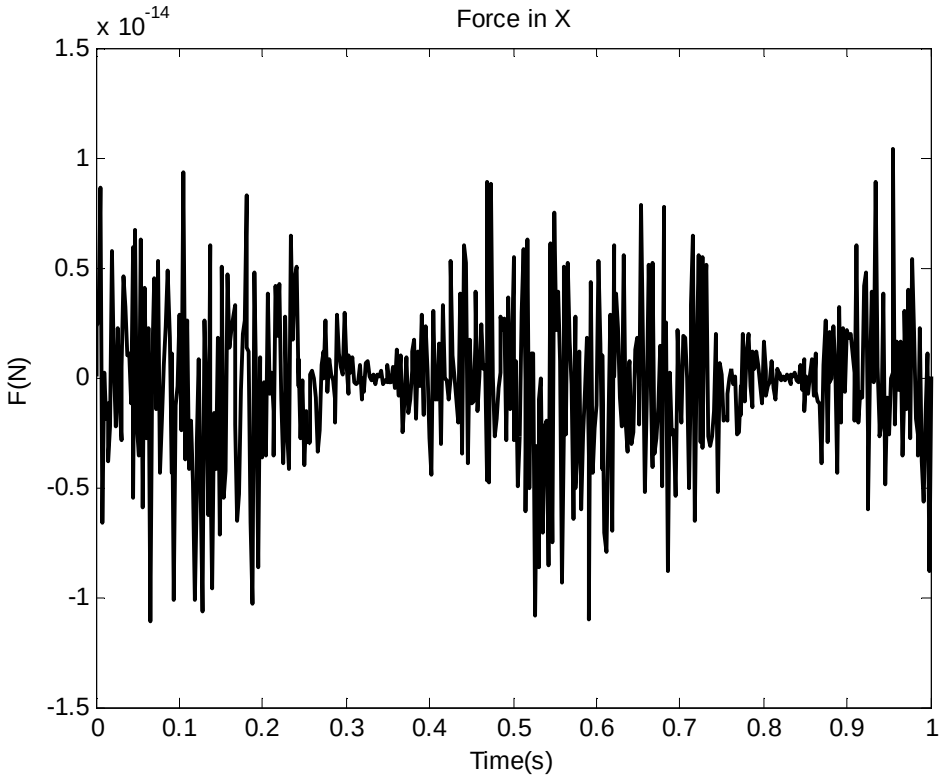

Fig. 4.2: The Force in X Direction Derived from the Vertical Displacement of CoM in Kinematic Condition

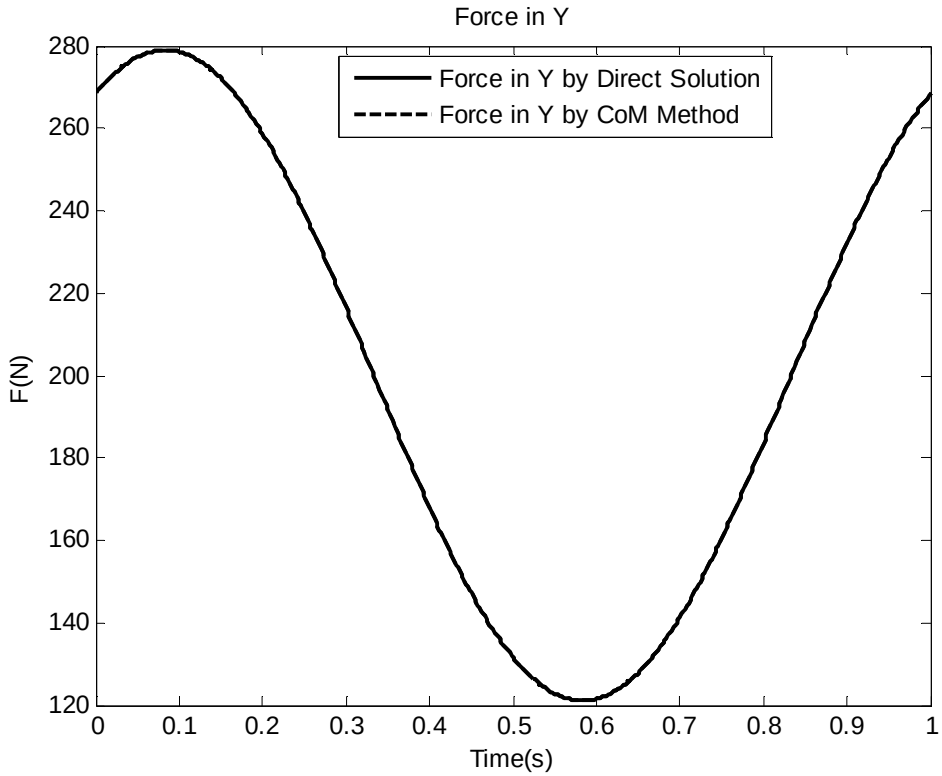

Fig. 4.3: The Force in Y Direction Derived from the Vertical Displacement of CoM in Kinematic Condition

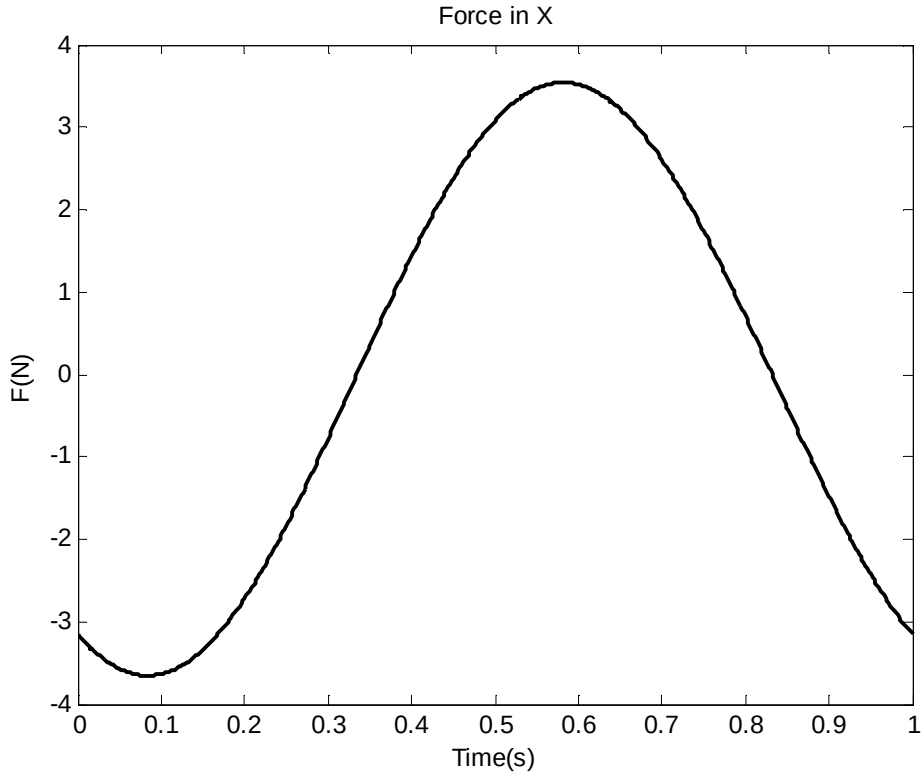

Fig. 4.4: The Force in X Direction Derived from the Vertical Displacement of CoM in Dynamic Condition

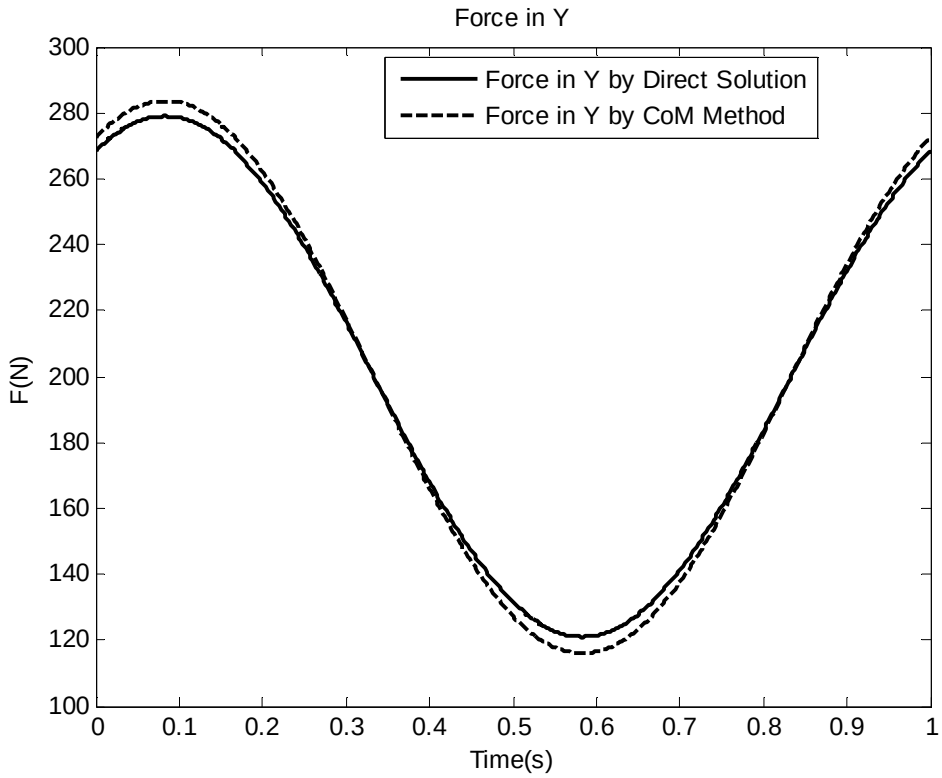

Fig. 4.5: The Force in Y Direction Derived from the Vertical Displacement of CoM in Dynamic Condition

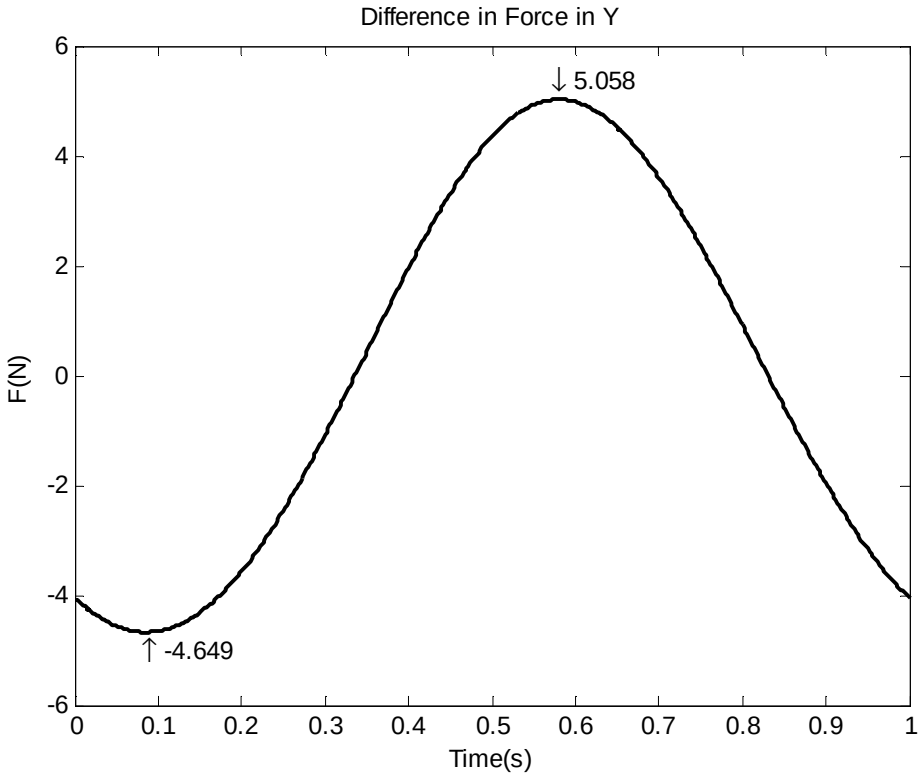

Fig. 4.6: The Difference in the Forces in Kinematic and Dynamic Condition

4.2 Trajectory Simulation

In the real application, it is not practical to ask the embedded system installed on the device which is in charge of control to compute the equations in real time basis. Since the force differences in both direction, it is reasonable to be simplified the applied force into:

$$F_{leg} = F_d + m_a \bullet a_y = F_d + m_a \bullet -\left(2\pi f\right)^2 \bullet A \bullet C\cos\left(2\pi ft + \frac{5}{6}\pi\right) \tag{4.8}$$

Using the same parameter setup in previous simulation, Eq. (4.7) is given as:

$$F_{leg} = 200 + 8\pi^2 Cos(2\pi t + \frac{5}{6}\pi) \tag{4.9}$$

Since the initial position is designated, the initial condition of angular displacement and velocity be found through Eq. (4.5) and (4.6). Consult Table C.2 for more details about the controller setup.

Comparing both the kinematic and the kinetic trajectories in Fig. 4.6 and 4.7, it is almost identical. Although there are small displacements in both directions in Fig. 4.8 and 4.9 due to disregard the force difference, the shift less than 0.01 m is acceptable after 60 seconds simulation. It can be shown in Fig. 4.12 that the error converge and oscillate around zero in 10 seconds. Despite the error is oscillating instead of decreasing to zero, the amplitude of the oscillation is less than 10^{-5} in radius which is small enough. The output torque of motor #1 and #2 are shown in Fig. 4.13. The output torque is continuous and around 2 Nm in maximum which means the control method is doable.

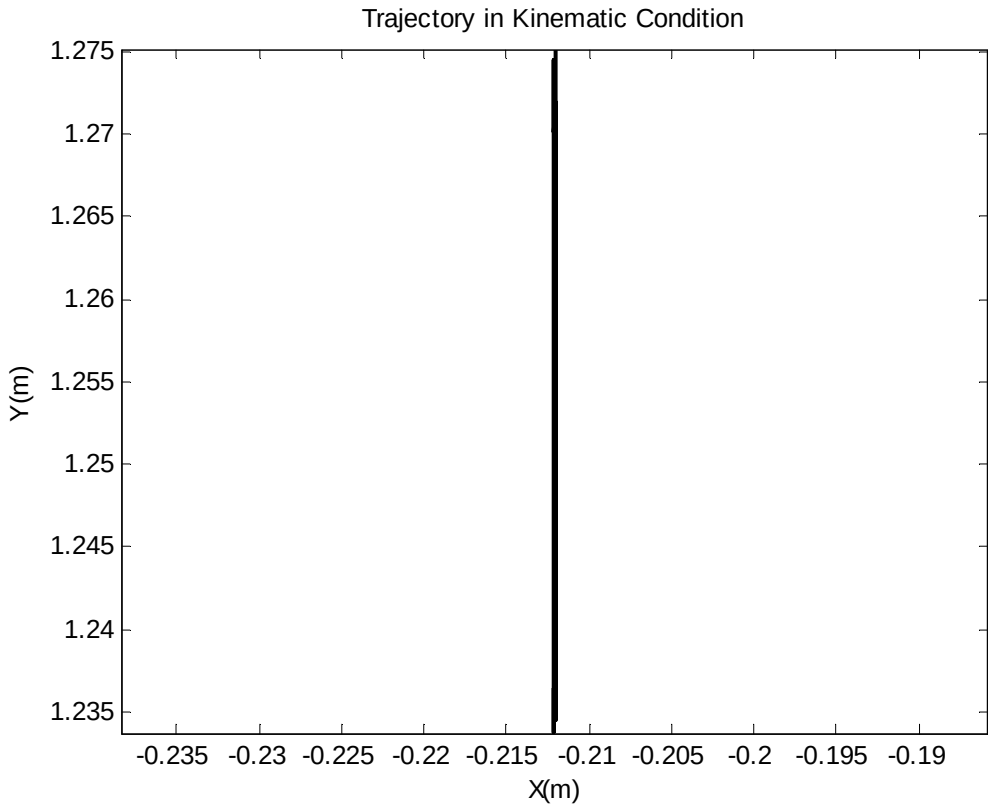

Fig. 4.7: The kinematic Trajectory in Walking Pattern Simulation

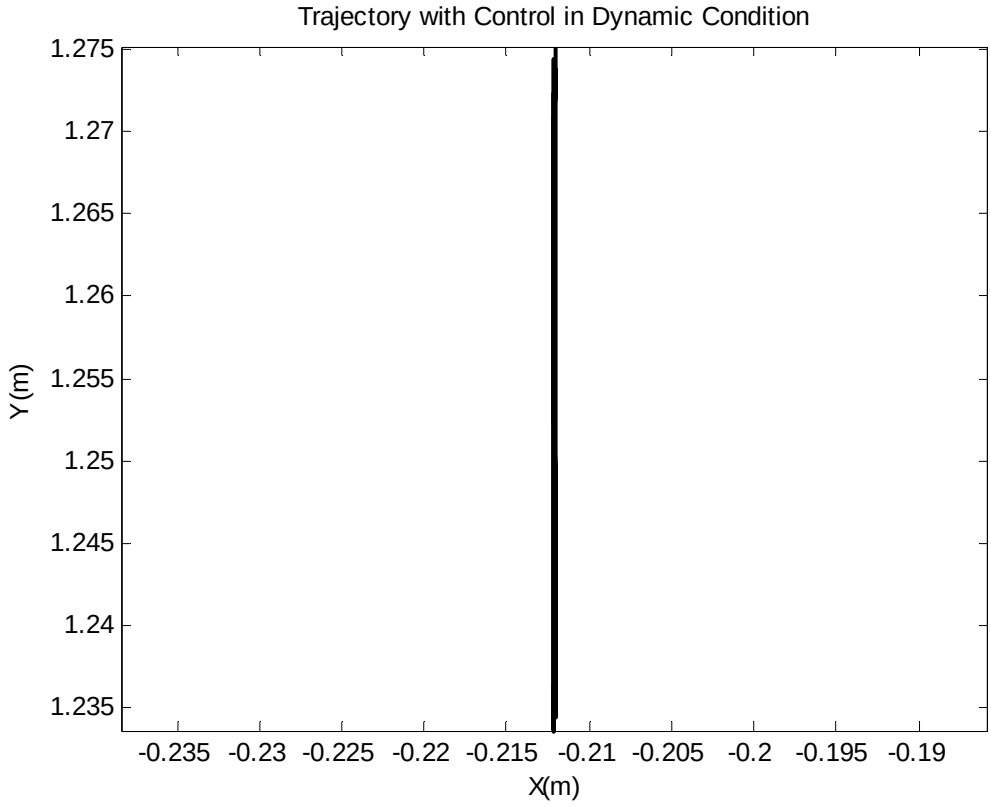

Fig. 4.8: The Dynamic Trajectory in Walking Pattern Simulation

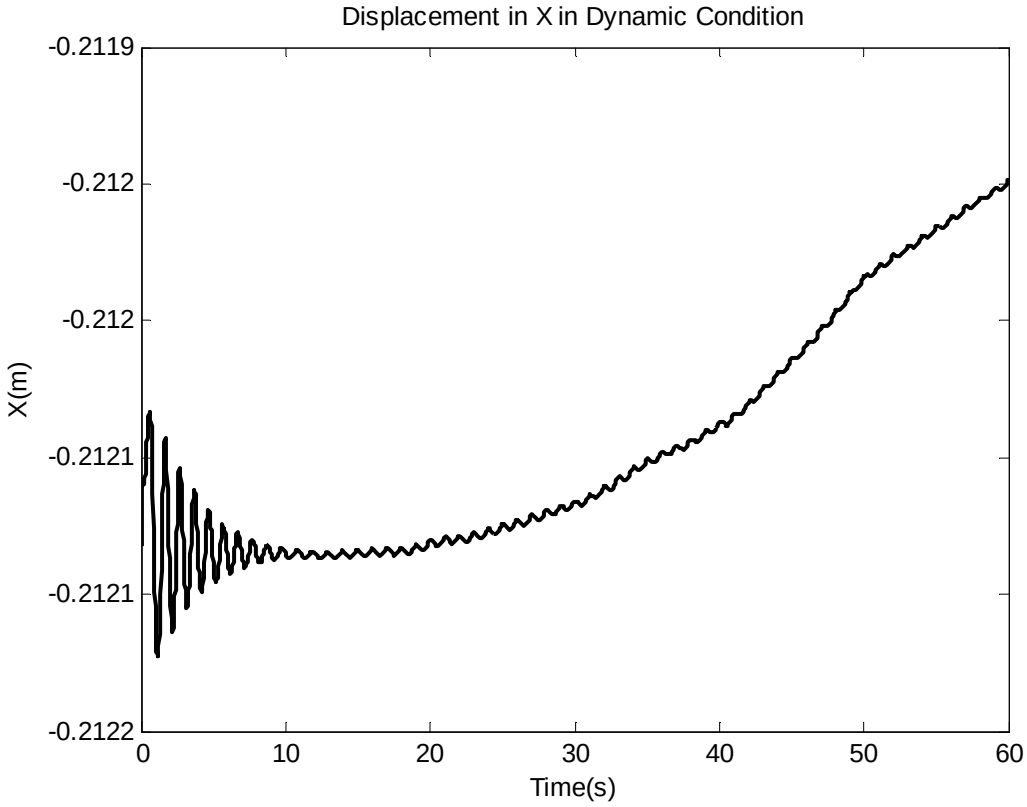

Fig. 4.9: The Dynamic Displacement in X Direction in Walking Pattern Simulation

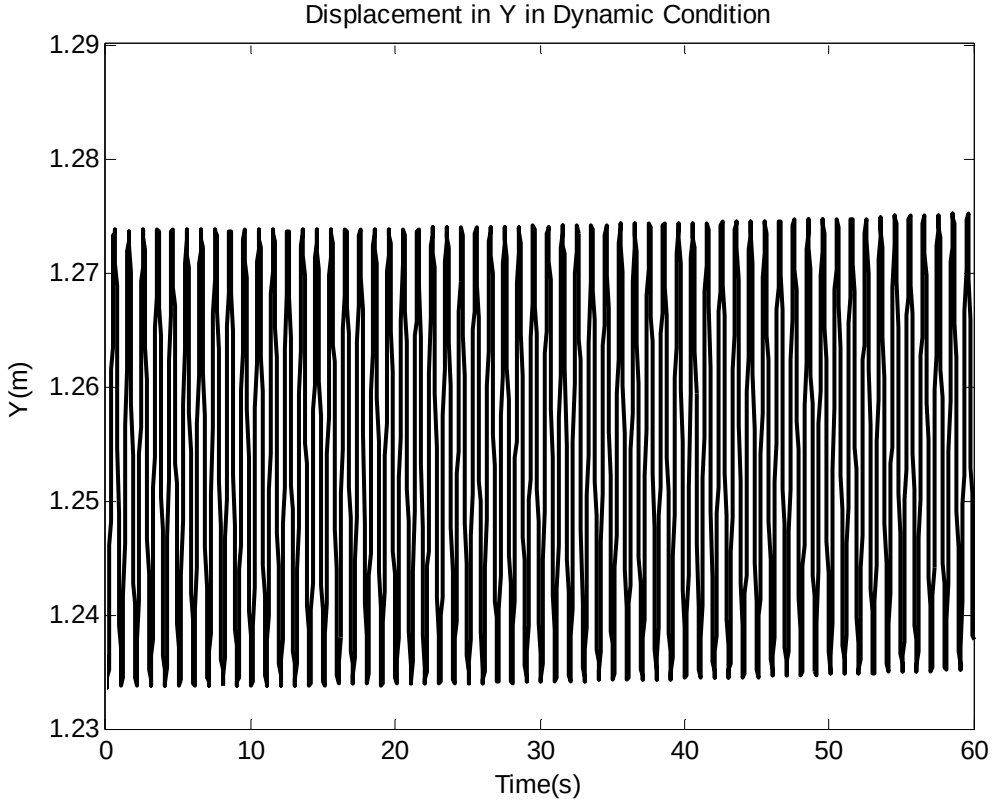

Fig. 4.10: The Dynamic Displacement in Y Direction in Walking Pattern Simulation

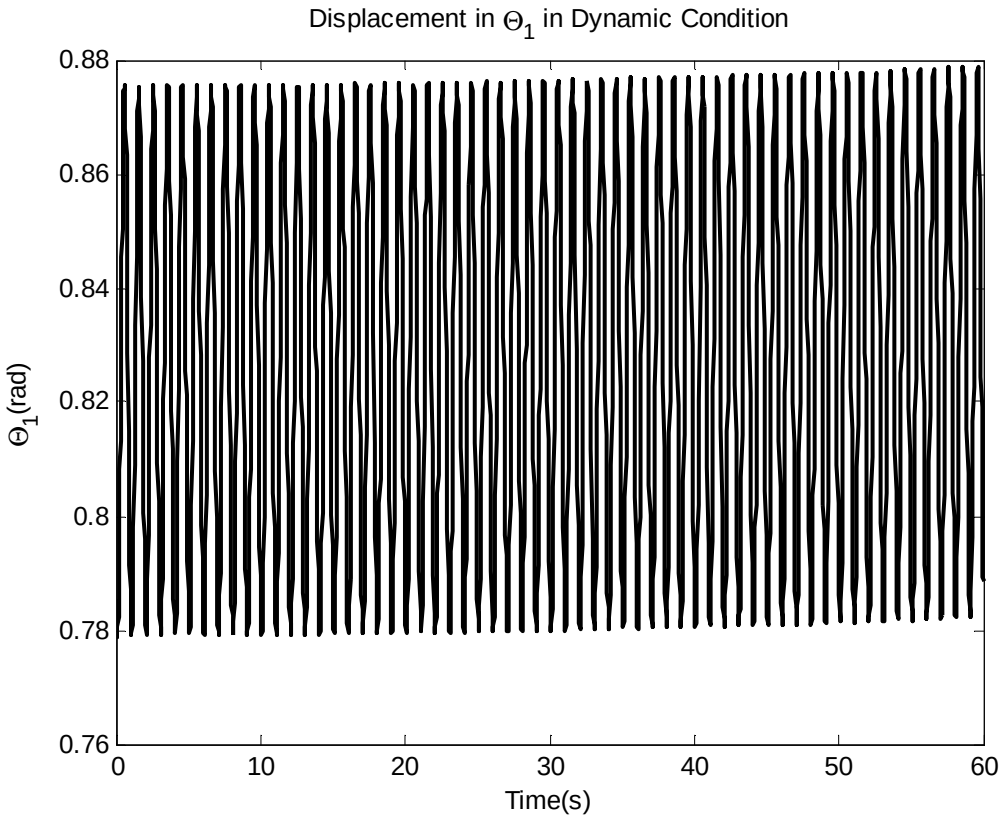

Fig. 4.11: The Dynamic Displacement in θ_1 in Walking Pattern Simulation

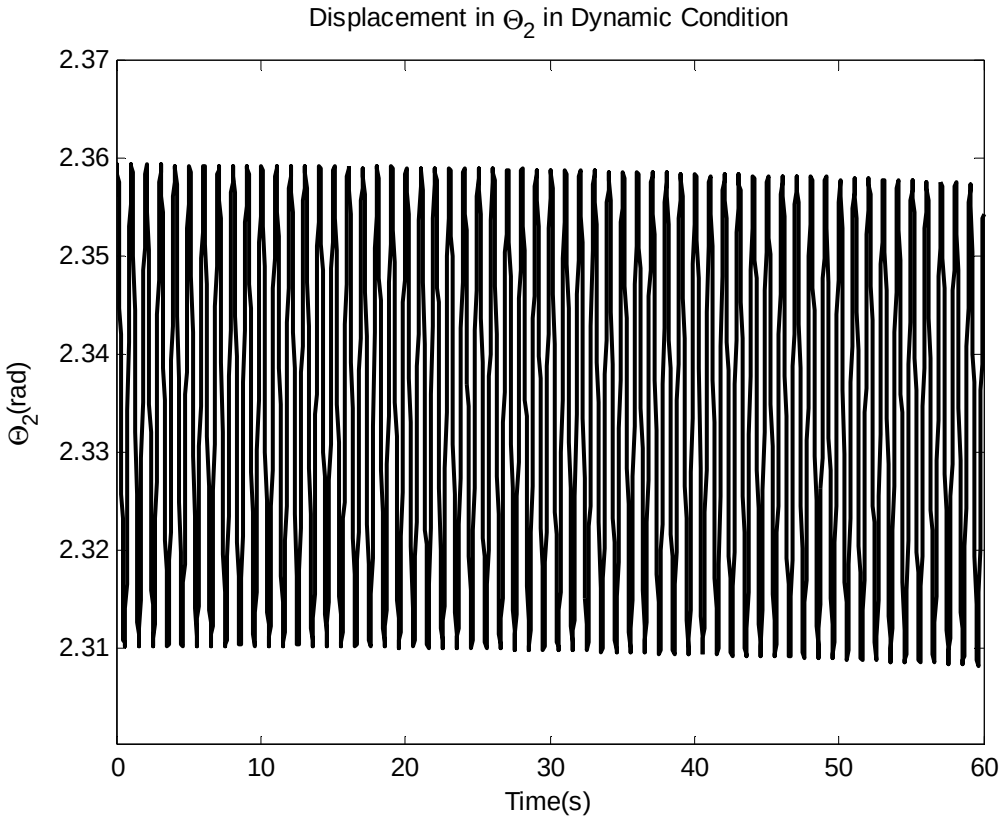

Fig. 4.12: The Dynamic Displacement in θ_2 in Walking Pattern Simulation

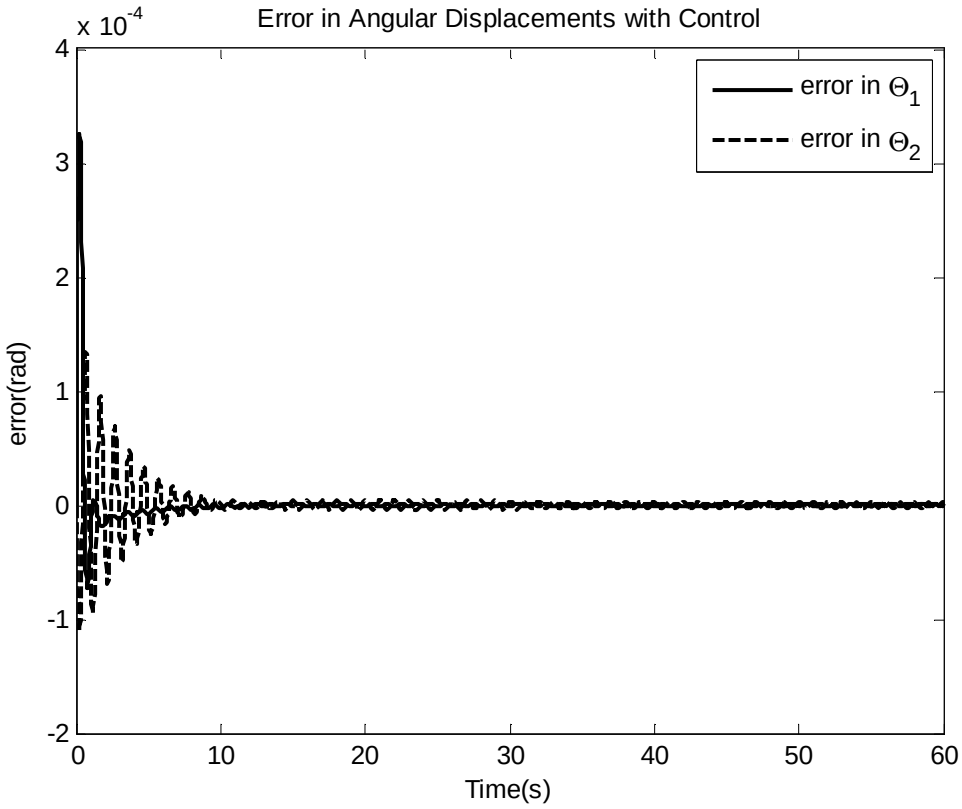

Fig. 4.13: The Error in $\theta_1\theta_2$ with Feed-Forward Adaptive Control

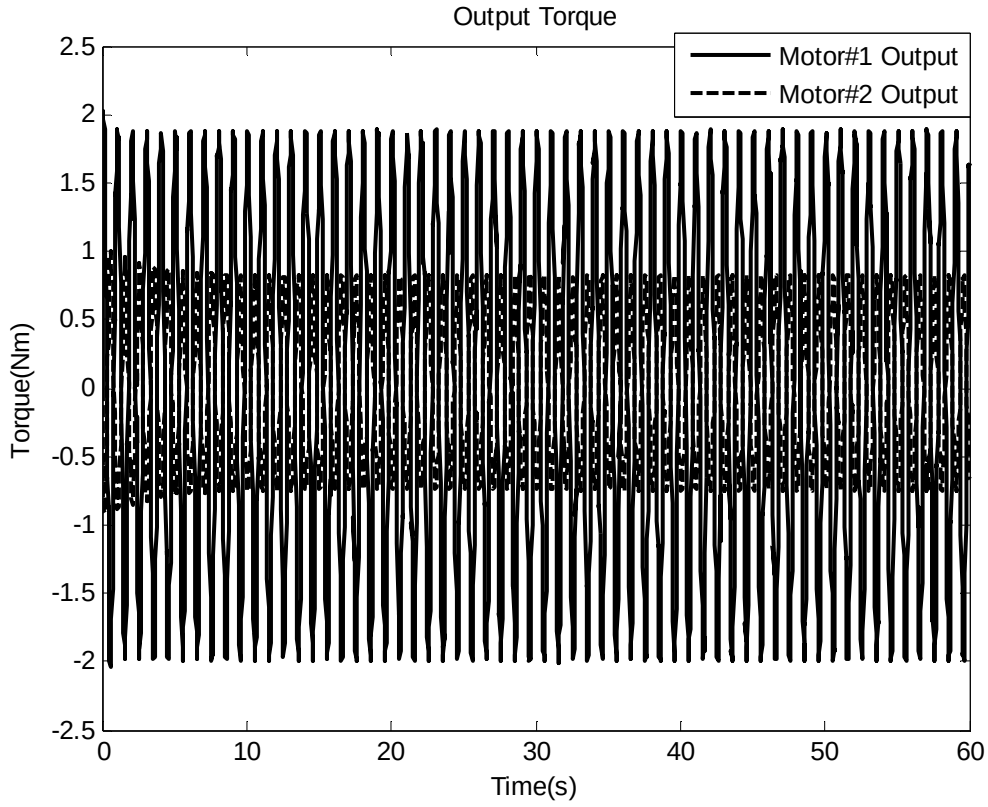

Fig. 4.14: The Output Torque from Motors

Chapter 5

Conclusion

A novel design of a two degree-of-freedom suspension system for gravity compensation purpose and its new application in rehabilitation has been presented. There are many mechanical designs trying to eliminate the gravitational effect on objects: the band wheel, the counter weight, and the linkage with springs. No matter how they work, it is inevitable that the devices all increase the inertia of the whole system. The influence of the inertia of linkage in dynamic has already been shown. All the system response to external impulse or force becomes slow and the rate of trajectories shifting with respect to time even keeps increasing. All of these compromise the performance and limits the loading weight.

To solve the issue, feed-forward adaptive control is introduced and it achieves excellent results. Although the error is not converge to zero, either oscillating around zero or asymptote to a certain value, the error in trajectory is still less than 0.1 mm. Since the goal is to use the device as a lower-limb rehabilitation machine the lifting force to the patient can be adjusted depending on the weight of the patient and keeps the suspension force constant no matter how patient moves. From the analysis and simulation, the suspension system has been shown to be a fully feasible design and it is lightweight and compact. This shows that by utilizing a novel mechanism in conjunction with controls, a significant improvement on such suspension systems can be achieved.

Reference

1. Joseph, E.W, *"Dynamics and control of Two Suspension Mechanisms for Ground-based Testing of Space Structures,"* Master Thesis, Old Dominion University, October, 1990.

2. Donalson, D.D. and Leondes, C.T., *"A Model Reference Parameter Tracking Technique for Adaptive Control System I – The Principle of Adaptation,"* Application and Industry, IEEE Transactions on, Sep. 1963, Vol. 82, pp. 241-252.

3. Dubowsky, S. and DesForges, D.T., *"The Application of Model-Reference Adaptive Control to Robotic Manipulators,"* ASME Journal of Dynamic Systems, Measurement, and Control, Sep. 1979, Vol. 101, pp. 193-200.

4. Yang, L.-F., Tzeng, R.-C., and Kou C.-P., *"Dynamics and Control of An Adaptive Disk Suspension System under Inertial Loading,"* ASME Design Engineering Technical Conference, Irvine, California, Aug. 1996.

5. Astrom, K.J. and Wittenmark, B.,*"Adaptive Control,"* 2nd Edition, Addison-Wesley Publishing Co., 1994.

6. Pons, J.L.,*"Wearable Robots: Biomechatronic Exoskeletons,"* Wiley Publishing Co., 2008.

7. Crowe, A., Schiereck, P., Boer R.W. and Keessen W., *"Characterization of Human Gait by Means of Body Center of Mass Oscillations Derived from Ground Reaction Forces,"* IEEE Transactions on Biomedical Engineering, Vol. 42, No. 3, March 1995.

8. Agrawal, S.K., Fattah, A. and Banala, S.K., *"Design and Prototype of a Gravity-Balanced Leg Orthosis,"* International Journal of Human-friendly Welfare Robotic System, 2003, pp.13-16.

9. Fattah, A., Agrawal, S.K., *"Gravity Balancing of a Human Leg using an External Orthosis,"* IEEE International Conference on Robotics and Automation, Roma, Italy, April 2007.

10. Colombo, G., Joerg, M., Schreier, R. and Dietz, V. *"Treadmill training of paraplegic patients using a robotic orthosis,"* Journal of Rehabilitation Research and Development, Vol. 37, No. 6, Dec, 2000, pp. 693-700.

APPENDIX A

Table A.1: Values of the design system parameters for the two degree-of-freedom suspension system for applied impulsive force.

Parameter	Value
l_1	0.3 m
l_2	0.3 m
l_3	0.6 m
l_4	1.2 m
l_{41}	0.6 m
l_{42}	0.6 m
m_1	1.6891 kg
m_2	1.6891 kg
m_3	3.3782 kg
m_4	6.7564 kg
w_a	1000 N
Initial θ_1	$\frac{\pi}{4}$
Initial θ_2	$\frac{3\pi}{4}$
g	9.81 m/s^2
K_1	2500 N/m
K_2	2500 N/m
P	10 kgm/s

Table A.2: Values of the design system parameters for the two degree-of-freedom suspension system for applied force.

Parameters	Value
l_1	0.3 m
l_2	0.3 m
l_3	0.6 m
l_4	1.2 m
l_{41}	0.6 m
l_{42}	0.6 m
m_1	1.6891 kg
m_2	1.6891 kg
m_3	3.3782 kg
m_4	6.7564 kg
w_a	1000 N
Initial θ_1	$\frac{\pi}{4}$
Initial θ_2	$\frac{3\pi}{4}$
g	9.81 m/s^2
K_1	2500 N/m
K_2	2500 N/m
F	10 N

APPENDIX B

Table B.1: Values of the parameters of the design system and the controller for the two degree-of-freedom suspension system for applied force.

Parameters	Value
l_1	0.3 m
l_2	0.3 m
l_3	0.6 m
l_4	1.2 m
l_{41}	0.6 m
l_{42}	0.6 m
m_1	1.6891 kg
m_2	1.6891 kg
m_3	3.3782 kg
m_4	6.7564 kg
w_a	1000 N
Initial θ_1	$\pi/4$
Initial θ_2	$3\pi/4$
g	9.81 m/s^2
K_1	2500 N/m
K_2	2500 N/m

P	10 kgm/s
g_d	600
g_v	400
γ	500

Table B.2: Values of the parameters of the design system and the controller for the two degree-of-freedom suspension system for applied force.

Parameters	Value
l_1	0.3 m
l_2	0.3 m
l_3	0.6 m
l_4	1.2 m
l_{41}	0.6 m
l_{42}	0.6 m
m_1	1.6891 kg
m_2	1.6891 kg
m_3	3.3782 kg
m_4	6.7564 kg
w_a	1000 N
Initial θ_1	$\pi/4$
Initial θ_2	$3\pi/4$
g	9.81 m/s^2
K_1	2500 N/m
K_2	2500 N/m
F	10 N
g_d	1200
g_v	800
γ	1000

APPENDIX C

Table C.1: Values of the parameters of the design system and the walking pattern for motion analysis on two degree-of-freedom suspension system

Parameters	Value
l_1	0.3 m
l_2	0.3 m
l_3	0.6 m
l_4	1.2 m
l_{41}	0.6 m
l_{42}	0.6 m
m_1	1.6891 kg
m_2	1.6891 kg
m_3	3.3782 kg
m_4	6.7564 kg
w_a	1000 N
Initial θ_1	$\pi/4$
Initial θ_2	$3\pi/4$
g	10 m/s^2
K_1	2500 N/m
K_2	2500 N/m
Lifting Force	800 N
f	1 Hz

Table C.2: Values of the parameters of the design system and the controller for the two degree-of-freedom suspension system in walking simulation

Parameter	Value
l_1	0.3 m
l_2	0.3 m
l_3	0.6 m
l_4	1.2 m
l_{41}	0.6 m
l_{42}	0.6 m
m_1	1.6891 kg
m_2	1.6891 kg
m_3	3.3782 kg
m_4	6.7564 kg
w_a	1000 N
Initial θ_1	$\pi/4$
Initial θ_2	$3\pi/4$
g	10 m/s^2
K_1	2500 N/m
K_2	2500 N/m
Lifting Force	800 N
f	1 Hz
F	$200 + 8\pi^2 Cos(2\pi t + 5\pi/6)$ N
g_d	1200
g_v	600
γ	800

Vita

The author was born on February 21st, 1985 to Chien-Hsiang Cheng and Liang-Li Jung. Born and raised in Taiwan, the author attended both the most prestigious high school and university in the country, Taipei Municipal Chien-Kuo High School and National Taiwan University (NTU). Motivated by Dr. Jung-Ho Cheng, Professor of NTU, in a seminar, the author decided to enroll in Mechanical Engineering Program at NTU with great interests and enthusiasm. During undergraduate years, he gained experience and mastered in electronic circuit design and embedded system under the instruction of Prof. Wen-Pin Shih. Followed his recommendation and encouragement, the author applied and was accepted into the M.S. Mechanical Engineering Program at Lehigh University, where his research is supervised by the advisor, Dr. Meng-Sang Chew. The author's studies involve mechanism design and the application of control methods. During his time at Lehigh University, he also served as a teaching assistant in the Mechanical Engineering and Mechanics department.